

This is to certify that the dissertation entitled

HIGGSLESS ELECTROWEAK SYMMETRY BREAKING FROM THEORY SPACE

presented by

ROSHAN FOADI

has been accepted towards fulfillment of the requirements for the

Ph.D. degree in Physics

All R. School

Major Professor's Signature

August 22, 2006

MSU is an Affirmative Action/Equal Opportunity Institution

Date

LIBRARY Michigan State University



PLACE IN RETURN BOX to remove this checkout from your record. TO AVOID FINES return on or before date due. MAY BE RECALLED with earlier due date if requested.

| DATE DUE | DATE DUE | DATE DUE |
|----------|----------|----------|
| | | |
| | | |
| | | |
| | | |
| | | |
| | | |
| | | |
| | | |
| | | |
| | | |

6/01 c:/CIRC/DateDue.p65-p.15

HIGGSLESS ELECTROWEAK SYMMETRY BREAKING FROM THEORY SPACE

By

Roshan Foadi

A DISSERTATION

Submitted to
Michigan State University
in partial fulfillment of the requirements
for the degree of

DOCTOR OF PHILOSOPHY

Department of Physics and Astronomy 2006

ABSTRACT

HIGGSLESS ELECTROWEAK SYMMETRY BREAKING FROM THEORY SPACE

Bv

Roshan Foadi

We propose a Higgsless model of electroweak symmetry breaking, with inspiration from the physics of one compactified extra-dimension. The gauge sector consists of an SU(2) Yang-Mills theory on an extra-dimensional interval, with boundary conditions breaking SU(2) to U(1) at one end, and large brane kinetic terms on both boundaries. Exchanges of Kaluza-Klein modes are shown to postpone the unitarity violation of longitudinal gauge boson scattering amplitudes to energy scales higher than the customary limits of Dicus-Mathur or Lee-Quigg-Thacker. Fermions are first implemented into the model as brane-localized fields, and then as bulk fields with large brane kinetic terms on both boundaries. Only in the latter case can unitarity and precision electroweak constraints coexist, as long as the amounts of leakage into the bulk of the Standard Model gauge bosons and the Standard Model left-handed fermions are properly related. In order to achieve a realistic top mass without violating unitarity of gauge boson scattering amplitudes, the gauge-sector compactification radius, R_g , and the fermion-sector compactification radius, R_f , are made independent by breaking the five-dimensional Lorentz invariance. Unitarity and experimental constraints are shown to impose, respectively, upper and lower bounds on $1/R_g$ and $1/R_f$.

I dedicate this thesis to my parents, Amalia and Hushyar, and to my brothers and sisters.

ACKNOWLEDGMENTS

I would like to thank my thesis advisor, Prof. Carl Schmidt, whose support and advice have helped me to successfully complete my research projects during my years at Michigan State University. I am especially grateful to him for teaching me how to focus on the important aspects of the research in theoretical physics, a field in which it is often easy to waste time on unessential technicalities. I am also grateful to Prof. R. Sekhar Chivukula. Since his arrival to Michigan State, in the Fall of 2003, he has been for me an endless source of knowledge and advice.

I am grateful to the Physics and Astronomy Department, and to the professors of the High Energy Physics Theory Group for their financial support. I also want to thank the Chairperson for the Graduate Programs, Prof. Bhanu Mahanti, for his advice, and the members of my thesis guidance committee, Prof. Kirsten Tollefson, Prof. Vladimir Zelevinsky, and Prof. Carlo Piermarocchi, for useful guidance. I am grateful to Prof. Scott Pratt for his participation to my thesis defense.

I would like to thank Prof. Wayne Repko, Prof. Wu-Ki Tung, and Prof. C.-P. Yuan for their advice, and Prof. Kaustubh Agashe, from Syracuse University, for useful discussions. I am further grateful to our current and former post-docs: Alexander S. Belyaev, Shrihari Gopalakrishna, Yu Jia, Daisuke Nomura, and Kazuhiro Tobe for illuminating discussions; to my graduate students colleagues: Aous Abdo, Jorge Benitez, Qing-Hong Cao, Chuan-Ren Chen, Stefano DiChiara, HyeongKwan Kim and Baradhwaj Panayancheri Coleppa, for the happy time in the office. I also want to thank Thomas Rockwell and the members of the departmental Computer Center for their technical support.

I am sincerely grateful to Debbie Simmons and Brenda Wenzlick for their help and kindness.

Contents

| | LIS | T OF FIGURES | vii |
|---|---------------------------------|--|------------|
| 1 | Intr | roduction | 1 |
| 2 | Unitarity in the Standard Model | | |
| | 2.1 | Partial Wave Expansion | 14 |
| | 2.2 | Longitudinal Gauge Boson Scattering in the Standard Model | 17 |
| | 2.3 | Unitarity and the Equivalence Theorem | 22 |
| 3 | Uni | tarity without the Higgs Boson | 26 |
| | 3.1 | Compactified Extra-Dimension | 27 |
| | 3.2 | Symmetry Breaking by Boundary Conditions | 3 0 |
| | 3.3 | Unitarity in Extra-Dimension | 37 |
| | 3.4 | Unitarity and the KK Equivalence Theorem | 41 |
| | 3.5 | Deconstructed Models | 44 |
| 4 | Hig | gsless Electroweak Symmetry Breaking | 51 |
| | 4.1 | Higgsless Models on a Warped Background | 52 |
| | 4.2 | Brane Kinetic Terms | 56 |
| | 4.3 | A Minimal Higgsless Model | 59 |
| | | 4.3.1 The $SU(2)_0 \times SU(2)_1 \times U(1)$ Model | 59 |
| | | 4.3.2 The $SU(2)\times SU(2)^N\times U(1)$ Model | 66 |
| | | 4.3.3 The $N \to \infty$ Limit | 70 |
| 5 | Cou | pling to Matter Fields and Experimental Constraints | 78 |
| | 5.1 | Model I | 79 |
| | 5.2 | Experimental Constraints on Model I | 81 |
| | | 5.2.1 Direct Constraints on Heavy Boson Production | 81 |
| | | 5.2.2 Indirect Constraints on the Low Energy Fermion Lagrangians | 81 |
| | | 5.2.3 Indirect Constraints on the Low Energy Gauge Lagrangian | 84 |
| | 5.3 | Model II | 86 |
| | | 5.3.1 Fermion Masses and Wave Functions | 88 |

| | | 5.3.2 | Generation Mixings | 95 |
|--------------|-------|--------|---|-----|
| | 5.4 | Experi | mental Constraints on Model II | 96 |
| | | 5.4.1 | Direct Constraints on Heavy Boson Production | 97 |
| | | 5.4.2 | Indirect Constraints on the Low Energy Fermion Lagrangians | 97 |
| | | 5.4.3 | Indirect Constraints on the Low Energy Gauge Lagrangian $$. $$. | 99 |
| 6 | The | Top S | Sector | 100 |
| | 6.1 | The T | op Mass in Theory Space | 100 |
| | 6.2 | Unitar | ity of Fermion Scattering Amplitudes | 103 |
| | 6.3 | Bound | s on the Model Parameters | 106 |
| 7 | Con | clusio | ns | 110 |
| A | Solu | itions | for the $\mathrm{SU}(2)_0{	imes}\mathrm{SU}(2)_1{	imes}\mathrm{U}(1)$ Model | 113 |
| В | Solu | itions | for the $SU(2) \times SU(2)^N \times U(1)$ Model | 115 |
| \mathbf{C} | Cou | pling | Constants in Model II | 120 |
| | C.1 | Gauge | Boson Couplings | 120 |
| | C_2 | Fermi | on Couplings | 123 |

List of Figures

| 1.1 | (a) Structure of a linear moose diagram. The circles represent gauge groups G_j , and their couplings g_j . A line connecting two circles represents a non-linear sigma model field, Σ_j , and its VEV f_j . Each Σ field transforms bilinearly under the adjacent gauge groups. (b) Moose diagram of a deconstructed model in a flat background: All gauge groups, couplings, and VEVs are identical, because of the translational invariance of the underlying five-dimensional theory. The only possible exception is for the first and the last site, depending on the boundary conditions. | 6 |
|-----|---|----|
| 1.2 | (a) Deconstruction of the $SU(2)_L \times SU(2)_R \times U(1)$ model on a flat background and brane kinetic terms on the Planck brane. (b) The same model can be unfolded to a single chain of $SU(2)$ groups, and a chain of $U(1)$ groups | 9 |
| 1.3 | Moose diagram for an $SU(2)\times SU(2)^N\times U(1)$ Higgsless model. The gauge couplings of the internal sites, and the Σ field VEV's are identical, as the underlying five-dimensional model is translationally invariant. If $g,g'\ll \tilde{g}/\sqrt{N+1}$, g and g' are approximately equal to the SM $SU(2)\times U(1)$ gauge couplings | 11 |
| 2.1 | The partial wave coefficients of elastic scattering amplitudes are complex numbers which must lie on the unitarity circle. When a tree-level amplitude – which is real – reaches $\pm 1/2$, radiative corrections become as large as the leading order contribution, forcing the theory to be strongly interacting. | 16 |
| 2.2 | Tree-level diagrams for the $W_L^+W_L^- \to W_L^+W_L^-$ elastic scattering, in the SM | 17 |
| 2.3 | $J=0$ partial wave amplitude for the $W_L^+W_L^- \to W_L^+W_L^-$ scattering, with (blue) and without (dashed red) the contribution of the Higgs boson, for $m_H=400$ GeV. Without the Higgs boson, the amplitude grows like s , leading to unitarity violation at ~ 1.6 TeV. The Higgs exchanges unitarize the amplitude by exactly canceling the energy growing terms. | 19 |

| 2.4 | $J=0$ partial wave amplitude for the $W_L^+W_L^- \to W_L^+W_L^-$ scattering in the SM, for $m_H=0.6$ TeV (green), well below the critical value (2.18), and $m_H=1$ TeV (red), above the critical value. In the first case unitarity is satisfied for all non-exponentially large energies. In the second case unitarity is already violated at energies above the Higgs | |
|-----|--|----|
| | pole | 20 |
| 2.5 | Tree-level diagrams for the $\pi^+\pi^- \to \pi^+\pi^-$ scattering, in the SM | 22 |
| 2.6 | Moose diagram for the GWS model with the Higgs boson integrated out. | 23 |
| 2.7 | Diagrams for the $\pi^+\pi^- \to \pi^+\pi^-$ scattering in the SM without the Higgs boson: (a) Tree-level amplitude. (b) One-loop corrections | 24 |
| 3.1 | Equivalence between the $SO(4) \sim SU(2)_L \times SU(2)_R$ gauge theory on a five-dimensional interval, with $SO(4)$ broken down to $SU(2)_{diagonal}$ at one end, and a single $SU(2)$ with double interval length | 34 |
| 3.2 | Diagrams contributing to the elastic scattering $A_n^a A_n^b \to A_n^c A_n^d$: Contact interaction plus s-channel, t-channel, and u-channel exchanges. | 37 |
| 3.3 | Rectangular Wilson loop in the $(\mu, 5)$ plane, with the fifth-dimensional interval on a lattice. | 45 |
| 3.4 | Moose diagram for the deconstructed SU(2) gauge theory on a five-dimensional interval, with BC's breaking SU(2) to U(1) at one end of the interval. | 48 |
| 3.5 | Moose diagram of the deconstructed $SU(2)_L \times SU(2)_R$ gauge theory on a five-dimensional interval, with BCs breaking $SU(2)_R$ to $U(1)$ at one end of the interval and $SU(2)_L \times SU(2)_R$ to $SU(2)_{diagonal}$ at the other end. This model is just a single chain of $SU(2)$ groups and a $U(1)$ group. | 49 |
| 3.6 | Moose diagram of the deconstructed $SU(2)_L \times SU(2)_R U(1)$ gauge theory on a five-dimensional interval, with BCs breaking $SU(2)_R \times U(1)$ to $U(1)$ at one end of the interval and $SU(2)_L \times SU(2)_R$ to $SU(2)_{diagonal}$ at the other end | 50 |
| 4.1 | Background of a Randall-Sundrum model (a). The same model after integrating out a large slice of AdS ₅ near the Planck brane (b). The new model has a smaller radius, an approximately flat background, and a large brane kinetic term on the UV brane | 57 |
| 4.2 | Moose diagram for a global $SU(2)_0 \times SU(2)_1 \times SU(2)_2$ NLSM whose $SU(2)_0 \times SU(2)_1 \times U(1)$ part is gauged. All parameters are taken to be independent quantities | 60 |
| 4.3 | Tree-level diagrams for the $W_L^+W_L^- \to W_L^+W_L^-$ elastic scattering, in the $SU(2)_0 \times SU(2)_1 \times U(1)$ NLSM model | 61 |
| 4.4 | The coefficient of the $(E/m_W)^2$ term in the $W_L^+W_L^- \to W_L^+W_L^-$ scattering amplitude in the $SU(2)_0 \times SU(2)_1 \times U(1)$ model (blue) as a function of the Z' and W' mass difference, with $m_{W'} = 500$ GeV fixed. The same quantity in the SM without a Higgs boson (red) is also plotted. | |
| | The vertical line indicates the position where $m_{Z'}^2 - m_{W'}^2 = m_Z^2 - m_W^2$. | 62 |

| 4.5 | The quantities f_1 (blue) and f_2 (red) as a function of the Z' and W' mass difference, with $m_{W'} = 500$ GeV fixed. The vertical line indicates | |
|------|--|----|
| | the position where $m_{Z'}^2 - m_{W'}^2 = m_Z^2 - m_W^2$ | 63 |
| 4.6 | The coupling constants $\alpha_g = g^2/4\pi$ (blue), $\alpha_{q'} = g'^2/4\pi$ (red), and | |
| | $\alpha_{\tilde{g}} = \tilde{g}^2/4\pi$ (green), as a function of the Z' and W' mass difference, with $m_{W'} = 500$ GeV fixed. The vertical line indicates the position where $m_{Z'}^2 - m_{W'}^2 = m_Z^2 - m_W^2$ | 64 |
| 4.7 | The $J=0$ partial wave amplitude as a function of \sqrt{s} for the SM without a Higgs boson (red) and the $\mathrm{SU}(2)_0\times\mathrm{SU}(2)_1\times\mathrm{U}(1)$ model (blue) with $m_{W'}=500$ GeV and $m_{Z'}^2-m_{W'}^2=m_Z^2-m_W^2$ | 65 |
| 4.8 | Moose diagram for the $SU(2) \times SU(2)^N \times U(1)$ Higgsless model | 66 |
| 4.9 | Tree-level diagrams for the $W_L^+W_L^- \to W_L^+W_L^-$ elastic scattering, in the $SU(2)\times SU(2)^N\times U(1)$ model | 68 |
| 4.10 | The $J=0$ partial wave amplitude as a function of \sqrt{s} for the SM without a Higgs boson (red) and the SU(2)×SU(2) ^N ×U(1) model (blue) for $N=1$ to 100 with $m_{W_1'}=500$ GeV | 69 |
| 4.11 | The coupling constants $\alpha_g = g^2/4\pi$ (blue), $\alpha_{g'} = g'^2/4\pi$ (red), and | |
| | $\alpha_{\hat{g}_5} = \hat{g}_5^2/4\pi$ (green), as a function of $1/R$ | 73 |
| 4.12 | Probability density for the position of the W boson (red), W_1 (green), and W_2 (blue) in the extra-dimensional interval, for $1/R = 500$ GeV, with $\delta(y)$ replaced by a narrow Gaussian | 74 |
| 4.13 | Probability density for the position of the photon (dashed), the Z boson (red), Z_1 (green), and Z_2 (blue) in the extra-dimensional interval, for $1/R=500$ GeV, with $\delta(y)$ and $\delta(\pi R-y)$ replaced by narrow Gaussians. | 75 |
| 4.14 | Unitarity violation curve for the $W_L^+W_L^- \to W_L^+W_L^-$ scattering, in the $(\sqrt{s}, 1/R)$ plane. For a given value of $1/R$, unitarity is satisfied for values of \sqrt{s} below the curve | 76 |
| 5.1 | Probability density for the position of the left-handed electron (red), and its KK resonances, e_{L_1} (green), and e_{L_2} (blue) in the extra- | |
| | dimensional (or TS) interval, for $1/R = 500$ GeV, and $t_L = \lambda/\sqrt{3}$, with $\delta(y)$ and $\delta(\pi R - y)$ replaced by narrow Gaussians | 92 |
| 5.2 | Probability density for the position of the right-handed electron (red), and its KK resonances, e_{R_1} (green), and e_{R_2} (blue) in the extra- | |
| | dimensional (or TS) interval, for $1/R = 500$ GeV, and $t_L = \lambda/\sqrt{3}$, with $\delta(y)$ and $\delta(\pi R - y)$ replaced by narrow Gaussians | 93 |
| 5.3 | Masses of fermions, as a function of the bulk mass, for $t_L = 10^{-1}$, $t_R = 1$, and $1/R = 500$ GeV | 94 |

| 6.1 | Mass of the lightest fermion, as a function of the bulk mass, for t_L chosen to adjust the S-parameter to zero, and $1/R = 500$ GeV. The curves correspond to several values of t_{χ_R} , from 10^{-1} to infinity | 101 |
|-----|---|-----|
| 6.2 | (a) Diagrams contributing to the $t\bar{t}\to W_L^+W_L^-$ tree-level scattering amplitude in the SM. (b) Same process, in our Higgsless model | 104 |
| 6.3 | Bounds imposed by unitarity constraints on the $t\bar{t} \to W_L^+ W_L^-$ scattering at $\sqrt{s}=10$ TeV (upper curve), and the $W_L^+ W_L^- \to W_L^+ W_L^-$ scattering at $\sqrt{s}=10$ TeV and $\sqrt{s}=5$ TeV (vertical lines), in the $(1/R_g,1/R_f)$ plane. Specifically, we have assumed the requirement of $a_0 < 1/2$ for both scattering processes. The $t\bar{t} \to W_L^+ W_L^-$ scattering at $\sqrt{s}=5$ TeV imposes no bound, since at this energy the no Higgs boson is required to unitarize the amplitude. The two curves on the bottom correspond to the minimum value of $1/R_f$ which allows a top mass of 175 GeV to be a solution of the mass equation for $M=0$ (lower), and the minimum value of $1/R_f$ which gives a tbW right-handed coupling in agreement with the experimental constraint (upper). The vertical curve on the left corresponds to the experimental bound on m_{W_1} from analysis of the WWZ vertex | 107 |
| 6.4 | Right-handed tbW coupling, in units of e/s , for $1/R_g = 550$ GeV, as a function of $1/R_f$. The horizontal line corresponds to the experimental bound of Ref. [80] | 108 |
| C.1 | Feynman rules for gauge interactions | 122 |
| | Feynman rules for charge-current and neutral-current interactions | 124 |

Chapter 1

Introduction

The $SU(3)_{color} \times SU(2)_L \times U(1)_Y$ gauge model of particle physics is a very successful theory, as decades of experiments have confirmed its predictions to a high level of accuracy. Nonetheless there are still several unanswered questions, the most prominent being the mechanism of electroweak symmetry breaking (EWSB). If the electroweak symmetry were unbroken, all particles so far discovered would be massless. Since most particles are massive, with masses which range from a few eV's for the lightest neutrino to ~ 174 GeV for the top quark, there must be some mechanism, lying at energies above the top mass, which spontaneously breaks the $SU(2)_L \times U(1)_Y$ electroweak symmetry to the $U(1)_Q$ symmetry of electromagnetism.

The process of mass acquisition via symmetry breaking is generically known as *Higgs mechanism* [1] [2] [3]. In its most common versions it consists of one or more scalar fields in a linear representation of the gauge group, with the scalar potential producing a non-zero *vacuum expectation value* (VEV) which spontaneously breaks a higher symmetry to a lower one.

The simplest renormalizable theory of EWSB with scalar fields is the Glashow-Weinberg-Salam model (GWS) [4] [5], in which one scalar doublet is coupled to the $SU(2)_L \times U(1)_Y$ gauge group. When the $SU(3)_{color}$ gauge group of Quantum Chromo-Dynamics is included, together with three generations of matter fields, the GWS model becomes the $Standard\ Model$ (SM) of particle physics. In this model, like in other models of EWSB, the W and Z boson masses depend on the gauge couplings

and the VEV. The latter is therefore constrained, and turns out to be around 250 GeV.

Theories of EWSB via scalar fields are particularly simple, but are also affected by problems like triviality, hierarchy, and vacuum stability. Nonetheless they have been proposed in a variety of theoretical frameworks, besides the SM: Supersymmetry, composite Higgs models, little Higgs models, extra-dimension, and so on. The main reason for this is unitarity. In any quantum field theory, a straightforward consequence of the S-matrix unitarity is that scattering amplitudes cannot grow indefinitely with energy. More specifically, the coefficients of the partial wave expansion computed in the theory must be less than 1/2, or else the theory becomes strongly interacting. This poses a serious problem for the scattering of longitudinal vector bosons, since the corresponding tree-level amplitudes grow with energy [6] [7] [8] [9]. In fact the polarization vector of a longitudinal gauge boson grows like E, where E is the particle energy, and the tree-level scattering amplitudes can potentially grow as badly as E^4 . Gauge invariance always guarantees the cancellation of the E^4 coefficient, but the coefficient of the E^2 term can be different from zero. However in renormalizable theories of EWSB via scalar fields this does not happen. For example, consider the SM Higgs doublet, which is complex and has therefore four real scalar fields. Three of these are absorbed by the W, and Z bosons to acquire the longitudinal component and become massive. These are the Goldstone bosons. However the unabsorbed scalar field corresponds to a physical spin-0 particle, the Higgs boson. In the scattering of longitudinal gauge bosons, the interactions with a virtual Higgs-boson exchange precisely cancel the bad high energy behavior and restore unitarity [7] [10] [11] [12]. Of course this is not a miracle, but just a consequence of the Goldstone boson equivalence theorem: At high energy, the longitudinal gauge boson scattering amplitudes become identical to the scattering amplitudes of the corresponding Goldstone bosons [9] [11] [13] [14] [15] [16] [17] [18] [19]. Analyzing these amplitudes in a linear representation of the gauge group shows that no terms growing with energy can be present, since the cubic and quartic interactions do not involve derivatives. It is important to stress, however, that the cancellation of the terms

which grow like E^2 is not enough to insure unitarity. This is easily understood if we decouple the Higgs boson from the theory by sending its mass to infinity, in which case the scattering amplitudes would no longer be unitarized. In fact in such case the Goldstone fields would necessarily be in a non-linear realization of the gauge group, with interaction terms involving derivatives, and the Goldstone boson scattering amplitudes would grow like E^2 . Therefore, unitarity poses an upper limit on the Higgs boson mass, which turns out to be below 1 TeV [10] [11].

After these considerations, the emerging picture is the following: in an $SU(2)_I \times$ $\mathrm{U}(1)_{Y}$ gauge theory, EWSB via scalar doublets is viable, as long as the VEV is close to 250 GeV, and the Higgs boson is a light particle (below 1 TeV), which should be detected in the upcoming generation of hadron and linear colliders. Recently it has been pointed out that the VEV and the Higgs mass can be raised if the gauge group is larger than $SU(2)_L \times U(1)_Y$. For example, Georgi has shown that an $SU(2)^{89} \times U(1)$ gauge theory can reproduce the SM results with a VEV greater than 2 TeV [20]. The reason for this (and the motivation for considering such a ridiculously large gauge structure) finds its origin in the physics of extra-dimension. A spatially compactified extra-dimension, substantially larger than the Planck length (10^{-33}cm) , but small enough to elude detection in the past generations of hadron and linear colliders, might exist [21] [22] [23] [24] [25] [26] [27] [28] [29] [30] [31] [32]. A gauge theory on a compactified extra-dimension can be seen from two different standpoints. First, it can be seen as a five-dimensional theory whose Lorentz invariance along the fifth dimension is explicitly violated by compactification. Effects of the Lorentz symmetry breaking would then be proportional to powers of 1/ER, where E is the typical energy of a physical process, and R is the size of the extra-dimension, which will be referred to as the *compactification radius*. Second, it can be seen as a four-dimensional theory, by expanding the four-dimensional components of the gauge field in a series of massive vector bosons, the Kaluza-Klein (KK) modes, whose mass spacing is of order of the inverse compactification radius. The fifth component of the gauge field would

¹The upper bound on the Higgs mass imposed by triviality is stronger than the bound imposed by unitarity.

then be expanded in a KK tower of massive scalar particles. These scalars cannot be physical, since in a five-dimensional gauge theory, under certain assumptions, the fifth component of a gauge field can be transformed away [33]. They are therefore to be interpreted as Goldstone bosons, eaten by the massive KK modes.

It is then clear that a gauge theory on a compactified extra-dimension has a spontaneously broken enhanced symmetry, with consequent generation of massive vector bosons and eaten Goldstone bosons. Chivukula et al. showed that this large symmetry structure has the important effect of delaying unitarity violation of scattering amplitudes to energy scales higher than the customary limit of Dicus-Mathur or Lee-Quigg-Thacker [7] [10] [11] [12]. The violation delay is achieved by introducing interactions with exchange of virtual KK modes [34] [35] [36]. In particular, the coefficient of the term growing like E^2 exactly vanishes. This can be understood by using a Kaluza-Klein equivalence theorem (KK-ET), which results from the geometric Higgs mechanism of compactification. From a four-dimensional point of view, the KK-ET relates the scattering amplitudes of longitudinal KK modes to the scattering amplitudes of the corresponding KK Goldstone bosons, which – as we argued before – do not grow with energy.

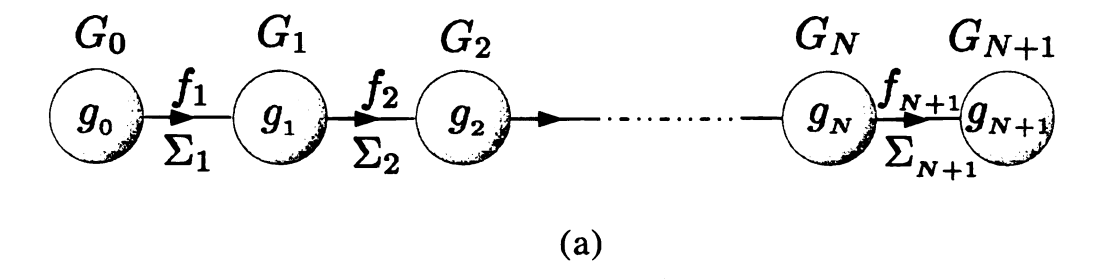
Eventually unitarity ends up being violated at large energies. The reason for this can be intuitively understood in two different ways. First, Yang-Mills theories are non renormalizable in 5D. Then a bad high-energy behavior of loop diagrams corresponds, through the optical theorem, to a bad high-energy behavior of the cut tree-level amplitudes. Second, even in absence of an E^2 term, a logarithmic growth in energy is still present: this comes from the infrared singularity in the t-channel. In the SM, or in other theories with a Higgs boson, such contribution is negligible for all non-exponentially large energies. However, in models from extra-dimension, as the number of exchanged KK modes is allowed to increase, the term proportional to $\log E$ becomes important, and eventually leads to a unitarity violation of any scattering amplitude. The scale of unitarity violation can be estimated by taking the extra-dimension to be infinite in size, because we are interested in the high energy behavior. Then the only mass scale is $1/g_5^2$, where g_5 is the gauge coupling of the

five-dimensional theory, with mass dimension -1/2. Therefore, we expect unitarity to be violated at energy scales of order $1/g_5^2$ times a numerical factor [37] [38].

This violation scale can be rather high, suggesting that perhaps there is a consistent way of breaking the electroweak symmetry without producing a Higgs boson, at least in the energy range predicted by $SU(2)_L \times U(1)_Y$ gauge theories with one or more Higgs doublets, as suggested by Georgi's model. The latter can be seen - when the Higgs fields are integrated out – as a deconstructed [39] [40], or latticized, version of a five-dimensional SU(2) gauge theory on an interval, rather than a circle, where each SU(2) group corresponds to a point on the extra-dimensional interval.² In fact when the extra-dimension is put on a lattice, a G-invariant gauge theory becomes a G^{N+2} non-linear sigma model (NLSM), where N+2 is the number of points in the lattice (two at the interval ends and N internal). NLSMs are usually depicted by moose diagrams, like the one in Fig.1.1(a). Each circle, or site, represents a gauge group G_i , and its coupling g_i . A line connecting two circles represents a NLSM field, Σ_j , and its VEV f_j . The field $\Sigma_j(x)$ transforms under both G_{j-1} and G_j , like $\Sigma_j(x) \to U_{j-1}^{-1}(x)\Sigma_j(x)U_j(x)$. In a deconstructed model all gauge groups are of course identical, and the Σ fields correspond to the value of the gauge-field fifth component at discrete points. If a flat background is assumed, all couplings and VEVs are also identical. The only possible exception is represented by the first and the last site, where boundary conditions (BCs) and brane kinetic terms, in the underlying five-dimensional theory, can result in different gauge groups and couplings in the deconstructed model. We will come back to this point later in this introduction. The moose diagram of a deconstructed model looks therefore like the one in Fig.1.1(b).

In deconstructed models the coefficient of the E^2 term does not vanish precisely, but it is suppressed by $1/N^2$, for $N \to \infty$. As a consequence, the delay of unitarity violation is not as large as in the full five-dimensional models [36] [41] [42]. Nonetheless deconstruction is still a powerful tool for model building for at least two reasons. First,

²In Georgi's model fermions are coupled in a peculiar way, which makes the interpretation as a deconstructed five-dimensional model not viable. Nonetheless such interpretation is valid for the gauge sector.



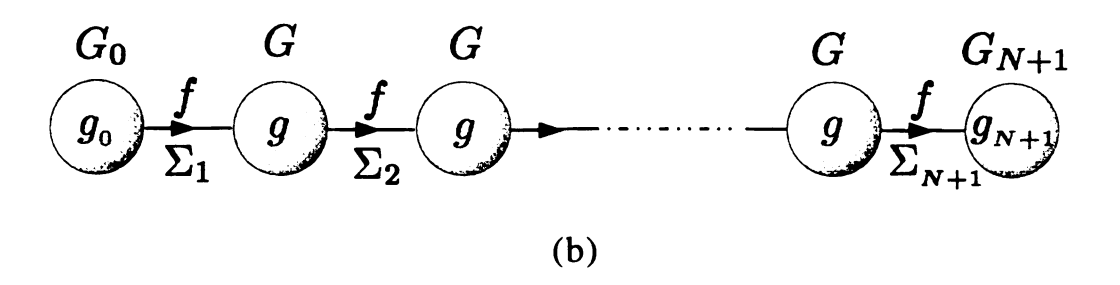


Figure 1.1: (a) Structure of a linear moose diagram. The circles represent gauge groups G_j , and their couplings g_j . A line connecting two circles represents a non-linear sigma model field, Σ_j , and its VEV f_j . Each Σ field transforms bilinearly under the adjacent gauge groups. (b) Moose diagram of a deconstructed model in a flat background: All gauge groups, couplings, and VEVs are identical, because of the translational invariance of the underlying five-dimensional theory. The only possible exception is for the first and the last site, depending on the boundary conditions.

it allows for common four-dimensional UV completions, like linear sigma models (as in Georgi's model) or dynamical symmetry breaking. This turns out to be particularly useful in Technicolor-like models, since a strongly coupled physics at the TeV scale is disfavoured by electroweak precision (EWP) data [43] [44], and deconstructed models with a large symmetry structure can raise the scale of unitarity violation by a factor 10 [45] [46]. Second, deconstructed models allow for more freedom in model building than strict five-dimensional theories. This feature is especially welcome when it comes to coupling a model to matter fields. As opposed to five-dimensional theories, where the interaction of fermions with the gauge-field fifth component has the same strength

as the ordinary gauge interactions, in deconstructed models the Yukawa coupling to the Σ fields can be made independent of the gauge interactions. Moreover, terms which are not local in a five-dimensional theory make perfect sense in deconstructed models. Theories represented by moose diagrams are commonly referred to as models from theory space (TS). As the number of sites goes to infinity, a theory-space chain of gauge groups becomes an extra-dimensional interval only under special assumptions. We will discuss the relation between extra-dimension and theory space in section 3.5.

Having established that extra-dimension and theory space provide new interactions which delay unitarity violation, the next step is to inquire whether EWSB can be implemented in these frameworks. Models with a compactified extra-dimension are usually mapped onto five-dimensional intervals, where the interval ends are fourdimensional branes with rather special properties, depending on the BC's. The fifthdimensional interval is commonly referred to as the bulk of the extra-dimension. Csaki et al. showed that an appropriate choice of the gauge group in the bulk, supplied with suitable BCs, can give a symmetry breaking pattern which contains EWSB. Therefore, Higgsless EWSB is indeed a potentially viable alternative to the more traditional models with a Higgs boson in the GeV range [36] [42] [45] [46] [47] [48] [49] [50]. The W boson would then be interpreted as the lightest mode of a charged KK tower, while the photon and the Z boson would be interpreted as the lightest modes of a neutral KK tower. The elastic scatterings $W^+W^- \to W^+W^-$ and $W^\pm Z \to W^\pm Z$ would be unitarized by exchanges of virtual Z_n and W_n^{\pm} KK modes, respectively, where $n=1,2,\ldots$ [36] [42]. However the cancellation of the terms which grow like E^2 is not enough to ensure unitarity. In gauge theories with a Higgs boson, we argued that unitarity requires an upper bound on the Higgs mass. Similarly, in extra-dimensional models the delay of unitarity violation imposes an upper bound on the compactification scale [46] [50].

Of course unitarity is not the only constraint we must consider. First, a realistic model of EWSB must reproduce the mass spectrum of the observed particles, top quark included. Second, it must satisfy the constraints imposed by EWP data. Third, low-energy anomalous interactions must be within the experimental bounds. Consid-

erable effort has been recently spent in the attempt to meet all these requirements. A model, in particular, has emerged as a potentially serious candidate: the $SU(2)_L \times SU(2)_R \times U(1)_{B-L}$ five-dimensional gauge theory, coupled to a warped anti-de Sitter (AdS), Randall-Sundrum (RS1) model [51], where BCs break $SU(2)_L \times SU(2)_R$ down to $SU(2)_{diagonal}$ at the infra-red, or "TeV" brane, and break $SU(2)_R \times U(1)_{B-L}$ down to $U(1)_Y$ at the ultra-violet, or "Planck" brane [46] [47] [52]. The electroweak symmetry $SU(2)_L \times U(1)_Y$ is therefore localized on the Planck brane, and is broken by the extra-dimensional bulk and the BCs on the TeV brane.

The $SU(2)_L \times SU(2)_R \rightarrow SU(2)_{diagonal}$ structure is designed to satisfy the bounds on the ρ parameter. The latter is defined as the ratio between the strength of the charged-current interactions and the neutral-current interactions at zero momentum. Experimental results show that ρ differs from unity by less than 2.5·10⁻³ [53]. The natural way to meet the constraints on the ρ parameter is to guarantee that a global isospin symmetry is still present even after EWSB, and is only broken by hypercharge and Yukawa interactions [54]. Such global symmetry is known as custodial isospin, and is naturally embedded in the SM. In the extra-dimensional model, the $SU(2)_L \times SU(2)_R \rightarrow SU(2)_{diagonal}$ structure guarantees a custodial symmetry if the five-dimensional profile of the matter fields is appropriately chosen. For example, with matter fields localized on the $x^5=0$ brane the tree-level ρ parameter does not differ from unity: This has been proved for a wide class of deconstructed models, with arbitrary gauge couplings and f-constants [55]. However in general the chargedcurrent and neutral-current interactions are not necessarily mediated by the W and the Z bosons only, since exchanges of the heavy KK modes might be equally important. This is potentially problematic, because a sizable contribution of the heavy KK exchanges means that the first heavy charged and neutral gauge bosons are relatively light, and could be below the direct-search experimental bounds. The AdS warping factor solves this problem, because it pushes the lightest KK ecitations toward the TeV range, while keeping the W and Z masses light [47]. This in turn means that the charged-current and neutral-current interactions, at zero momentum, are almost entirely mediated by the SM gauge bosons.

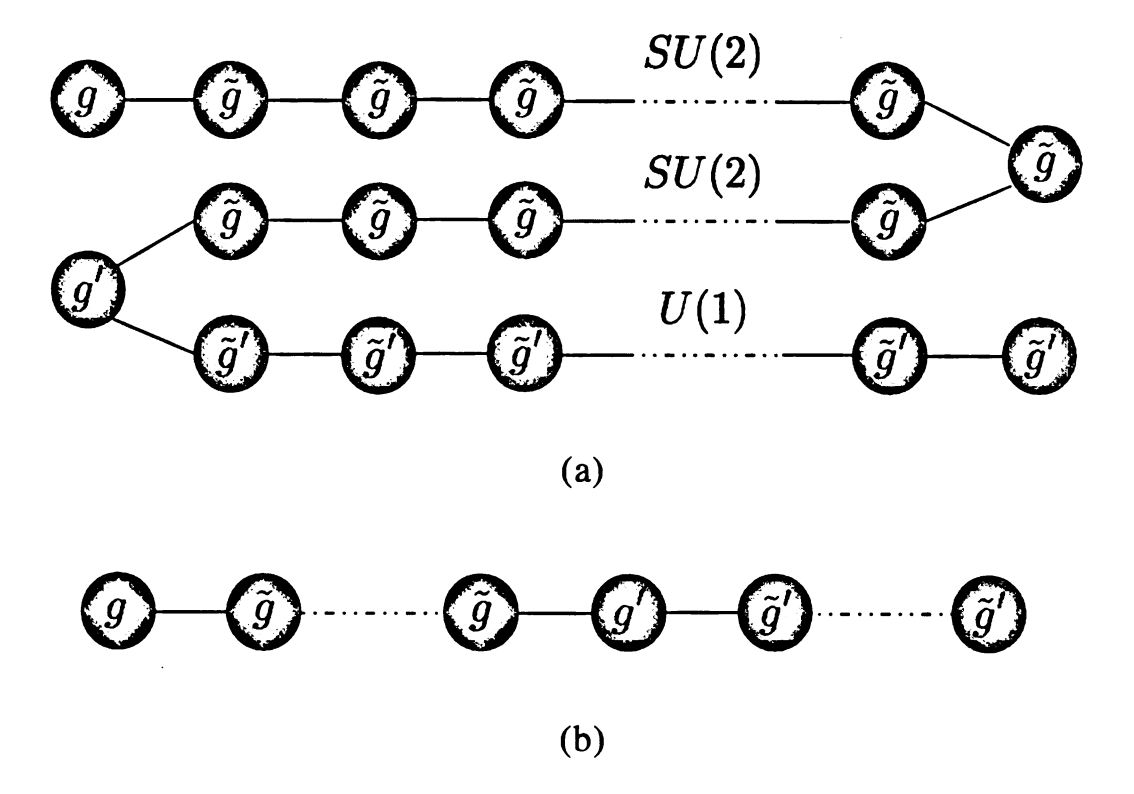


Figure 1.2: (a) Deconstruction of the $SU(2)_L \times SU(2)_R \times U(1)$ model on a flat background and brane kinetic terms on the Planck brane. (b) The same model can be unfolded to a single chain of SU(2) groups, and a chain of U(1) groups.

Warping seems therefore to be a necessary ingredient for a five-dimensional Higgsless model to meet the experimental contraints on the direct search of heavy gauge bosons. However, integrating out a large slice of AdS₅ in the proximity of the Planck brane leaves an effective field theory with a nearly flat background, and a kinetic term localized on one of the boundaries, which "mimics" the warping of the extra-dimension [56] [57] [58]. In this way we can still work with a flat extra-dimension, which means that we can work with sines and cosines, rather than Bessel functions, thereby simplifying the mathematical content of the model. This approach is only valid as long as the energy is much smaller than the curvature of the AdS₅ profile, which lies in the Planck scale, and begins to break down as the energy increases. The corresponding deconstructed model is shown in Fig. 1.2(a). The brane kinetic terms

force the first SU(2) and U(1) gauge groups to have different couplings. The same model has been unfolded in Fig. 1.2(b). Notice that the unfolded moose diagram shows explicitly the equivalence between an $SU(2)_L \times SU(2)_R$ gauge symmetry in the bulk, broken to $SU(2)_{diagonal}$ on one brane, and a single SU(2). We will demonstrate this in section 3.2.

Of course there are more constraints to be considered, other than the ρ parameter. If the contribution of the new physics on the low energy observables is approximately oblique - that is, it does not change the form of the interactions, but only modifies their relative strength - then it can be parametrized in terms of the Peskin-Takeuchi S, T, and U variables, where S = T = U = 0 corresponds to the SM [43] [44] [59]. T is directly related to the ρ parameter, and for models with a custodial symmetry is zero at tree level. U is usually expected to differ from zero by only a percent of T, and is therefore negligible. The constraints on the S parameter are usually more difficult to meet, since a small S often requires the new physics scale to be higher, which is harmful for unitarity. In Higgsless models from extra-dimension the value of S depends on the fermion profiles. It is well known that when the matter fields are localized on the Planck brane, the S parameter is positive, while matter fields localized on the TeV brane give a negative S value [60]. It is then clear that in order for S to vanish, the matter fields must be delocalized. This has been proved for a wide class of Higgsless models [46] [55] [61] [62] [63] [64]. We will return to these results in chapter 5.

The model of Fig. 1.2(b) can be simplified by reducing the number of U(1) groups to one, as in Fig. 1.3. By eliminating the chain of U(1) groups, we necessarily introduce interactions which would be non-local in a deconstructed five-dimensional theory [42] [45]. In fact, in order to maintain gauge invariance, all fermions in the bulk must couple to the U(1) group with left-handed hypercharge Y_L . However from a purely TS point of view this is perfectly legitimate. This is a first example of what was mentioned before, namely that TS offers more freedom, in model building, than the rigid structure of a real extra-dimension.

The $\mathrm{SU}(2) \times \mathrm{SU}(2)^N \times \mathrm{U}(1)$ model of Fig. 1.3 is arguably a minimal Higgsless model

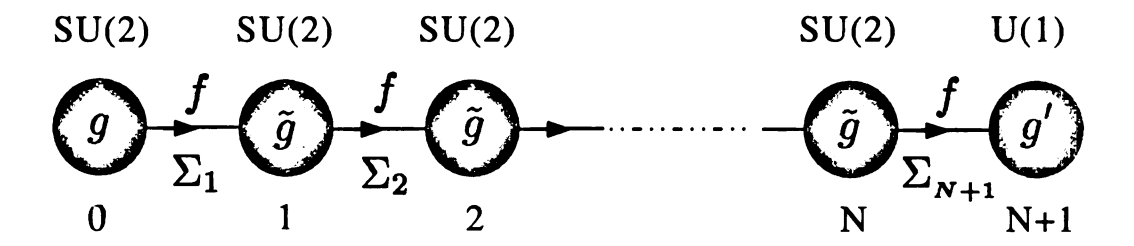


Figure 1.3: Moose diagram for an $SU(2)\times SU(2)^N\times U(1)$ Higgsless model. The gauge couplings of the internal sites, and the Σ field VEV's are identical, as the underlying five-dimensional model is translationally invariant. If $g, g' \ll \tilde{g}/\sqrt{N+1}$, g and g' are approximately equal to the SM $SU(2)\times U(1)$ gauge couplings.

of EWSB, and is the model we will consider in this dissertation. The SU(2) and U(1) gauge groups on the two edges of the moose chain act approximately as the SM SU(2)_L×U(1)_Y, and the SU(2)^N gauge group represents approximately the new-physics contribution. This approximation is valid as long as the the effective SU(2)^N gauge coupling, $\tilde{g}/\sqrt{N+1}$, is large, if compared to the coupling of the first SU(2) group, g, and the coupling of the U(1) group, g'. Then g and g' have approximately their SM values. The fermion sector follows the same pattern of the gauge sector. If matter fields are delocalized, as required by the experimental contraints on the S parameter, then the SM fermions are mainly, but not exclusively, charged under the SU(2) and U(1) gauge groups on the chain edges, with SM quantum numbers. The new, heavy fermions are mainly coupled to the SU(2)^N group, with approximately vector-like couplings [42] [45].

As $N \to \infty$, this theory becomes a model from continuum TS: The discrete site index of Fig. 1.3 becomes a continuous variable, but the non-local couplings of matter fields disfavour the extra-dimensional interpretation. Despite this, the continuum TS limit is more convenient for calculational purposes: Recurrence relations and eigenvalue equations become differential equations and transcendental equations, which are simpler to solve. Therefore, in this dissertation we will carry out most of the calculations in the continuum limit.

The main source of tension, in Higgsless models of this kind, is between the uni-

tarity bounds, and the constraints from EWP data and the top-quark sector. In particular, a heavy top mass is problematic, if the compactification scale is to be within the unitarity bounds. In order to solve this problem, two compactification scales are introduced: one for the gauge sector, and one, higher, for the fermion sector. This makes the extra-dimensional interpretation even more problematic: It corresponds to a microscopic breaking of the five-dimensional Lorentz invariance, in addition to the macroscopic breaking due to compactification. On the other hand, from a discrete TS standpoint this just corresponds to Yukawa couplings being independent of gauge couplings [20] [45].

This dissertation is organized as it follows. In chapter 2 the unitarity of longitudinal gauge boson scattering amplitudes is analyzed in the SM, as well as the role of the Higgs boson and the corresponding bounds on its mass. In chapter 3 the role of extradimension as a tool to delay unitarity violation is discussed in details. Deconstructed models, and TS are then shown to be viable alternatives. The goal of this chapter is to show how to build theories without Higgs bosons, which are weakly coupled and unitary up to high energy scales. In chapter 4 these concepts are applied to models of EWSB. We first consider the extra-dimensional $SU(2)_L \times SU(2)_R \times U(1)$ model. Then we introduce the model which is the object of our study. The gauge sector is an SU(2)Yang-Mills theory on an extra-dimensional interval, with BCs breaking SU(2) down to U(1) on one end. In order to obtain the right masses for the SM gauge bosons, large kinetic terms are added on both branes, without affecting the delay of unitarity violation. Unitarity upper bounds on the compactification scale are calculated numerically in terms of the cutoff scale. Deconstruction is then shown to preserve the important features of the extra-dimensional model, in a familiar four-dimensional context. In chapter 5 matter fields are coupled to the model in two different ways: First, with brane-localized fermions, and second, with slightly delocalized fermions. In both cases the extra-dimensional interpretation is not viable, because non-local interactions must be introduced. Therefore, the $N \to \infty$ limit of the deconstructed model should be interpreted as a continuum TS. The constraints from the EWP data are analyzed for both ways of coupling fermions, including lower bounds on the

mass of the W_1 and Z_1 bosons. While the tree-level T parameter is naturally suppressed by custodial isospin in both cases, the bounds on the S parameter can only be satisfied by the delocalized model, as long as the fermion leakage into the bulk is appropriately tuned. Also, multiple generations and fermion mixings are shown to be naturally implemented in the delocalized model. In chapter 6 a heavy top mass is shown to be unattainable, when the unitarity bounds of gauge boson scattering amplitudes are imposed. However, from a continuum TS standpoint, the compactification scales for the gauge sector and the fermion sector are shown to be independent quantities. This allows to accommodate the top mass without violating the gauge-sector unitarity bounds. Unitarity of $t\bar{t} \to W_L^+W_L^-$, and experimental constraints on the right-handed tbW coupling are translated into upper and lower bounds, respectively, for the fermion-sector compactification scale. Finally, in chapter 7 we offer our conclusions.

Chapter 2

Unitarity in the Standard Model

Any respectable quantum theory must return probabilities between zero and one. In scattering theory this requirement is guaranteed by unitarity of the S matrix: The wavefunctions of scattered particles differ from the wavefunctions of incident particles by unitary transformations. This forces the partial wave amplitudes to lie on a radius-one circle in the complex plane. In this chapter we derive the precise formulation of this constraint, and find its implications for the scattering of longitudinal vector bosons in the SM.

2.1 Partial Wave Expansion

Let us consider a two-particle elastic scattering process in the spin-0 channel. In the center-of-mass (COM) frame, this process is equivalent to a one-particle scattering off a spinless fixed target, and can be described in the context of ordinary one-particle quantum mechanics.

With all couplings turned off, the total wavefunction is just a plane wave propagating, say, along the z axis. An expansion in spherical waves gives

$$\psi_{i} = e^{ipz} = \frac{i}{2pr} \sum_{I=0}^{\infty} (2J+1) \left[(-1)^{J} e^{-ipr} - e^{ipr} \right] P_{J}(\cos \theta) , \qquad (2.1)$$

where p is the magnitude of the particle momentum in the COM frame, θ is the scattering angle, and r is the radial distance from the COM. This expansion is a

superposition of incoming and outgoing spherical waves, e^{-ipr} and e^{ipr} , respectively. The scattering center can only affect the outgoing wave. For an elastic scattering, with no absorption, unitarity of the S matrix implies that the corresponding partial wave coefficients are multiplied by phase factors, which we denote by $e^{2i\delta_J(p)}$. Therefore, the total wavefunction is

$$\psi_{\text{total}} = \frac{i}{2pr} \sum_{J=0}^{\infty} (2J+1) \left[(-1)^{J} e^{-ipr} - e^{2i\delta_{J}(p)} e^{ipr} \right] P_{J}(\cos \theta) . \tag{2.2}$$

The scattered wave represents the difference between the outgoing waves in ψ_{total} and ψ_{i} ,

$$\psi_{\text{scattered}} = \frac{e^{ipr}}{pr} \sum_{J=0}^{\infty} (2J+1) \frac{e^{2i\delta_J(p)} - 1}{2i} P_J(\cos \theta)$$
$$= \frac{e^{ipr}}{r} F(p, \theta), \tag{2.3}$$

where $F(p, \theta)$ is the scattering amplitude,

$$F(p,\theta) = \frac{1}{p} \sum_{J=0}^{\infty} (2J+1) \frac{e^{2i\delta_J(p)} - 1}{2i} P_J(\cos\theta) . \tag{2.4}$$

The scattered outgoing flux in a solid angle $d\Omega$, through a sphere of radius r, is

$$v_{\rm o}|\psi_{\rm scattered}|^2r^2d\Omega=v_{\rm o}|F(p,\theta)|^2d\Omega$$
,

where v_0 is the outgoing particles speed. This expression is by definition equal to the product of the scattering cross-section and the incident flux, $v_i \psi_i \psi_i^* = v_i$:

$$v_{\rm o}|F(p,\theta)|^2d\Omega=v_{\rm i}d\sigma$$
.

Since the collision is elastic, $v_i = v_0$, and

$$\left(\frac{d\sigma}{d\Omega}\right)_{\text{COM, elastic}} = |F(p,\theta)|^2.$$
 (2.5)

In quantum field theory, at high energy, with Lorentz-invariant normalization of the quantum states, equation (2.5) reads

$$\left(\frac{d\sigma}{d\Omega}\right)_{\text{COM, elastic}} = \frac{|M(p,\theta)|^2}{64\pi^2 \cdot 4p^2} ,$$
(2.6)

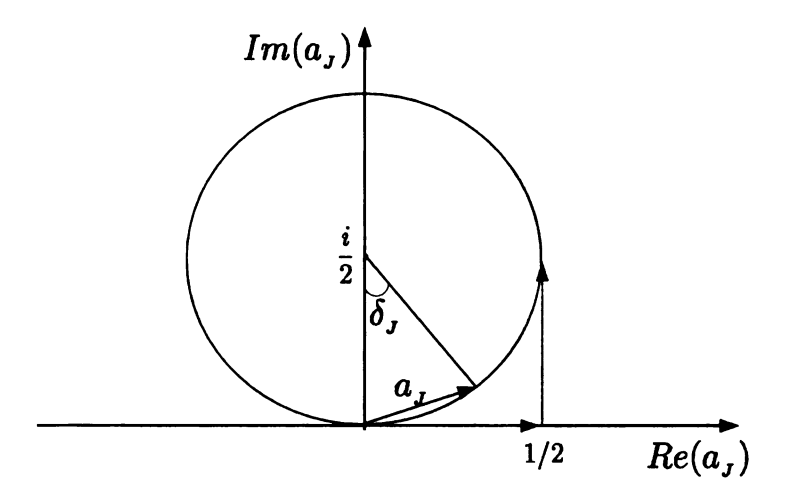


Figure 2.1: The partial wave coefficients of elastic scattering amplitudes are complex numbers which must lie on the unitarity circle. When a tree-level amplitude – which is real – reaches $\pm 1/2$, radiative corrections become as large as the leading order contribution, forcing the theory to be strongly interacting.

where $M(p,\theta)$ is the scattering amplitude [65]. Equating the right-hand side of (2.5) and (2.6), and using (2.4), leads to the partial wave expansion of $M(p,\theta)$, with the appropriate normalization factor,

$$M(p,\theta) = 16\pi \sum_{J=0}^{\infty} (2J+1)a_J(p)P_J(\cos\theta) , \qquad (2.7)$$

where

$$a_J(p) = \frac{e^{2i\delta_J(p)} - 1}{2i}$$
 (2.8)

In the complex plane, $a_J(p)$ lies on a radius-1/2 circle centered on i/2, the unitarity circle, as shown in Fig 2.1. Since tree-level scattering amplitudes are real, $a_J(p)$ can only lie on the circle if loop corrections are included. These become more and more important as the tree-level amplitude increases in magnitude. When the latter reaches $\pm 1/2$, radiative corrections become as important as the leading-order contribution. Therefore, at tree level, either

$$|a_J(p)| \le \frac{1}{2} \,, \tag{2.9}$$

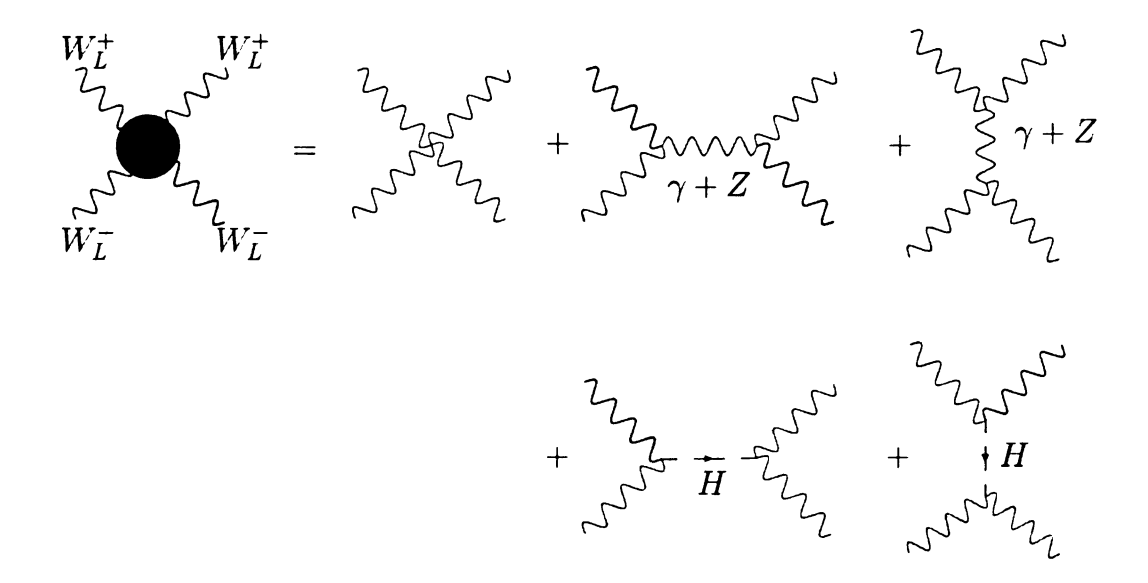


Figure 2.2: Tree-level diagrams for the $W_L^+W_L^- \to W_L^+W_L^-$ elastic scattering, in the SM.

or the theory must be strongly interacting.

2.2 Longitudinal Gauge Boson Scattering in the Standard Model

We now apply last section results to the scattering amplitude of longitudinal W bosons in the SM. As before, we consider the scattering in the COM frame, with initial momenta along the z-axis. The four momenta, for the scattering particles and the scattered particles, are, respectively, $(E,0,0,\pm p)$ and $(E,0,\pm p\sin\theta,\pm p\cos\theta)$, where $E=\sqrt{p^2+m_W^2}$. The polarization vectors are respectively $(p,0,0,\pm E)/m_W$ and $(p,0,\pm E\sin\theta,\pm E\cos\theta)/m_W$. At tree level, in unitary gauge, there are seven diagrams, as shown in Figure 2.2. A simple power counting shows that the amplitude can diverge as badly as $(E/m_W)^4$, for large values of E/m_W , because each polarization vector grows like E/m_W , and longitudinal gauge boson propagators do not fall off with energy.

The contact interaction, plus the photon and Z exchanges give the amplitude

$$M^{\text{gauge}} = \frac{g^2}{m_W^4} \left[p^2 E^2 (-2 + 6\cos\theta) - E^4 \sin^2\theta \right]$$

$$+ \frac{1}{m_W^4} \left[\frac{e^2}{s} + \frac{g^2 \cos^2\theta_W}{s - m_Z^2} \right] \left(-4p^2 (p^2 - 3E^2)^2 \right) \cos\theta$$

$$+ \frac{1}{m_W^4} \left[\frac{e^2}{t} + \frac{g^2 \cos^2\theta_W}{t - m_Z^2} \right] \left[-4E^2 \left(p^2 + (E^2 - 2p^2)\cos\theta \right)^2 \right]$$

$$-2p^2 (1 + \cos\theta) \left(2E^2 - p^2 - E^2 \cos\theta \right)^2 \right], (2.10)$$

where $s = 4E^2$, and $t = -2p^2(1 - \cos \theta)$. In the limit of large E/m_W , this expression becomes

$$M^{\text{gauge}} = g^2 \frac{1 + \cos \theta}{2} \left(\frac{E}{m_W}\right)^2 + g^2 \frac{3 - 2\cos^2 \theta_W (1 - \cos \theta)^2 + \cos^2 \theta}{4\cos^2 \theta_W (1 - \cos \theta)} + \mathcal{O}\left((m_W/E)^2\right). \tag{2.11}$$

The term proportional to $(E/m_W)^4$ vanishes because of gauge invariance, which guarantees the special relation $e^2 = g^2 \sin^2 \theta_W$ between different coupling constants. Nonetheless the term proportional to $(E/m_W)^2$ does not cancel. Therefore, if only interactions from the gauge sector were to be included, the J=0 partial wave would violate unitarity at

$$\sqrt{s} \simeq \frac{8\sqrt{\pi}m_W \sin\theta_W}{e} \sim 1.7 \text{ TeV},$$
 (2.12)

and the J=1 partial wave would violate unitarity at $\sqrt{s}\simeq 2.9$ TeV.

However there are two more diagrams in Fig.2.2 which have not been considered yet, the Higgs exchanges. Their contribution to the scattering amplitude is

$$M^{\text{Higgs}} = -\frac{g^2}{4m_W^2} \left[\frac{(s - 2m_W^2)^2}{s - m_H^2} + \frac{(t + 2m_W^2 \cos \theta)^2}{t - m_H^2} \right] . \tag{2.13}$$

For $E^2, m_H^2 \gg m_W^2$ this becomes

$$M^{\text{Higgs}} \simeq -g^2 \frac{1 + \cos \theta}{2} \left(\frac{E}{m_W}\right)^2 - \frac{g^2}{4} \frac{m_H^2}{m_W^2} \left[\frac{s}{s - m_H^2} + \frac{t}{t - m_H^2}\right].$$
 (2.14)

A comparison of (2.14) and (2.11) shows that the coefficients of the $(E/m_W)^2$ term exactly cancel. The J=0 partial wave amplitude for the $W_L^+W_L^- \to W_L^+W_L^-$

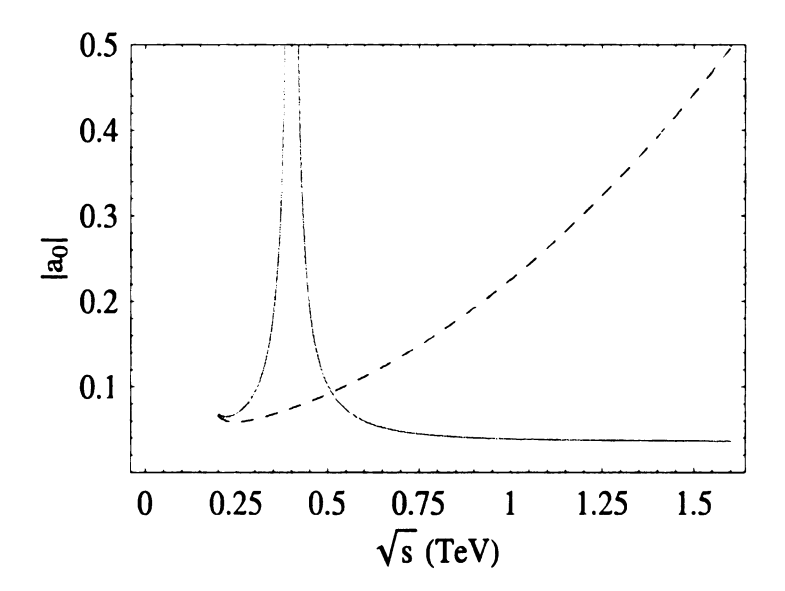


Figure 2.3: J=0 partial wave amplitude for the $W_L^+W_L^- \to W_L^+W_L^-$ scattering, with (blue) and without (dashed red) the contribution of the Higgs boson, for $m_H=400$ GeV. Without the Higgs boson, the amplitude grows like s, leading to unitarity violation at ~ 1.6 TeV. The Higgs exchanges unitarize the amplitude by exactly canceling the energy growing terms.

scattering is then shown in Fig 2.3, with and without the Higgs boson contribution, for m_H =400 GeV. (A small m_{γ} =1 GeV photon mass has been included, in order to regulate the singularity in the t-channel. This is inconsequential in the high energy region in which we are interested.) It is evident that the Higgs boson exchanges are essential to maintain unitarity in the TeV range. Notice that near the Higgs pole the amplitude is tamed by finite-width effects, which are sufficient to keep a_0 below 1/2.

The cancellation of the quadratically divergent term is not enough to prevent unitarity violation at sufficiently high energies, since the term proportional to $(m_W/E)^0$ can be of order one. The contributions to the J=0 partial wave of the contact interaction, plus the photon and Z exchanges, give an $\mathcal{O}\left((m_W/E)^0\right)$ term of order $(g^2/32\pi)\log(E/m_W)$, and is therefore safe for non-exponentially large energies. (The logarithmic growth comes from the integration near $\cos\theta=1$, where

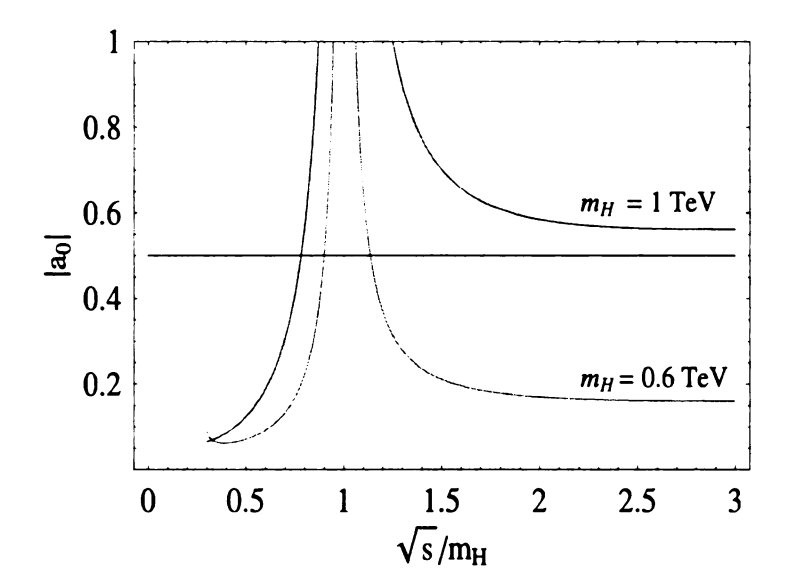


Figure 2.4: J=0 partial wave amplitude for the $W_L^+W_L^- \to W_L^+W_L^-$ scattering in the SM, for $m_H=0.6$ TeV (green), well below the critical value (2.18), and $m_H=1$ TeV (red), above the critical value. In the first case unitarity is satisfied for all non-exponentially large energies. In the second case unitarity is already violated at energies above the Higgs pole.

 m_Z^2/t becomes large, and high energy regions become important.) On the other hand, the contribution of the Higgs exchanges give an $\mathcal{O}\left((m_W/E)^0\right)$ term of order $(g^2/32\pi)(m_H^2/m_W^2)$, and can be large, depending on the Higgs boson mass. Therefore, for $s, m_H^2 \gg m_W^2, m_Z^2$, the $W_L^+W_L^- \to W_L^+W_L^-$ scattering amplitude is to a good approximation given by the second term of (2.14),

$$M(W_L^+ W_L^- \to W_L^+ W_L^-) \simeq \frac{g^2}{4} \frac{m_H^2}{m_W^2} \left[\frac{s}{s - m_H^2} + \frac{t}{t - m_H^2} \right] ,$$
 (2.15)

and the J=0 partial wave amplitude is

$$a_0(W_L^+W_L^- \to W_L^+W_L^-) \simeq -\frac{g^2}{64\pi} \frac{m_H^2}{m_W^2} \left[2 + \frac{m_H^2}{s - m_H^2} - \frac{m_H^2}{s} \log\left(1 + \frac{s}{m_H^2}\right) \right].$$
 (2.16)

In the limit of large energy, this amplitude approaches a constant value:

$$a_0(W_L^+W_L^- \to W_L^+W_L^-) \simeq -\frac{g^2}{32\pi} \frac{m_H^2}{m_W^2}$$
 (2.17)

Then unitarity demands

$$m_H < \frac{4\sqrt{\pi}m_W \sin\theta_W}{e} \sim 0.9 \text{ TeV} \ .$$
 (2.18)

If the Higgs mass is well below this critical value, the J=0 amplitude satisfies the unitarity bound at all (non-exponentially large) energies. If the Higgs mass attains or exceeds the critical value, unitarity is already violated at energies above the Higgs pole, as shown in Fig.2.4.

It is possible to refine the bound (2.18) by considering the neutral four-channel system $W_L^+W_L^-$, $(1/\sqrt{2})Z_LZ_L$, $(1/\sqrt{2})HH$, and HZ_L , rather than just $W_L^+W_L^-$ [10]. Then (2.17) is replaced by a 4×4 matrix:

$$a_{0} = -\frac{g^{2}}{32\pi} \frac{m_{H}^{2}}{m_{W}^{2}} \begin{pmatrix} 1 & \frac{1}{\sqrt{8}} & \frac{1}{\sqrt{8}} & 0\\ \frac{1}{\sqrt{8}} & \frac{3}{4} & \frac{1}{4} & 0\\ \frac{1}{\sqrt{8}} & \frac{1}{4} & \frac{3}{4} & 0\\ 0 & 0 & 0 & \frac{1}{2} \end{pmatrix} . \tag{2.19}$$

This scattering matrix has a surprising simple eigenchannel structure. The largest eigenvalue corresponds to the elastic scattering of the channel $2W_L^+W_L^- + Z_L + Z_L + HH$, and leads to the most stringent unitarity bound on the Higgs mass:

$$m_H < \frac{8\sqrt{\pi}m_W \sin\theta_W}{3e} \sim 0.6 \text{ TeV} \ .$$
 (2.20)

At this point, two questions naturally arise: (i) Why do terms growing like E^2 exactly cancel out from longitudinal vector boson scattering amplitudes? (ii) What makes the four neutral-channel system $W_L^+W_L^-$, $(1/\sqrt{2})Z_LZ_L$, $(1/\sqrt{2})HH$, and HZ_L , so special and so simple, compared to other two-body neutral channels? The answer to these questions can be found in the Goldstone boson equivalence theorem, which relates amplitudes for absorption and emission of longitudinal vector bosons, to amplitudes for absorption and emission of the corresponding eaten Goldstone bosons. This will be the subject of the next section.

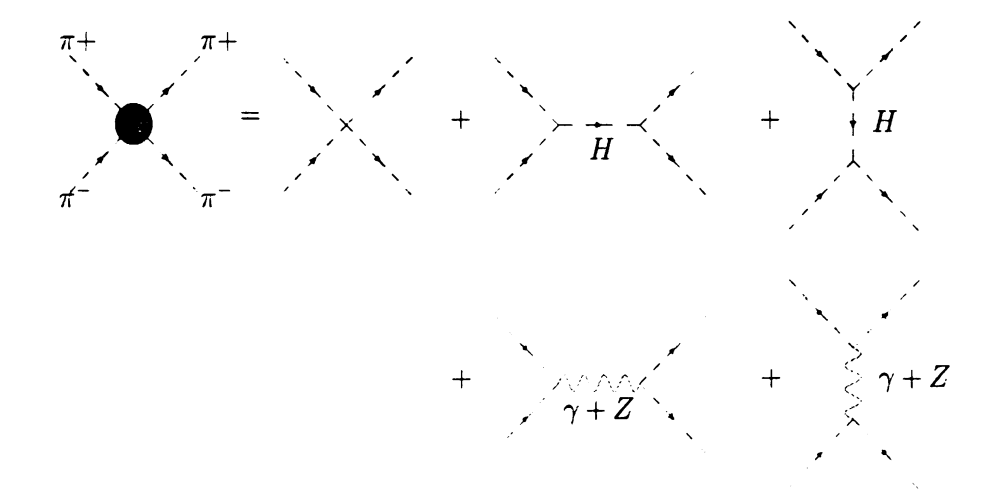


Figure 2.5: Tree-level diagrams for the $\pi^+\pi^- \to \pi^+\pi^-$ scattering, in the SM.

2.3 Unitarity and the Equivalence Theorem

Consider the $\pi^+\pi^-\to\pi^+\pi^-$ scattering in the SM, where π^\pm are the Goldstone bosons eaten by the W^\pm boson. At tree level there are seven diagrams, which are shown in Fig. 2.5. For $s, m_H^2 \gg m_W^2, m_Z^2$, the interactions from the Higgs sector are dominant, because the corresponding couplings are enhanced by a factor m_H^2/m_W^2 . Therefore, the amplitude is approximately given by the first three diagrams. In a general R_ξ gauge, and ignoring the Goldstone boson masses, we obtain

$$M(\pi^+\pi^- \to \pi^+\pi^-) \simeq -\frac{g^2}{4} \frac{m_H^2}{m_W^2} \left[\frac{s}{s - m_H^2} + \frac{t}{t - m_H^2} \right] ,$$
 (2.21)

in agreement with (2.15). This is an expected result. In fact, the Goldstone boson equivalence theorem tells us that the amplitudes for absorption or emission of a longitudinal gauge boson approach, at high energies, the same amplitudes with the gauge boson replaced by its eaten Goldstone boson [9] [11] [13] [14] [15] [16] [17] [18] [19].

We are therefore in a position to answer the two questions posed at the end of sec. 2.2. (i) The cancellation of the terms growing like $(E/m_W)^2$ occurs because at high energy longitudinal gauge boson scattering amplitudes become identical to Goldstone boson scattering amplitudes. These cannot steadily grow with energy, as a simple power counting shows. In fact, in a general R_{ξ} gauge, gauge boson propagators

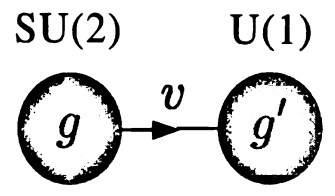


Figure 2.6: Moose diagram for the GWS model with the Higgs boson integrated out.

fall off with energy, and – working in a linear representation of the gauge group – the coupling with the Goldstone bosons involves only one power of momentum. Then gauge boson exchange amplitudes approach a constant value, of order g^2 . In the Higgs sector, the coupling Higgs-Goldstone does not depend on momentum, thus the Higgs exchanges fall off with energy, for $\sqrt{s} \gg m_H$. Therefore, as the energy increases, only the contact interaction – which is constant, and of order $g^2 m_H^2 / m_W^2$ – becomes relevant. (ii) The four channels $W_L^+ W_L^-$, $(1/\sqrt{2})Z_L Z_L$, $(1/\sqrt{2})HH$, and HZ_L have a simple eigenchannel structure because they correspond, via the equivalence theorem, to the Higgs-sector neutral channels: $\pi^+\pi^-$, $(1/\sqrt{2})\pi^0\pi^0$, $(1/\sqrt{2})HH$, and $H\pi^0$, where π^0 is the Goldstone boson eaten by the Z. The simplicity of the scattering matrix (2.19) is then a consequence of the underlying global symmetries of the Higgs sector.

Of course the equivalence theorem by itself is not enough to guarantee the cancellation of the terms growing like $(E/m_W)^2$: The key ingredient here is the Higgs boson. This has been shown explicitly in sec. 2.2, and can be seen also using the equivalence theorem. If we take the GWS model, and integrate out the Higgs boson, what is left is an $SU(2)_L \times SU(2)_R$ NLSM whose $SU(2)_L \times U(1)$ part is gauged. The corresponding moose diagram is shown in Fig. 2.6. At low external momenta, and before the gauge couplings are turned on, the Goldstone boson Lagrangian is

$$\mathcal{L}_{\text{Goldstone}} = \frac{v^2}{4} \text{Tr} \left[\partial^{\mu} \Sigma \partial_{\mu} \Sigma \right], \qquad (2.22)$$

where v is the SM VEV, and

$$\Sigma = \exp\left(i\pi^a \sigma^a/v\right). \tag{2.23}$$

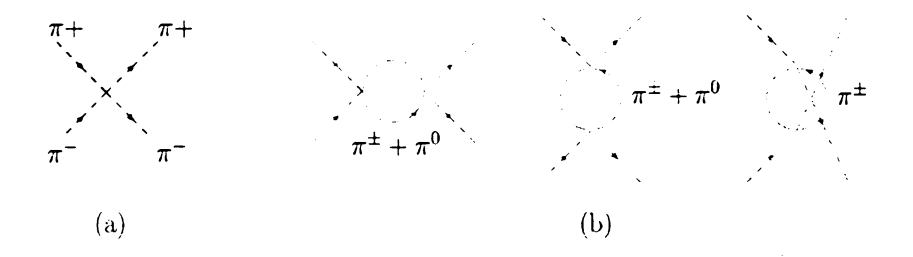


Figure 2.7: Diagrams for the $\pi^+\pi^- \to \pi^+\pi^-$ scattering in the SM without the Higgs boson: (a) Tree-level amplitude. (b) One-loop corrections.

The π^a 's are the usual SM Goldstone bosons, and the σ^a 's are the Pauli matrices. Expanding the exponential, the first non-zero interacting term is a quartic interaction:

$$\mathcal{L}^{(4)} = \frac{1}{6v^2} \Big[\left((\pi^+)^2 (\partial \pi^-)^2 + (\pi^-)^2 (\partial \pi^+)^2 - 2\pi^+ \pi^- (\partial \pi^+) (\partial \pi^-) \right) - 2 \left((\partial \pi^+) (\partial \pi^-) (\pi^0)^2 + \pi^+ \pi^- (\partial \pi^0)^2 - (\partial \pi^+) \pi^- (\partial \pi^0) \pi^0 \right) \Big].$$
 (2.24)

The tree-level $\pi^+\pi^- \to \pi^+\pi^-$ scattering is only given by a contact interaction, Fig.2.7(a). The corresponding amplitude is

$$M(\pi^{+}\pi^{-} \to \pi^{+}\pi^{-}) = -\frac{u}{v^{2}}$$

= $g^{2}\frac{1+\cos\theta}{2}\left(\frac{E}{m_{W}}\right)^{2}$, (2.25)

in agreement with the leading term of (2.11): The equivalence theorem still works. But the term growing like $(E/m_W)^2$ does not cancel. The difference, with the Higgs sector of the SM, is in the couplings, which involve derivatives of the Goldstone fields, and thus the external momenta. This happens because a model with only Goldstone bosons and no physical scalars is necessarily in a non linear realization of the symmetry group. Then the Lagrangian can only be built out of derivative terms, because terms without derivatives vanish. Therefore, in an $SU(2)\times U(1)$ gauge theory the Higgs boson is a necessary ingredient for unitarity.

This example sheds some light on the connection between unitarity violation and non-renormalizability. As the tree-level amplitude grows like E^2 , the one-loop corrections, Fig.2.7(b), grow like E^4 , by simple power counting. Then, at the unitarity

violation scale the loop corrections become as important as the leading order contribution, and the perturbative expansion breaks down. Moreover, as the external momenta grow, higher order terms must be added to (2.22), and new terms in the expansion of the Σ field must be considered, because they cease to be negligible. Thus, as the energy increases, the non renormalizable operators become important. Above the unitarity violation scale a new theory must take over. Such theory must reproduce the low-energy physics of the SU(3)_{color} \times SU(2)_L \times U(1) model, and restore unitarity, or delay unitarity violation to higher energy scales.

Chapter 3

Unitarity without the Higgs Boson

The non-linearly realized $SU(2)_{L} \times U(1)_{Y}$ gauge theory has been shown to violate unitarity of longitudinal gauge boson scattering amplitudes at few TeV's. In order to restore unitarity, or delay unitarity violation to higher energy scales, new particles must come into play, and mediate interactions which cancel the bad high energy behavior. In the SM, the Higgs boson suffices to restore unitarity at (almost) all energies. Recently, models with one compactified extra-dimension have been shown to violate unitarity at energy scales higher than the customary limit of Dicus-Mathur or Lee-Quigg-Thacker. The violation delay is mediated by a tower of massive gauge bosons, rather than a scalar particle.

In this chapter the physics of one compactified extra-dimension is introduced and discussed. From a four-dimensional standpoint, the extra-dimensional compactification breaks a countable infinity of gauge symmetries, with a corresponding generation of towers of Goldstone bosons and massive gauge bosons. The residual gauge symmetry can be further broken by an appropriate choice of BCs. Gauge symmetry breaking via compactification and BCs is shown to be *soft* (spontaneous), rather than *hard* (explicit), for all BCs consistent with the variational principle. Deconstructed models, where the extra-dimension is put on a lattice, and models from theory space are introduced as viable alternatives.

3.1 Compactified Extra-Dimension

The structure of our universe may be larger than the ordinary space-time four dimensions. There might be a compactified spatial extra-dimension, substantially larger than the Planck scale, but small enough to elude detection in the past generation of hadron and linear colliders [21] [22] [23] [24] [25] [26] [27] [28] [29] [30] [31] [32]. Being compact, the fifth-dimension is usually taken to be an interval. For instance, a circular fifth-dimension of radius R can be mapped onto a $[0, 2\pi R]$ interval with periodic BCs. As a second example, if a Z_2 symmetry is imposed on the circle, the fifth-dimension can be conveniently represented on a $[0, \pi R]$ interval, with BCs which follow from the field transformations under Z_2 .

In order to maintain generality, it is therefore convenient to specify a gauge theory on a $[0, \pi R]$ interval, where R is an arbitrary length, and derive the most general class of allowed BCs¹. For an arbitrary gauge group G, the action of a Yang-Mills theory on a flat background is

$$S_{\text{gauge}} = \int d^4x \int_0^{\pi R} dx^5 \left[-\frac{1}{4g_5^2} F_{MN}^a F^{aMN} - \frac{1}{2g_5^2 \xi} \left(\partial_\mu A^{a\mu} + \xi \partial_5 A^{a5} \right)^2 \right], \qquad (3.1)$$

where

$$F_{MN}^{a} = \partial_{M} A_{N}^{a} - \partial_{N} A_{M}^{a} + f^{abc} A_{M}^{b} A_{M}^{c} . \tag{3.2}$$

Here a is the gauge index, f^{abc} the structure constants, and g_5 the five-dimensional gauge coupling, with mass dimension -1/2. Notice that with this normalization, the gauge fields have mass dimension 1, as in 4D. The five-dimensional coordinates are labeled by $M, N \in (\mu, 5)$, with $\mu \in (0, 1, 2, 3)$, and the metric tensor – assuming a flat background – is $G_{MN} = \text{diag}(1,-1,-1,-1,-1)$. The gauge-fixing term we have chosen explicitly violates the five-dimensional gauge invariance. However the latter is already broken by compactification, which forces the A^a_μ and A^a_5 fields to behave differently. It is therefore convenient to get rid of the $\partial_5 A^a_\mu \partial^\mu A^a_5$ mixing term from $F^a_{\mu 5} F^{a \mu 5}$, and the gauge-fixing term of (3.1) is especially designed for this purpose.

¹This and the next two sections follow closely the content of Ref. [36].

The variation of the action (3.1) leads to the equations of motion (EOM)

$$\partial_{M}F^{aM\nu} - f^{abc}F^{bM\nu}A^{c}_{M} + \frac{1}{\xi}\partial^{\nu}\partial^{\sigma}A^{a}_{\sigma} - \partial^{\nu}\partial_{5}A^{a}_{5} = 0 ,$$

$$\partial^{\sigma}F^{a}_{\sigma5} - f^{abc}F^{b}_{\sigma5}A^{c\sigma} + \partial_{5}\partial_{\sigma}A^{a\sigma} - \xi\partial_{5}^{2}A^{a}_{5} = 0 .$$

$$(3.3)$$

However the boundary pieces must vanish as well. This leads to the requirement

$$[F_{\nu 5}^{a} \delta A^{a\nu} + (\partial_{\sigma} A^{a\sigma} - \xi \partial_{5} A_{5}^{a}) \delta A_{5}^{a}]_{0}^{\pi R} = 0.$$
 (3.4)

Periodic BCs (with period πR) clearly satisfy (3.4). If the fields are not periodic, (3.4) implies that the equations

$$F_{\nu 5}^{a} \delta A^{a\nu} = 0 ,$$

$$(\partial_{\sigma} A^{a\sigma} - \xi \partial_{5} A_{5}^{a}) \delta A_{5}^{a} = 0$$

$$(3.5)$$

hold at $x^5 = 0$ and $x^5 = \pi R$. For instance, if the extra-dimension is a radius-R circle, and a Z_2 symmetry is imposed on the gauge fields [66] [67],

$$A_{\mu}^{a}(x, x^{5}) = A_{\mu}^{a}(x, -x^{5}) , \quad A_{5}^{a}(x, x^{5}) = -A_{5}^{a}(x, -x^{5}) ,$$
 (3.6)

the independent degrees of freedom lie on only one half of the circle, say, the upper half. Then the BCs on the $[0, \pi R]$ interval are

$$\left. \begin{array}{l} \partial_5 A^a_\mu = 0 \ , \\ A^a_5 = 0 \end{array} \right\} \ , \ x^5 = 0, \pi R \ .$$
(3.7)

It is not difficult to prove that (3.7) satisfies (3.5). However the requirement (3.5) allows for a broader set of BCs, even those which have no interpretation in terms of an orbifolded circle. There are three choices of BCs which respect the four-dimensional Lorentz invariance:

$$A^a_{\mu} = 0 \; , \; A^a_5 = \text{const.}$$
 (3.8)

$$A_{\mu}^{a}=0\ ,\ \partial_{5}A_{5}^{a}=0 \eqno (3.9)$$

$$F_{\mu 5}^a = 0 , A_5^a = \text{const.}$$
 (3.10)

Notice that the orbifold BCs (3.7) correspond to the choice (3.10), although the condition $F_{\mu 5}^a = 0$ is satisfied in a trivial way. In addition to (3.8)-(3.10), there are

also more interesting choices in which the sum of different terms in (3.5) vanish, rather than each individual term. We will return to this points later in this section.

Although the EOM (3.3) are uniquely determined by the principle of least action, the BCs are arbitrary, and correspond to different physical scenarios. An illuminating analogy is given by the physics of a vibrating rod. The wave equation governs the displacements inside the rod, but the BCs determine what kind of motion can actually take place. If both ends of the rod are fixed, the displacement at the boundaries is zero, which is analogous to $A^a_\mu = 0$ in the extra-dimensional model. However if only one end is fixed, the behavior at the loose end is governed by a non-trivial equation, which is analogous to $F^a_{\mu 5} = 0$.

We are interested in the four-dimensional implications of the five-dimensional theory. It is then convenient to expand the five-dimensional gauge fields in KK modes, that is, in eigenfunctions of $-\hat{p}_5^2 \equiv \partial_5^2$ satisfying the chosen BCs. For simplicity, we first consider BCs which do not depend on the gauge index a. Then we can write

$$A^{a}_{\mu}(x, x^{5}) = \sum_{n=0}^{\infty} f_{n}(x^{5}) A^{a}_{n\mu}(x) ,$$

$$A^{a}_{5}(x, x^{5}) = \sum_{n=0}^{\infty} \phi_{n}(x^{5}) \pi^{a}_{n}(x) ,$$
(3.11)

where x is a four-dimensional coordinate, and the expansion coefficients are obviously x-dependent. The eigenfunctions $f_n(x^5)$ and $\phi_n(x^5)$ satisfy the equations

$$f_n''(x^5) = -m_n^2 f_n(x^5) ,$$

$$\phi_n''(x^5) = -M_n^2 \phi_n(x^5) ,$$
(3.12)

and the BCs. These requirements determine m_n , M_n , $f_n(x^5)$, and $\phi_n(x^5)$ up to a normalization constant for the wavefunctions. A canonical normalization of the four-dimensional fields requires

$$\int_0^{\pi R} dx^5 f_n(x^5) f_m(x^5) = g_5^2 \delta_{nm} .$$

$$\int_0^{\pi R} dx^5 \phi_n(x^5) \phi_m(x^5) = g_5^2 \delta_{nm} . \tag{3.13}$$

Inserting (3.11) in the free part of the action (3.1), and using (3.12) and (3.13), leads

to

$$S_{\text{free}} = \sum_{n=0}^{\infty} \int d^4x \left[\frac{1}{2} A_{n\mu}^a \left(g^{\mu\nu} \partial^2 - \left(1 - \frac{1}{\xi} \right) \partial^{\mu} \partial^{\nu} + g^{\mu\nu} m_n^2 \right) A_{n\nu}^a + \frac{1}{2} (\partial_{\mu} \pi_n^a)^2 - \frac{1}{2} \xi M_n^2 (\pi_n^a)^2 \right]. \tag{3.14}$$

This action describes a tower of mass- m_n gauge bosons, and a tower of mass- $\sqrt{\xi}M_n$ Goldstone bosons. The Goldstone bosons can be removed from (3.14) by going to unitary gauge, $\xi \to \infty$, except for the massless mode, if there is any. Since the natural size for the mass spacing is 1/R, as $R \to \infty$ all gauge boson masses go to zero. This shows that compactification – that is, the acquisition of a finite value for R – acts as a "geometrical" Higgs mechanism, which breaks a countable infinity of gauge symmetries, with consequent generation of a tower of massive gauge bosons, and a tower of eaten Goldstone bosons.

If the BCs on A_5^a are $\partial_5 A_5^a = 0$ on both ends, then the lowest KK mode in the expansion of A_5^a is a physical massless scalar field, π_0^a , in the adjoint representation of the gauge group. As we shall see later in this chapter, such field is not essential for unitarity. Moreover, it does not behave as a Higgs boson, because it does not have the appropriate quantum numbers. Therefore, in the following we will always impose BCs which do not allow for such massless state to exist.

3.2 Symmetry Breaking by Boundary Conditions

We have just seen that compactification is a symmetry-breaking mechanism. However compactification cannot break the symmetries which are localized on the fourdimensional branes. Therefore, if the gauge group G is unbroken on both branes, then the four-dimensional theory will be G-invariant, and the mass of the lowest KK mode will be zero, $m_0 = 0$. As an example, consider the gauge group SU(2), and impose the BCs

$$\left. \begin{array}{l} \partial_5 A_\mu^a = 0 \ , \\ A_5^a = 0 \end{array} \right\} \ , \ x^5 = 0, \pi R \ .$$
(3.15)

Notice that these are the orbifold BCs (3.7). Since only the derivative of $A^a_{\mu}(x, x^5)$ is fixed by (3.15), the gauge fields can have any value on the boundaries. This means that SU(2) is unbroken on both branes, and therefore also in the four-dimensional theory. The BCs on A^a_5 do not allow for a massless scalar, thus in unitary gauge we only have to consider A^a_{μ} . The solution of (3.12) for $f_n(x^5)$ is

$$f_n(x^5) = A_n \cos(m_n x^5) + B_n \sin(m_n x^5)$$
.

The BCs (3.15) imply $B_n = 0$ and $\sin(m_n \pi R) = 0$, whence

$$m_n = \frac{n}{R}$$
 , $n = 0, 1, 2, \dots$ (3.16)

As expected, there is a triplet of massless gauge bosons, due to the unbroken SU(2). Notice that the wavefunction of the massless fields is flat, which means that the corresponding particles have equal probability of being anywhere, in the extra-dimensional interval.

A more interesting case is when only a subgroup of G is unbroken on the two branes. Then the four-dimensional theory will not be invariant under the full group G, but only under the subgroup which is unbroken on both branes. In other words, BCs can be used to break four-dimensional gauge symmetries. In order to better understand this concept, we consider three examples of symmetry breaking via BCs.

(1) G=SU(2), and BCs breaking SU(2) down to U(1) at one end of the interval:

$$\left.\begin{array}{l}
\partial_{5}A_{\mu}^{a}=0,\\ A_{5}^{a}=0\end{array}\right\}, x^{5}=0 \qquad \left.\begin{array}{l}
A_{\mu}^{1,2}=0, \ \partial_{5}A_{\mu}^{3}=0,\\ \partial_{5}A_{5}^{1,2}=0, \ A_{5}^{3}=0\end{array}\right\}, x^{5}=\pi R.$$
(3.17)

These BCs can be seen as deriving from a $Z_2 \times Z_2$ orbifold on a radius-2R circle,

$$A_{\mu}(x, -x^{5}) = A_{\mu}(x, x^{5}) .$$

$$A_{5}(x, -x^{5}) = -A_{5}(x, x^{5}) ,$$

$$A_{\mu}(x, \pi R + x^{5}) = PA_{\mu}(x, \pi R - x^{5})P^{-1} ,$$

$$A_{5}(x, \pi R + x^{5}) = -PA_{5}(x, \pi R - x^{5})P^{-1} ,$$
(3.18)

where P = diag(1, -1) is the orbifold projection operator. The BCs (3.17) do not allow for a massless scalar, thus in unitary gauge $A_5^a \equiv 0$, and we can focus on the four-dimensional components only.

There are two different KK towers, one for the charged sector, and one for the neutral sector. The KK expansions are²

$$A^{\pm}_{\mu}(x, x^{5}) = \sum_{n=0}^{\infty} f_{n}(x^{5}) W^{\pm}_{n\mu}(x) ,$$

$$A^{3}_{\mu}(x, x^{5}) = \sum_{n=0}^{\infty} g_{n}(x^{5}) Z_{n\mu}(x) .$$
(3.19)

The eigenfunctions are as usual combinations of sines and cosines, and the BCs (3.17) lead to the mass equations.

$$\cos(m_n \pi R) = 0,$$

$$\sin(M_n \pi R) = 0,$$
(3.20)

Here and in the examples below m_n (M_n) is the mass of the *n*-th charged-boson (neutral-boson). The solutions are

$$m_n = \frac{n-1/2}{R}$$
 , $n = 1, 2, ...$, $M_n = \frac{n}{R}$, $n = 0, 1, 2 ...$ (3.21)

The lowest mode of the charged KK tower is a massive particle. However the lowest mode of the neutral tower is a massless particle: It is the massless gauge boson of the unbroken U(1) symmetry. Finally, the normalized wavefunctions are

$$f_n(x^5) = \sqrt{\frac{2g_5^2}{\pi R}} \cos(m_n x^5) ,$$

$$g_n(x^5) = \sqrt{\frac{2g_5^2}{\pi R}} \cos(M_n x^5) ,$$
(3.22)

which include the flat wavefunction of the massless neutral boson, $g_0(x^5) = \mathrm{const.}.$

²Here and in the following, the superscript "±" in A^{\pm} refers to the SU(2) linear combination $(A^1 \mp iA^2)/\sqrt{2}$.

(2) $G=SO(4)\sim SU(2)_L\times SU(2)_R$, and BCs breaking $SU(2)_R$ down to U(1) at one end of the interval, and SO(4) down to $SU(2)_{\rm diagonal}$ at the other end. In addition to the gauge fields A^a_{LM} and A^a_{RM} , it is convenient to define $A^a_{\pm M}$ by

$$A_{\pm M}^{a} \equiv \frac{A_{LM}^{a} \pm A_{RM}^{a}}{\sqrt{2}} \ . \tag{3.23}$$

Then the BCs read

$$\left. \begin{array}{l} \partial_{5}A_{L\mu}^{a} = 0 \; , \; A_{L5}^{a} = 0 \; , \\ A_{R\mu}^{1,2} = 0 \; , \; \partial_{5}A_{R5}^{1,2} = 0 \; , \\ \partial_{5}A_{R\mu}^{3} = 0 \; , \; A_{R5}^{3} = 0 \end{array} \right\} \; , \; x^{5} = 0 \qquad \left. \begin{array}{l} A_{-\mu}^{a} = 0 \; , \; \partial_{5}A_{-5}^{a} = 0 \; , \\ \partial_{5}A_{+\mu}^{a} = 0 \; , \; A_{+5}^{a} = 0 \end{array} \right\} \; , \; x^{5} = \pi R \; .$$

$$(3.24)$$

These BCs do not allow for a zero-mode scalar, thus in unitary gauge $A_{L5}^a \equiv A_{R5}^a \equiv 0$. As in example (1), there is a charged KK tower, and a neutral KK tower:

$$A_{L\mu}^{\pm}(x,x^{5}) = \sum_{n=0}^{\infty} f_{Ln}(x^{5}) W_{n\mu}^{\pm}(x) ,$$

$$A_{L\mu}^{3}(x,x^{5}) = \sum_{n=0}^{\infty} g_{Ln}(x^{5}) Z_{n\mu}(x) ,$$

$$A_{R\mu}^{\pm}(x,x^{5}) = \sum_{n=0}^{\infty} f_{Rn}(x^{5}) W_{n\mu}^{\pm}(x) ,$$

$$A_{R\mu}^{3}(x,x^{5}) = \sum_{n=0}^{\infty} g_{Rn}(x^{5}) Z_{n\mu}(x) .$$

$$(3.25)$$

The BCs (3.24) lead to the mass equations

$$\cos(2m_n\pi R) = 0,$$

$$\sin(2M_n\pi R) = 0.$$
(3.26)

The solutions are

$$m_n = \frac{n - 1/2}{2R}$$
 , $n = 1, 2, \dots$, $M_n = \frac{n}{2R}$, $n = 0, 1, 2 \dots$, (3.27)

and the normalized wavefunctions are

$$f_{Ln}(x^5) = \sqrt{\frac{g_5^2}{\pi R}} \cos(m_n x^5) ,$$

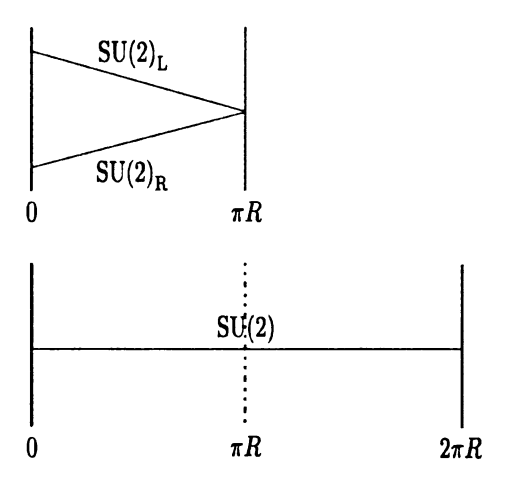


Figure 3.1: Equivalence between the $SO(4) \sim SU(2)_L \times SU(2)_R$ gauge theory on a five-dimensional interval, with SO(4) broken down to $SU(2)_{diagonal}$ at one end, and a single SU(2) with double interval length.

$$f_{Rn}(x^{5}) = \sqrt{\frac{g_{5}^{2}}{\pi R}} \cos\left(m_{n}(2\pi R - x^{5})\right) ,$$

$$g_{Ln}(x^{5}) = \sqrt{\frac{g_{5}^{2}}{\pi R}} \cos(M_{n}x^{5}) ,$$

$$g_{Rn}(x^{5}) = \sqrt{\frac{g_{5}^{2}}{\pi R}} \cos\left(M_{n}(2\pi R - x^{5})\right) .$$
(3.28)

Comparing (3.26)-(3.27) with (3.20)-(3.21), we observe that model (2) can be obtained from model (1) by replacing R with 2R. In fact the boundary πR acts as a mirror: The SU(2)_R wavefunctions are just the mirror images of the SU(2)_L wavefunctions, as a comparison between (3.28) and (3.22) shows explicitly. Then we arrive at the conclusion that an SU(2)_L×SU(2)_R gauge group in the bulk, with SU(2)_L×SU(2)_R broken down to SU(2)_{diagonal} at one end of the interval, is equivalent to a single SU(2) in a bulk with double interval length. This is schematically shown in Fig. 3.1.

(3) $G=SO(4)\times U(1)\sim SU(2)_L\times SU(2)_R\times U(1)$, BCs breaking $SU(2)_R\times U(1)$ to U(1) at one end of the interval, and SO(4) to $SU(2)_{diagonal}$ at the other end. Defining the

 A_{+}^{a} fields as in (3.23), the BCs are

$$\left. \begin{array}{l} \partial_{5}A_{L\mu}^{a} = 0 \; , \; A_{L5}^{a} = 0 \; , \\ A_{R\mu}^{1,2} = 0 \; , \; \partial_{5}A_{R5}^{1,2} = 0 \; , \\ A_{R\mu}^{3} - B_{\mu} = 0 \; , \; \partial_{5}(A_{R5}^{3} - B_{5}) = 0 \; , \\ \partial_{5}(g_{5}^{\prime 2}A_{R\mu}^{3} + g_{5}^{2}B_{\mu}) = 0 \; , \; g_{5}^{\prime 2}A_{R5}^{3} + g_{5}^{2}B_{5} = 0 \end{array} \right\} \; , \; x^{5} = 0 \; , \\ A_{-\mu}^{a} = 0 \; , \; \partial_{5}A_{-5}^{a} = 0 \; , \\ \partial_{5}A_{+\mu}^{a} = 0 \; , \; A_{+5}^{a} = 0 \; , \\ \partial_{5}B_{\mu} = 0 \; , \; B_{5} = 0 \; , \end{array} \right\} \; , \; x^{5} = \pi R \; . \tag{3.29}$$

Once again the gauge-field fifth components can be transformed away. As in models (1) and (2) there is a charged-boson KK tower, which is identical to the one of model (2), and a neutral-boson KK tower. The KK expansions are

$$A_{L\mu}^{\pm}(x,x^{5}) = \sum_{n=0}^{\infty} f_{Ln}(x^{5}) W_{n\mu}^{\pm}(x) ,$$

$$A_{L\mu}^{3}(x,x^{5}) = \sum_{n=0}^{\infty} g_{Ln}(x^{5}) Z_{n\mu}(x) ,$$

$$A_{R\mu}^{\pm}(x,x^{5}) = \sum_{n=0}^{\infty} f_{Rn}(x^{5}) W_{n\mu}^{\pm}(x) ,$$

$$A_{R\mu}^{3}(x,x^{5}) = \sum_{n=0}^{\infty} g_{Rn}(x^{5}) Z_{n\mu}(x) ,$$

$$B_{\mu}(x,x^{5}) = \sum_{n=0}^{\infty} h_{n}(x^{5}) Z_{n\mu}(x) .$$
(3.30)

The BCs (3.29) lead to the mass equations

$$\cos(2m_n\pi R) = 0,$$

$$\tan(M_n\pi R) = \sqrt{1 + \frac{2g_5'^2}{g_5^2}}.$$
(3.31)

The solutions are

$$m_n = \frac{n - 1/2}{2R} , n = 1, 2, \dots ,$$

$$M_n = \begin{cases} 0 & n = 0 \\ \frac{1}{2R} \left(\frac{2}{\pi} \arctan \sqrt{1 + 2g_5'^2/g_5^2} + n - 1 \right) & n = 1, 3, 5, \dots , \\ \frac{1}{2R} \left(-\frac{2}{\pi} \arctan \sqrt{1 + 2g_5'^2/g_5^2} + n \right) & n = 2, 4, 6, \dots \end{cases}$$
(3.32)

and the normalized wavefunctions are

$$f_{Ln}(x^{5}) = \frac{g_{5}}{\sqrt{\pi R}} \cos(m_{n}x^{5}) ,$$

$$f_{Rn}(x^{5}) = \frac{g_{5}}{\sqrt{\pi R}} \cos\left(m_{n}(2\pi R - x^{5})\right) ,$$

$$g_{L0}(x^{5}) = \frac{1}{\sqrt{\pi R}} \frac{g_{5}g_{5}'}{\sqrt{g_{5}^{2} + 2g_{5}'^{2}}} ,$$

$$g_{Ln}(x^{5}) = -\sqrt{\frac{2}{\pi R}} \frac{g_{5}^{2}}{\sqrt{g_{5}^{2} + 2g_{5}'^{2}}} \frac{\cos(M_{n}x^{5})}{2\cos(M_{n}\pi R)} , n \ge 1 ,$$

$$g_{R0}(x^{5}) = \frac{1}{\sqrt{\pi R}} \frac{g_{5}g_{5}'}{\sqrt{g_{5}^{2} + 2g_{5}'^{2}}} ,$$

$$g_{Rn}(x^{5}) = -\sqrt{\frac{2}{\pi R}} \frac{g_{5}^{2}}{\sqrt{g_{5}^{2} + 2g_{5}'^{2}}} \frac{\cos\left(M_{n}(2\pi R - x^{5})\right)}{2\cos(M_{n}\pi R)} , n \ge 1 ,$$

$$h_{0}(x^{5}) = \frac{1}{\sqrt{\pi R}} \frac{g_{5}g_{5}'}{\sqrt{g_{5}^{2} + 2g_{5}'^{2}}} ,$$

$$h_{n}(x^{5}) = \sqrt{\frac{2}{\pi R}} \frac{g_{5}g_{5}'}{\sqrt{g_{5}^{2} + 2g_{5}'^{2}}} \cos\left(M_{n}(\pi R - x^{5})\right) , n \ge 1 .$$

$$(3.33)$$

In all these examples there is an unbroken U(1) symmetry, and therefore a massless gauge boson. However, from a purely four-dimensional standpoint, it is not clear yet what symmetry is actually broken down to U(1). A better understanding can be achieved by putting the extra-dimensional interval on a lattice: The corresponding model will then be purely four-dimensional, with a larger symmetry group, but also with a clear symmetry breaking pattern. We will come back to this point in sec. 3.5. Also, we still have to show that symmetry breaking via compactification and BCs is soft (spontaneous), rather than hard (explicit). In other words, we must show that the symmetry-breaking mechanism preserves the special relation between gauge couplings which guarantees the cancellation of the energy-growing terms, in longitudinal gauge boson scattering amplitudes. This will be the subject of the next section.

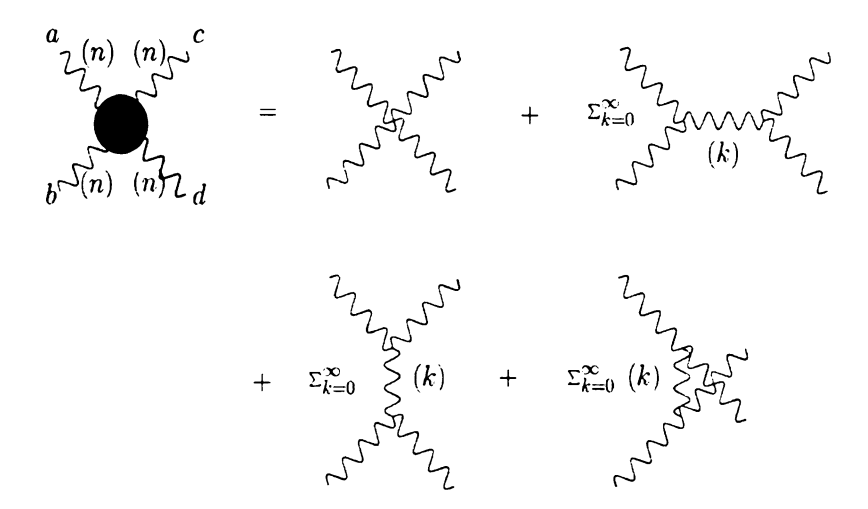


Figure 3.2: Diagrams contributing to the elastic scattering $A_n^a A_n^b \to A_n^c A_n^d$: Contact interaction plus s-channel, t-channel, and u-channel exchanges.

3.3 Unitarity in Extra-Dimension

In the last section we have seen that BCs may lead to different symmetry breaking patterns. We now want to show that symmetry breaking via compactification and BCs is soft. In other words, we want to show that the terms growing like E^4 and E^2 , in longitudinal gauge boson scattering amplitudes, exactly vanish when the BCs satisfy (3.5).

Let us consider the elastic scattering amplitude for the process $A_n^a A_n^b \to A_n^c A_n^d$. In general we expect four diagrams, as shown in Fig.3.2: The four-point interaction, plus s, t, and u exchanges of KK modes. We will assume that the external modes satisfy the same BCs, but we will not assume this for the exchanged modes. At high energy, the scattering amplitude can be expanded in powers of E/m_n , where m_n is the A_n^a mass:

$$M = M^{(4)} \left(\frac{E}{m_n}\right)^4 + M^{(2)} \left(\frac{E}{m_n}\right)^2 + M^{(0)} + \mathcal{O}\left((m_n/E)^2\right) . \tag{3.34}$$

It might seem inappropriate to formally expand the amplitude in powers of E/m_n , when for a given energy E there is an infinite number of exchanged KK modes whose mass is larger than E, and the series is potentially divergent. On the other hand,

imposing a sharp cutoff on the spectrum would explicitly break the gauge invariance. However such a hard breaking would have little effect on the scattering amplitudes, because the couplings with the heavy KK modes are suppressed. This can be seen by considering the higher-order gauge-invariant operators which result from integrating out the KK modes above a spectrum cutoff Λ . In D dimensions, an example of such operators is

$$\frac{1}{\Lambda^{6-D}}(F_{MN})^3 \,\,\,\,(3.35)$$

where we are still using the normalization of (3.1), with $-1/(4g_D^2)$ multiplying the kinetic term: Then $(F_{MN})^3$ has dimension 6, whence the Λ^{6-D} factor in the denominator of (3.35). Alternatively, we can see that this operator contains three gauge fields, so if it comes from loops of heavy KK modes it should contain three powers of the coupling in canonical normalization, and zero powers in the normalization of (3.1).

We would like to compare the contribution of the $(F_{MN})^3$ and $(F_{MN})^2$ operators to the $A_n^a A_n^b \to A_n^c A_n^d$ scattering amplitude. The ordinary $(F_{MN})^2$ operator gives a contribution of order

$$g_D^2(ER)^4$$
 . (3.36)

This can be seen from the four-point interaction: There are two powers of the coupling, and four polarization vectors, each carrying a power of $E/m_n \sim ER$.

The contribution of $(F_{MN})^3$ can potentially scale like E^6 . However this contribution comes from two factors of $\partial_{\mu}A_{\nu} - \partial_{\nu}A_{\mu}$ and two factors of the gauge fields. This implies that two of the polarization vectors appear in the combination $p_{\mu}\epsilon_{\nu} - p_{\nu}\epsilon_{\mu}$, which, after substitution in the scattering amplitude, turns out to give a contribution proportional to the mass of the external gauge bosons, rather than growing with energy. Therefore, the $(F_{MN})^3$ term gives a contribution of order

$$\frac{g_D^4}{\Lambda^{6-D}}E^2 \,, \tag{3.37}$$

where two powers of g_D come from the $\partial_{\mu}A_{\nu} - \partial_{\nu}A_{\mu}$ terms, and the remaining two powers come from the quadratic term. The ratio between the $(F_{MN})^3$ and $(F_{MN})^2$

contributions is

$$\frac{g_D^2}{\Lambda^{6-D}E^2R^4} \sim \frac{g_4^2}{(\Lambda R)^{6-D}(ER)^2} \,, \tag{3.38}$$

where we scaled g_D^2 as $g_4^2 R^{D-4}$. For $E \gg 1/R$, $\Lambda R > 1$, and D < 6, the contribution from the large-n KK modes is suppressed. This remains true also when the non-trivial cancellation of the $(ER)^4$ term in (3.36) is taken into account, as long as $\Lambda R > 1$ and D < 6. For a five-dimensional theory ΛR can be as large as $24\pi^3$ [68].

In practice we can therefore extend the series of virtual KK modes to infinity: It is just a simple way to preserve the gauge invariance. Then we obtain the following coefficients for the expansion (3.34):

$$M^{(4)} = i \left(g_{nnnn}^2 - \sum_{k} g_{nnk}^2 \right) \left[(3 + 6\cos\theta - \cos^2\theta) f^{abe} f^{cde} + 2(3 - \cos^2\theta) f^{ace} f^{bde} \right] , \qquad (3.39)$$

$$M^{(2)} = \frac{i}{m_n^2} f^{ace} f^{bde} \left(4g_{nnnn}^2 m_n^2 - 3\sum_{k} g_{nnk}^2 M_k^2 \right) - \frac{i}{2m_n^2} f^{abe} f^{cde} \left[4g_{nnnn}^2 m_n^2 - 3\sum_{k} g_{nnk}^2 M_k^2 + \left(12g_{nnnn}^2 m_n^2 + \sum_{k} g_{nnk}^2 (3m_k^2 - 16m_n^2) \right) \cos\theta \right] , \qquad (3.40)$$

where g_{nnn}^2 is the contact-interaction coupling, g_{nnk} is the coupling of the external modes to the k-th exchanged KK mode, and M_k is the mass of the k-th exchanged KK mode. Notice that the KK indices should be interpreted as double indices, including both KK and color index, e.g., $k \to (k,e)$. Since the external modes are assumed to satisfy the same BCs, the KK index n is color-blind. In the expression for $M^{(2)}$, the Jacobi identity on the structure constants has been used. This requires summations like $\sum_k g_{nnk}^{abe}$ or $\sum_k g_{nnk}^{abe} (M_k^e)^2$ to be independent of the color index e, which will be confirmed below.

If
$$g_{nnn}^2 = \sum_k g_{nnk}^2$$
, $M^{(4)}$ cancels, and $M^{(2)}$ becomes

$$M^{(2)} = \frac{i}{m_n^2} \left(4g_{nnnn}^2 m_n^2 - 3\sum_k g_{nnk}^2 M_k^2 \right) \left(f^{ace} f^{bde} - \sin^2 \frac{\theta}{2} f^{abe} f^{cde} \right) . \tag{3.41}$$

Therefore, the conditions for the cancellation of E^4 and E^2 terms are

$$g_{nnnn}^2 = \sum_{k} g_{nnk}^2 , \qquad (3.42)$$

$$4g_{nnn}^2 m_n^2 = 3\sum_k g_{nnk}^2 M_k^2 . (3.43)$$

In terms of the wavefunctions, the condition (3.42) reads

$$\int_0^{\pi R} dx_1^5 f_n^4(x_1^5) = \sum_k \int_0^{\pi R} dx_1^5 \int_0^{\pi R} dx_2^5 f_n^2(x_1^5) f_n^2(x_2^5) g_k(x_1^5) g_k(x_2^5) , \qquad (3.44)$$

where f_n and g_k are the wavefunctions of the external modes and the exchanged modes, respectively. This condition is indeed satisfied for any set of BCs which guarantee the hermiticity of the ∂_5^2 operator, because in such case the wavefunctions g_k satisfy the completeness relation $\sum_k g_k(y)g_k(z) = \delta(y-z)$, which immediately implies (3.44). The ∂_5^2 operator is hermitian for a large class of "mixed" BCs,

$$\partial_5 A^a_\mu(0,\pi R) = V^{ab}_{0,\pi R} A^b_\mu(0,\pi R) , \qquad (3.45)$$

where $V_{0,\pi R}^{ab}=0$ corresponds von Neumann BCs , and $V_{0,\pi R}^{ab}=\infty$ corresponds Dirichlet BCs. The BCs (3.8)-(3.10) are indeed either of the Dirichlet or the von Neumann type.³

Since (3.42) is satisfied, the condition for the cancellation of the E^2 terms is (3.43), or, in terms of the wavefunctions,

$$3\sum_{k}M_{k}^{2}\int_{0}^{\pi R}dx_{1}^{5}\int_{0}^{\pi R}dx_{2}^{5}f_{n}^{2}(x_{1}^{5})f_{n}^{2}(x_{2}^{5})g_{k}(x_{1}^{5})g_{k}(x_{2}^{5}) = 4m_{n}^{2}\int_{0}^{\pi R}dx_{1}^{5}f_{n}^{4}(x_{1}^{5}).$$

$$(3.46)$$

Using the equations of motion $\partial_5^2 f_n = -m_n^2 f_n$ and $\partial_5^2 g_k = -M_k^2 g_k$, integrating by parts, and using the completeness relation, it is not difficult to show that (3.46) is satisfied up to contact terms like $[f_n^3 f_n']_0^{\pi R}$, $[f_n^2 g_k']_0^{\pi R}$, and $[f_n f_n' g_k]_0^{\pi R}$, which vanish for Dirichlet or von Neumann BCs. Therefore, we arrive at the conclusion that the BCs (3.8)-(3.10) guarantee the cancellation of both E^4 and E^2 terms in longitudinal gauge boson scattering amplitudes. Notice that mixed BCs, eq. (3.45), only insure

³Notice that (3.10) is a von Neumann BC in unitary gauge, $A_5^a \equiv 0$, or for A_5^a vanishing on the boundaries.

the cancellation of the E^4 terms, but the E^2 terms are in general non-zero. In fact mixed BCs can be obtained by including brane mass terms for the gauge fields, which explicitly break the gauge invariance. A brane localized Higgs field would then be necessary to cancel the bad high energy behavior.

The cancellation of the E^4 and E^2 terms delays unitarity violation to higher energy scales rather than restoring unitarity at all energies. In fact even after the cancellation there is still a logarithmic growth in the partial wave amplitudes, which becomes more and more important as the number of the exchanged KK modes is allowed to increase. The high energy behavior will be analyzed in chapter 4 for a specific model of EWSB. However the scale of unitarity violation can be estimated by taking the extra-dimension to be infinite in size, because the high energy limit corresponds to distances short compared to the interval length. Then the only mass scale is $1/g_5^2$, and we therefore expect unitarity to be violated at energy scales of order $1/g_5^2$ times a numerical factor [34] [37] [38].

3.4 Unitarity and the KK Equivalence Theorem

In section 3.3 we have seen that the terms growing like E^4 and E^2 , in longitudinal gauge boson scattering amplitudes, exactly vanish for BCs consistent with the variational principle. This can be seen also by using the Goldstone boson equivalence theorem. In a five-dimensional theory the Goldstone bosons are the KK excitations of the gauge field fifth component. This interacts with the four-dimensional components via cubic and quartic terms in the action (3.1):

$$S_{\text{gauge}} \supset \int d^4x \int_0^{\pi R} dx^5 \left[-\frac{1}{2g_5^2} F_{\mu 5}^a F^{a \mu 5} \right]$$

$$\supset \int d^4x \int_0^{\pi R} dx^5 \left[f^{abc} \frac{1}{2g_5^2} \left(\partial_{\mu} A_5^a - \partial_5 A_{\mu}^a \right) A^{b\mu} A_5^c + \frac{1}{2g_5^2} f^{abc} f^{ade} A_{\mu}^b A_5^c A^{d\mu} A_5^e \right].$$
(3.47)

A quick dimensional analysis shows that the Goldstone boson scattering amplitudes cannot grow with energy, because each cubic vertex carries only one power of momentum.

However we have seen in section 3.3 that in longitudinal gauge boson scattering amplitudes the term growing like E^2 only cancels for BCs consistent with the variational principle. (While the term growing like E^4 cancels for a broader set of BCs.) On the other hand we have just seen that the Goldstone boson scattering amplitudes cannot grow like E^2 , by simply power counting. This again proves that symmetry breaking via BCs which are not consistent with with the variational principle is not soft, and the equivalence theorem does not apply.

It is not our intention to give here a proof of the KK equivalence theorem, but we want to show that the KK excitations of A_5^a behave properly as eaten Goldstone bosons when the gauge fields satisfy the BCs (3.8)-(3.10). In the action (3.1) the quadratic term mixing the μ -component with the 5-component is

$$S_{\text{mixing}}^{(2)} = \int d^4x \int_0^{\pi R} dx^5 \left[-\frac{1}{g_5^2} \partial_5 A^{a\mu} \partial_{\mu} A_5^a \right]$$
$$= -\frac{1}{g_5^2} \left[A^{a\mu} \partial_{\mu} A_5^a \right]_0^{\pi R} + \int d^4x \int_0^{\pi R} dx^5 \frac{1}{g_5^2} A^{a\mu} \partial_{\mu} \partial_5 A_5^a .$$

The contact terms vanish for BCs of the type (3.8)-(3.10), and the last term has the right form to be a gauge-Goldstone quadratic term. For simplicity, we consider BCs which do not depend on the gauge index a. Then, using the expansions (3.11) leads to

$$S_{\text{mixing}}^{(2)} = \sum_{m=0}^{\infty} \sum_{n=0}^{\infty} \int d^4x \int_0^{\pi R} dx^5 \frac{1}{g_5^2} f_m(x^5) A_m^{a\mu}(x) \phi_n'(x^5) \partial_\mu \pi_n^a(x) . \tag{3.48}$$

From this expression we find that the Goldstone boson $\tilde{\pi}_m^a$ eaten by the *m*-th gauge boson is a superposition of the mass eigenstates

$$\tilde{\pi}_{m}^{a} = \frac{1}{N_{m}} \int_{0}^{\pi R} dx^{5} \frac{1}{g_{5}^{2}} f_{m}(x^{5}) \partial_{5} A_{5}^{a}(x, x^{5})$$

$$= \frac{1}{N_{m}} \sum_{n=0}^{\infty} \left[\int_{0}^{\pi R} dx^{5} \frac{1}{g_{5}^{2}} f_{m}(x^{5}) \phi'_{n}(x^{5}) \right] \pi_{n}^{a}(x) , \qquad (3.49)$$

where the constant N_m is determined by requiring that $\tilde{\pi}_m^a$ is properly normalized, and is therefore given by

$$N_m = \sqrt{\sum_{n=0}^{\infty} \left[\int_0^{\pi R} dx^5 \frac{1}{g_5^2} f_m(x^5) \phi_n'(x^5) \right]^2} \ . \tag{3.50}$$

Then (3.48) gives a four-dimensional mixing Lagrangian

$$\mathcal{L}_{\text{mixing}}^{(2)} = \sum_{m=0}^{\infty} N_m A_m^{a\mu}(x) \partial_{\mu} \tilde{\pi}_m^a(x) , \qquad (3.51)$$

from which it is clear that $\tilde{\pi}_m^a$ beahves properly as an eaten Goldstone boson (giving tree-level vacuum polarization amplitudes with a transverse structure) only if N_m equals the mass of the m-th KK gauge boson,

$$N_m = m_m (3.52)$$

In order to prove (3.52) we start from the definition of N_m , eq. (3.50), which gives

$$N_{m}^{2} = \sum_{n=0}^{\infty} \int_{0}^{\pi R} dx^{5} \frac{1}{g_{5}^{2}} \int_{0}^{\pi R} dx'^{5} \frac{1}{g_{5}^{2}} f_{m}(x^{5}) f_{m}(x'^{5}) \phi'_{n}(x^{5}) \phi'_{n}(x'^{5})$$

$$= \sum_{n=0}^{\infty} \int_{0}^{\pi R} dx^{5} \frac{1}{g_{5}^{2}} \int_{0}^{\pi R} dx'^{5} \frac{1}{g_{5}^{2}} f'_{m}(x^{5}) f'_{m}(x'^{5}) \phi_{n}(x^{5}) \phi_{n}(x'^{5})$$

$$+ [f_{m} \phi_{n}]_{0}^{\pi R} \text{ terms} . \tag{3.53}$$

The contact terms are zero for gauge fields satisfying the BCs (3.8)-(3.10)⁴. Then, using the completeness relation

$$\sum_{n=0}^{\infty} \frac{1}{g_5^2} \phi_n(x^5) \phi_n(x^{\prime 5}) = \delta(x^5 - x^{\prime 5}) , \qquad (3.54)$$

which is valid for a broader set of BCs, (3.53) becomes

$$N_m^2 = \int_0^{\pi R} dx^5 \frac{1}{g_5^2} f_m'(x^5) f_m'(x'^5)$$

$$= \frac{1}{g_5^2} \left[f_m f_m' \right]_0^{\pi R} - \int_0^{\pi R} dx^5 \frac{1}{g_5^2} f_m(x^5) f_m''(x'^5) . \tag{3.55}$$

⁴Strictly speaking the BCs (3.10) involve a non-trivial dynamics on the boundaries, which requires a more detailed analysis. Here we only demand that (3.10) is trivially satisfied by the choice $\partial_5 A_\mu^a = 0$ and $A_5^a = 0$, in which case the contact terms in eq. (3.53) vanish.

The contact terms $\left[f_m f_m'\right]_0^{\pi R}$ are zero under the same conditions which guarantee that $\left[f_m \phi_n\right]_0^{\pi R} = 0$. Therefore, using the equation of motion (3.12) and the normalization condition (3.13) we obtain (3.52).

With these results, the KK equivalence theorem for the $A_n^a A_n^b \to A_n^c A_n^d$ elastic scattering reads

$$M(A_n^a A_n^b \to A_n^c A_n^d) = C_{\text{mod}} M(\tilde{\pi}_n^a \tilde{\pi}_n^b \to \tilde{\pi}_n^c \tilde{\pi}_n^d) + \mathcal{O}\left((m_n/E)^2\right) , \qquad (3.56)$$

where the radiative modification factor $C_{\text{mod}} = 1 + \mathcal{O}(\text{loop})$ arises only at one-loop level [15] [16] [17] [18] [19]. We have already noticed that in general the eaten Goldstone bosons are not mass eigenstates. For the $\tilde{\pi}_n^a$'s to be mass eigenstates, with the same masses m_n of the KK gauge bosons A_n^a (in Feynman-'t Hooft gauge), the condition

$$\phi_n'(x^5) = m_n f_n(x^5) \tag{3.57}$$

must be satisfied. For instance, this is true for the BCs of an orbifolded circle, eq. (3.7), because the corresponding gauge-boson and Goldstone-boson wavefunctions are cosines and sines, respectively, of the same argument [34].

3.5 Deconstructed Models

The KK expansion is a way to see five-dimensional gauge theories on an interval from a four-dimensional point of view. A different, purely four-dimensional approach is provided by deconstruction, in which the extra-dimensional interval is put on a regular lattice [39] [40] [41]. In the five-dimensional action

$$S = \int d^4x \int_0^{\pi R} dx^5 \left[-\frac{1}{4g_5^2} F_{MN}^a F^{aMN} \right]$$
$$= \int d^4x \int_0^{\pi R} dx^5 \left[-\frac{1}{4g_5^2} F_{\mu\nu}^a F^{a\mu\nu} - \frac{1}{2g_5^2} F_{\mu5}^a F^{a\mu5} \right]$$
(3.58)

the x^5 coordinate is replaced by a discrete index j, and the integral in dx^5 is replaced by a summation over j.

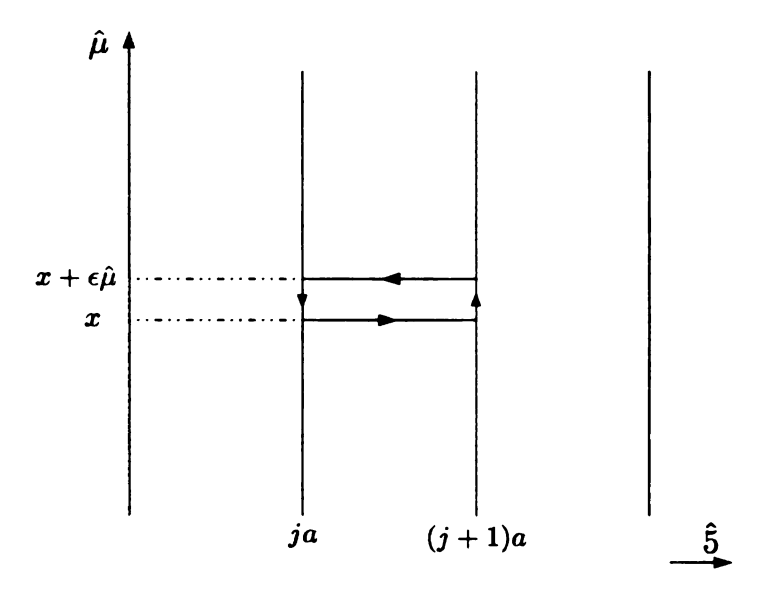


Figure 3.3: Rectangular Wilson loop in the $(\mu, 5)$ plane, with the fifth-dimensional interval on a lattice.

In order to evaluate $F_{\mu 5}$, we consider a rectangular Wilson loop in the $(\mu, 5)$ plane, as shown in Fig. 3.3. We denote the unitary link operator (or comparator) between the points (x_1, x_1^5) and (x_2, x_2^5) by $U(x_1, x_1^5|x_2, x_2^5)$, and the position in the latticized fifth dimension by ja, where $a \equiv \pi R/(N+1)$ is the lattice spacing, and N+2 is the number of points in the lattice (N internal plus the two endpoints). The U(X|Y) operator is defined by its transformation law under the gauge group,

$$U(X|Y) \to e^{i\alpha^a(X)G^a} U(X|Y)e^{-i\alpha^b(Y)G^b} , \qquad (3.59)$$

where the G^a 's are the group generators, and the $\alpha(X)^a$'s are the transformation parameters. (Here X and Y are points in the five-dimensional space.) Therefore, the trace of the unitary operator

$$U(x,ja) \equiv U(x,ja|x,(j+1)a) U(x,(j+1)a|x+\epsilon\hat{\mu},(j+1)a)$$

$$U(x+\epsilon\hat{\mu},(j+1)a|x+\epsilon\hat{\mu},ja) U(x+\epsilon\hat{\mu},ja|x,ja) , \qquad (3.60)$$

where $\hat{\mu}$ is a unit vector in the μ direction, is invariant under a gauge transformation. For $\epsilon \ll 1$, we can express the link $U(x, ja|x + \epsilon \hat{\mu}, ja)$ in terms of the gauge field μ -th component,

$$U(x, ja|x + \epsilon \hat{\mu}, ja) = e^{-i\epsilon A_{\mu} \left(x + \frac{\epsilon}{2}\hat{\mu}, ja\right) + \mathcal{O}(\epsilon^3)}, \tag{3.61}$$

where $A_{\mu} \equiv A_{\mu}^{a}G^{a}$. On the other hand, U(x,ja|x,(j+1)a) cannot be properly expressed in terms of A_{5} , because a is not an infinitesimal quantity. Then we define the $\Sigma_{j}(x)$ field by

$$\Sigma_j(x) \equiv U(x, ja|x, (j+1)a) . \tag{3.62}$$

Its transformation law can be derived directly from (3.59),

$$\Sigma_j(x) \to e^{i\alpha_j^a(x)G^a} \Sigma_j(x) e^{-i\alpha_{j+1}^b(x)G^b}$$
(3.63)

where $\alpha_j^a(x) \equiv \alpha^a(x, ja)$. (The "color" index a should not be confused with the lattice spacing a.) Expanding in powers of ϵ , the operator (3.60) becomes

$$U(x, ja) = 1 + \epsilon \Sigma_j(x) \left(D_\mu \Sigma_j(x) \right)^{\dagger} + \mathcal{O}(\epsilon^2) , \qquad (3.64)$$

where

$$D_{\mu}\Sigma_{j} = \partial_{\mu}\Sigma_{j} - iG^{a}A^{a}_{j-1\mu}\Sigma_{j} + i\Sigma_{j}G^{a}A^{a}_{j\mu} , \qquad (3.65)$$

and $A_{j\mu}(x) \equiv A_{\mu}(x,ja)$ is the gauge field corresponding to the j-th rotation, $\alpha_j(x) = \alpha(x,ja)$. $D_{\mu}\Sigma_j(x)$ is the covariant derivative of $\Sigma_j(x)$. In fact, from the transformation law of the five-dimensional gauge fields,

$$A_M^a(X)G^a \to e^{i\alpha^b(X)G^b} \left(A_M^a(X)G^a + i\partial_M \right) e^{-i\alpha^c(X)G^c},\tag{3.66}$$

it follows

$$A_{j\mu}^{a}(x)G^{a} \to e^{i\alpha_{j}^{b}(x)G^{b}} \left(A_{j\mu}^{a}(x)G^{a} + i\partial_{\mu} \right) e^{-i\alpha_{j}^{c}(x)G^{c}}, \tag{3.67}$$

and $D_{\mu}\Sigma_{j}(x)$ transforms like $\Sigma_{j}(x)$. Therefore, $\operatorname{Tr}\left((D_{\mu}\Sigma_{j}(x))^{\dagger}D^{\mu}\Sigma_{j}(x)\right)$ is invariant, and $D_{\mu}\Sigma_{j}(x)$ must be proportional to $F_{\mu 5}^{a}(x,ja)$, the deconstructed version of $F_{\mu 5}^{a}(x,x^{5})$. The proportionality factor can be found by letting a to be small, so that $\Sigma_{j}(x)$ can be expressed in terms of $A_{5}(X) \equiv A_{5}^{a}(X)G^{a}$:

$$\Sigma_j(x) \equiv U(x, ja|x, (j+1)a) = e^{-iaA_5(x, (j+\frac{1}{2})a)}.$$
 (3.68)

Expanding in a, and taking the ∂_{μ} -derivative, gives

$$F_{\mu 5}^{a}(x, ja) = \frac{i}{a} D_{\mu} \Sigma_{j}(x). \tag{3.69}$$

Therefore, replacing the integral over x^5 with a sum over j,

$$\int_0^{\pi R} dy \to \sum_{j=0}^{N+1} a,\tag{3.70}$$

the Lagrangian of a deconstructed five-dimensional gauge theory becomes

$$\mathcal{L} = -\frac{1}{4\tilde{g}^2} \sum_{j=0}^{N+1} F_{j\mu\nu}^a F_j^{a\mu\nu} + \frac{f^2}{4} \sum_{j=1}^{N+1} \text{Tr}\left((D_\mu \Sigma_j)^\dagger D^\mu \Sigma_j \right), \tag{3.71}$$

where $F^a_{j\mu\nu}$ is the field-strength tensor for the gauge field $A^a_{j\mu}$. The dimensionless four-dimensional gauge coupling \tilde{q} is

$$\tilde{g} = \frac{g_5}{\sqrt{a}} = \frac{g_5}{\sqrt{\pi R}} \sqrt{N+1},$$
 (3.72)

and the dimension-one f constant is

$$f = \frac{2}{g_5\sqrt{a}} = \frac{2}{g_5\sqrt{\pi R}}\sqrt{N+1} \tag{3.73}$$

Notice that both \tilde{g} and f grow like $\sqrt{N+1}$, but what really enters in the calculation of scattering amplitudes are the effective coupling $\tilde{g}/\sqrt{N+1}$ and the effective mass scale $f/\sqrt{N+1}$, which are independent on the number of sites.

This results prove what was claimed in chapter 1, namely that deconstructed fivedimensional gauge theories on a flat background are NLSMs with identical couplings and VEV's. The Σ_j field can be expressed in terms of the Goldstone boson fields:

$$\Sigma_j(x) = e^{2i\pi_j^a(x)G^a/f}. (3.74)$$

Comparing this equation with (3.68) we see that the Goldstone fields are related to the fifth component of the gauge field,

$$\pi_j^a(x) = -\frac{1}{g} A_5^a \left(x, (j + \frac{1}{2})a \right). \tag{3.75}$$

Therefore, in deconstruction the four-dimensional components of the gauge fields are taken at the lattice points, while the fifth component is taken between the points. This picture corresponds precisely to the circles and lines of a moose diagram.

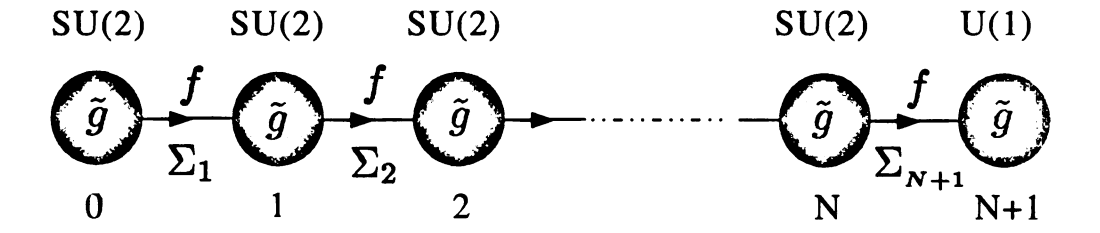


Figure 3.4: Moose diagram for the deconstructed SU(2) gauge theory on a five-dimensional interval, with BC's breaking SU(2) to U(1) at one end of the interval.

Notice that: (i) If the five-dimensional theory is invariant under a gauge group G, and BCs break G down to G_0 and G_1 , at $x^5 = 0$ and $x^5 = \pi R$, respectively, the corresponding deconstructed four-dimensional model is invariant under a larger gauge group, $G_0 \times G^N \times G_1$. (ii) In the five-dimensional theory spontaneous symmetry breaking is due to compactification, while in the four-dimensional deconstructed model spontaneous symmetry breaking is achieved through the Σ fields VEV, $\Sigma_j^0 = f \cdot 1$, where 1 is the identity operator. (iii) As the mechanism which leads to compactification is not explained in the five-dimensional model, and must be supplied by a UV completion of the theory, so the deconstructed model does not explain the origin of the VEV, and must be UV completed by a more fundamental theory whose low-energy content is described by the NLSM.

Deconstruction makes the symmetry breaking pattern more explicit. For example, a five-dimensional SU(2) gauge theory, with BCs which leave the symmetry unbroken on both branes, corresponds to an SU(2)^{N+2} gauge symmetry which is spontaneously broken to SU(2) by the Σ fields VEV. We now consider the three examples of section 3.2, with symmetry-breaking BCs, and deconstruct the corresponding five-dimensional theories.

(1) G=SU(2), and BCs breaking SU(2) down to U(1) at one end of the interval. The deconstructed model is an $SU(2)^{N+2}$ NLSM whose $SU(2)^{N+1} \times U(1)$ part is gauged, with the U(1) coupling identical to the $SU(2)^{N+1}$ coupling. With the BCs

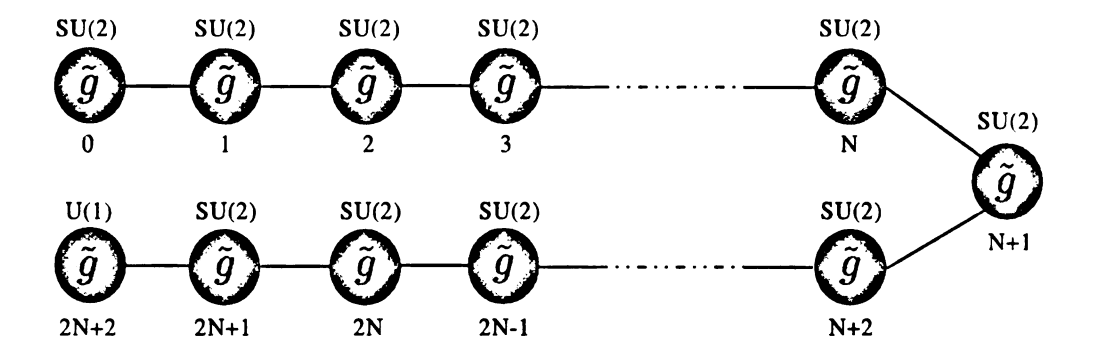


Figure 3.5: Moose diagram of the deconstructed $SU(2)_L \times SU(2)_R$ gauge theory on a five-dimensional interval, with BCs breaking $SU(2)_R$ to U(1) at one end of the interval and $SU(2)_L \times SU(2)_R$ to $SU(2)_{diagonal}$ at the other end. This model is just a single chain of SU(2) groups and a U(1) group.

 $A^{\pm}_{\mu}(\pi R) = 0$, from (3.65) we obtain, for $D_{\mu}\Sigma_{N+1}$, the expression

$$D_{\mu}\Sigma_{N+1} = \partial_{\mu}\Sigma_{N+1} - iG^{a}A_{N\mu}^{a}\Sigma_{N+1} + i\Sigma_{N+1}G^{3}A_{N+1\mu}^{3}, \qquad (3.76)$$

which shows how the U(1) group is embdded in the SU(2) structure, with the G^3 generator of SU(2) acting as the U(1) generator. The SU(2)^{N+1}×U(1) gauge symmetry is broken to U(1) by the Σ fields VEV. The moose diagram of this model is then shown in Fig. 3.4.

(2) $G=SO(4)\sim SU(2)_L\times SU(2)_R$, and BCs breaking $SU(2)_R$ to U(1) at one end of the interval, and SO(4) to $SU(2)_{diagonal}$ at the other end. The deconstructed model is described by two SU(2) moose diagrams, one for the $SU(2)_L$ group and one for the $SU(2)_R$ group, with the $SU(2)_{diagonal}$ site connecting the two chains. Therefore, the deconstructed model is an $SU(2)^{2N+3}$ NLSM whose $SU(2)^{2N+2}\times U(1)$ part is gauged, as shown in Fig. 3.5. It is then evident that this model is identical to model (1), with N replaced by 2N+1. The identity between these two models, which was demonstrated in section 3.2 by considering the mass spectrum and the wavefunctions, is even more explicit after deconstruction.

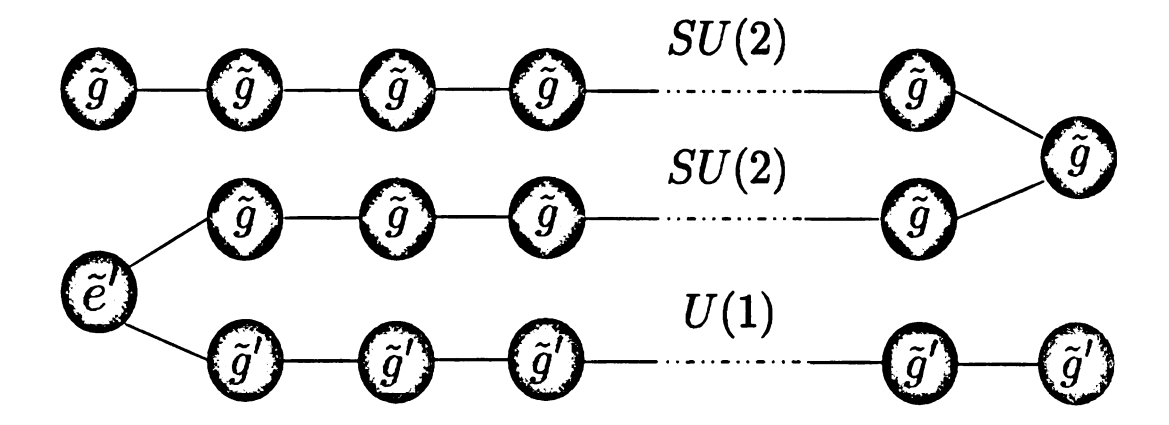


Figure 3.6: Moose diagram of the deconstructed $SU(2)_L \times SU(2)_R U(1)$ gauge theory on a five-dimensional interval, with BCs breaking $SU(2)_R \times U(1)$ to U(1) at one end of the interval and $SU(2)_L \times SU(2)_R$ to $SU(2)_{diagonal}$ at the other end.

(3) $G=\mathrm{SO}(4)\times\mathrm{U}(1)\sim\mathrm{SU}(2)_{\mathrm{L}}\times\mathrm{SU}(2)_{\mathrm{R}}\times\mathrm{U}(1)$, with BCs breaking $\mathrm{SU}(2)_{\mathrm{R}}\times\mathrm{U}(1)$ to $\mathrm{U}(1)$ at one end of the interval, and $\mathrm{SO}(4)$ to $\mathrm{SU}(2)_{\mathrm{diagonal}}$ at the other end. The deconstructed model is an $\mathrm{SU}(2)^{3N+4}$ NLSM whose $\mathrm{SU}(2)^{2N+2}\times\mathrm{U}(1)^{N+2}$ part is gauged. This gauge symmetry is then broken to $\mathrm{U}(1)$ by the Σ fields VEV. In this model there are three coupling constants: The coupling of the 2N+2 SU(2) groups, \tilde{g} , the coupling of N+1 U(1) groups, \tilde{g}' , and the coupling of the unbroken U(1) group on the $x^5=0$ boundary, $\tilde{e}\equiv\tilde{g}\tilde{g}'/\sqrt{\tilde{g}^2+2\tilde{g}'^2}$. The moose diagram is shown in Fig. 3.6.

Chapter 4

Higgsless Electroweak Symmetry Breaking

In chapter 3 we have seen that a gauge theory on an extra-dimensional interval has, from a four-dimensional point of view, an enhanced and spontaneously broken gauge symmetry, which postpones the unitarity violation of longitudinal gauge boson scattering amplitudes to energy scales higher than the customary limits of Dicus-Mathur or Lee-Quigg-Thacker [7] [10] [11] [12]. We have also seen that different choices of gauge group and BCs lead to different symmetry breaking patterns, in the four-dimensional theory.

In this chapter we will show that EWSB can be implemented in this framework. We will first consider an $SO(4)\times U(1)$ gauge theory in the bulk, with BCs breaking $SO(4)\sim SU(2)_L\times SU(2)_R$ to $SU(2)_{diagonal}$ at one end of the interval, and $SU(2)_R\times U(1)$ at the other end. This model will be briefly described in a flat background, where it proves to be inconsistent with EWP data, in a Randall-Sundrum warped backround, and with brane kinetic terms [69] [70]. A more minimal model is then introduced, with an SU(2) symmetry in the bulk, BCs breaking SU(2) to U(1) at one end, and brane kinetic terms. From a deconstructed viewpoint, this theory is an $SU(2)^{N+2}$ NLSM whose $SU(2)\times SU(2)^N\times U(1)$ part is gauged. We study the N=1, arbitrary N, and $N\to\infty$ models, with the latter corresponding to the extra-dimensional case.

4.1 Higgsless Models on a Warped Background

In section 3.2 we considered three examples of Yang-Mills theories on a flat extradimensional interval, with BCs breaking the gauge symmetry. Those models share some common features: First, the unbroken symmetry is U(1). Second, there is a charged-boson KK tower and a neutral-boson KK tower. Third, the lowest mode of the neutral tower is the massless gauge boson of the unbroken U(1) symmetry. In section 3.5 we considered the corresponding deconstructed versions. Each of them has a symmetry breaking pattern which contains $SU(2)\times U(1)\rightarrow U(1)$, and is therefore potentially a model of EWSB.

Model (1) has an SU(2) gauge symmetry in the bulk, with BCs breaking SU(2) to U(1) at one end of the extra-dimensional interval. We found that the mass of the lightest massive neutral boson is twice as large the mass of the lightest charged boson, and so they cannot be interpreted as the SM W and Z bosons. Therefore, model (1) has obviously no chance of being a realistic model of EWSB. Neither does model (2), which we saw being equivalent to model (1).

Model (3) has an $SO(4)\times U(1)$ gauge symmetry in the bulk, with BCs breaking $SO(4)\sim SU(2)_L\times SU(2)_R$ to $SU(2)_{diag}$ at one end of the interval, and $SU(2)_R\times U(1)$ to U(1) at the other end [36]. The mass of the KK modes are given by (3.32). For the lightest massive charged and neutral boson we have¹

$$m_{W_0} = \frac{1}{4R},$$

$$m_{Z_0} = \frac{1}{2R} \frac{2 \arctan \sqrt{1 + 2g_5'^2/g_5^2}}{\pi}.$$
(4.1)

Notice that for $g_5'=0$ we obtain $m_{W_0}=m_{Z_0}$, while for $0<2g_5'^2< g_5^2$ the neutral boson mass becomes slightly larger than the charged boson mass, as in the SM. To check whether this can be a realistic model of EWSB, we must also consider the heavy KK modes. For m_{W_1} and m_{Z_1} (3.32) gives

$$m_{W_1} = m_{W_0} + 2m_{W_0}$$

¹Here we substitute the KK index n of (3.32) with n-1, so that the lightest massive modes correspond to n=0, rather than n=1.

$$m_{Z_1} = m_{Z_0} + 2m_{W_0} . (4.2)$$

These values are very low, and can only be realistic if the fermion couplings with the heavy gauge bosons are suppressed.

In five dimensions the smallest irreducible representation of the Lorentz group is four-dimensional, thus our fundamental objects are Dirac spinors. In order to obtain a low-energy effective Lagrangian in agreement with the SM, we introduce two fermion SU(2) doublets, Ψ_L and Ψ_R , whose Lorentz-Dirac structures are

$$\Psi_L = \begin{pmatrix} \psi_L \\ \chi_L \end{pmatrix} , \Psi_R = \begin{pmatrix} \chi_R \\ \psi_R \end{pmatrix} .$$

To be more specific, ψ_L and χ_L (ψ_R and χ_R) are doublets under SU(2)_L (SU(2)_R), and singlets under SU(2)_R (SU(2)_L). The U(1) charge is chosen to be (B-L)/2 for both Ψ_L and Ψ_R , where B stands for baryon number, and L for lepton number. Then the five-dimensional Lagrangian for one generation (of quarks or leptons) is

$$\mathcal{L}_{\text{fermion}}^{(5)} = \bar{\Psi}_L i \Gamma^M \left(\partial_M - i A_{LM}^a T^a - i B_M \frac{B - L}{2} \right) \Psi_L + \bar{\Psi}_R i \Gamma^M \left(\partial_M - i A_{RM}^a T^a - i B_M \frac{B - L}{2} \right) \Psi_R . \tag{4.3}$$

The matrices $T^a \equiv \sigma^a/2$ are the SU(2) generators, where σ^a is the a-th Pauli matrix. The matrices Γ^M are the five-dimensional version of the four-dimensional γ^μ matrices, and are defined by $\Gamma^M = (\gamma^\mu, -i\gamma^5)$ [71]. In this Lagrangian we omitted the mass terms, which are not of our concern now.

Since the electroweak symmetry is unbroken on the $x^5=0$ brane, it is natural to try first with fermions which are strictly localized at $x^5=0$. Using the BCs (3.29) for the gauge fields, working in unitary gauge, (all gauge-field fifth components equal to zero), and imposing the BCs $\chi_L(x,0)=\chi_R(x,0)=0$ for the fermion fields², the fermion action becomes

$$S_{\text{fermion}} = \int d^4x \int_0^{\pi R} dx^5 \delta(x^5) \mathcal{L}_{\text{fermion}}^{(5)}$$
$$= \int_{x^5=0} d^4x \left[\bar{\psi}_L i \gamma^\mu \left(\partial_\mu - i A_{L\mu}^a T^a - i B_\mu \frac{B-L}{2} \right) \psi_L \right]$$

²Consistent BCs for fermion fields are discussed in Ref. [71].

$$+\bar{\psi}_{R}i\gamma^{\mu}\left(\partial_{\mu}-iB_{\mu}\left(T^{3}+\frac{B-L}{2}\right)\right)\psi_{R}\right]$$

$$=\int_{x^{5}=0}d^{4}x\left[\bar{\psi}_{L}i\gamma^{\mu}\left(\partial_{\mu}-iA_{L\mu}^{a}T^{a}-iB_{\mu}Y\right)\psi_{L}\right]$$

$$+\bar{\psi}_{R}i\gamma^{\mu}\left(\partial_{\mu}-iB_{\mu}Y\right)\psi_{R}\right]$$
(4.4)

where we used the SM relations $(B-L)/2 = Y_L$ and $T^3 + (B-L)/2 = Y_R$. Notice that Y_L is proportional to the 2×2 unit matrix, while Y_R is diagonal but not proportional to the unit matrix. Writing ψ_R in terms of its SU(2) components, $\psi_R = (u_R, d_R)$, we recognize in (4.4) the electroweak fermion Lagrangian, with the four-dimensional gauge fields replaced by the five-dimensional fields $A_{L\mu}^a$ and B_μ , taken at $x^5 = 0$.

In order to evaluate the effective couplings of the fermion fields with the KK gauge fields, we must substitute the expansions (3.30) in (4.4). The charged-current and neutral-current Lagrangians are

$$\mathcal{L}_{CC} = \sum_{n=0}^{\infty} \left[\frac{g_n^{CC}}{\sqrt{2}} \, \bar{\psi} \gamma^{\mu} P_L T^+ \psi \, W_{n\mu}^+ \right] + \text{h.c.} ,$$

$$\mathcal{L}_{NC} = \sum_{n=0}^{\infty} \left[\bar{\psi} \gamma^{\mu} \left(g_n^{NC} P_L T^3 + g_{Qn}^{NC} Q \right) \psi \, Z_{n\mu} \right] , \qquad (4.5)$$

where $\psi \equiv \psi_L + \psi_R$, $P_L \equiv (1 - \gamma^5)/2$ is the usual left-handed projection matrix, $T^{\pm} \equiv T^1 \pm i T^2$ are the isospin raising and lowering matrices, and $Q \equiv T^3 + Y$ is the charge matrix. The effective couplings are related to the W_n and Z_n wavefunctions at $x^5 = 0$:

$$g_n^{CC} = f_{Ln}(0) ,$$

 $g_n^{NC} = g_{Ln}(0) - h_n(0) ,$
 $g_{Qn}^{NC} = h_n(0) .$ (4.6)

From (3.33) we obtain

$$g_n^{CC} = \frac{g_5}{\sqrt{\pi R}},$$

$$g_n^{NC} = -\sqrt{\frac{2}{\pi R}} g_5 \sin(M_n \pi R) ,$$

$$g_{Qn}^{NC} = \sqrt{\frac{2}{\pi R}} \frac{g_5^{\prime 2}}{\sqrt{g_5^2 + 2g_5^{\prime 2}}} \cos(M_n \pi R) .$$
(4.7)

From these equations we notice that the fermion couplings with the heavy KK gauge bosons are not suppressed, relative to the couplings with W_0 and Z_0 . Therefore, the values (4.2) for the first heavy KK modes are well below the experimental lower bounds from the direct searches [72] [73].

In order for the extra-dimensional model to be realistic, m_{W_1} and m_{Z_1} must be heavier, and this can be achieved by replacing the flat background with a warped RS1 metric. The latter is given by

$$ds^{2} = e^{-2kx^{5}} \eta_{\mu\nu} dx^{\mu} dx^{\nu} - dx^{5} dx^{5} , \qquad (4.8)$$

where, as usual, $x^5 \in [0, \pi R]$, and k measures the AdS₅ curvature. With an exponential factor multiplying the Minkowskian metric, the EWSB scale and the Planck scale can be naturally embedded in the same model, for a factor $k\pi R$ of order $\log(M_{Planck}/\text{TeV}) \sim 30$ is sufficient to achieve the goal. The metric (4.8) is often written as

$$ds^{2} = \frac{1}{(kz)^{2}} \left[\eta_{\mu\nu} dx^{\mu} dx^{\nu} - (dz)^{2} \right] , \qquad (4.9)$$

where z is defined by

$$z \equiv \frac{1}{k} e^{kx^5} , \qquad (4.10)$$

and belongs to the interval

$$\left(z_h \equiv \frac{1}{k}\right) \le z \le \left(z_v \equiv \frac{e^{k\pi R}}{k}\right) ,$$
 (4.11)

where z_h^{-1} is of order of the Planck scale, and z_v^{-1} is in the TeV range. (The subscripts "h" and "v" stand respectively for hidden and visible.)

With the warped metric (4.9), the wavefunctions are superpositions of Bessel functions, rather than sines and cosines. Therefore, mass equations and normalization integrals become more complicated than in the flat-metric case [47]. For the gauge boson masses, a perturbative expansion in $1/\log(z_v/z_h)$ gives, to leading order,

$$m_W = \frac{1}{z_v} \frac{1}{\sqrt{\log\left(\frac{z_v}{z_h}\right)}},$$

$$m_Z = \sqrt{\frac{g_5^2 + 2g_5'^2}{g_5^2 + g_5'^2} \frac{1}{z_v} \frac{1}{\sqrt{\log\left(\frac{z_v}{z_h}\right)}}},$$
(4.12)

for the W and the Z boson, while numerical results show that the W_1 and Z_1 masses are around 1.2 TeV, heavy enough to have evaded detection at the Tevatron, but within the reach of the next generation of colliders.

4.2 Brane Kinetic Terms

The main motivation for using the AdS_5 geometry is of course the large hierarchy between the TeV scale and the Planck scale. However, since we are only interested in the EWSB scale, it is sufficient to consider an effective field theory where the high momentum modes – all the way down from the Planck scale to the TeV scale – are integrated out. In other words, for our purposes it is sufficient to consider an effective theory with a new hidden brane bounding the space at $z_v > a \gg z_h$, with the requirement for the new theory to reproduce the same physics from the point of view of an observer living at z > a [56] [57] [58]. The resulting five-dimensional model has still the same bulk and TeV brane Lagrangians, due to the conformal invariance, but new kinetic terms localized on the hidden brane. For example, for a free photon field the coefficient of the localized kinetic term runs like [57]

$$\frac{1}{e^2(a)} = \frac{1}{e^2(z_h)} + 2\log\left(\frac{a}{z_h}\right),\tag{4.13}$$

where $1/e^2(z_h)$ is the coefficient of the initial kinetic term localized on the Planck brane. If a large slice of AdS₅ is integrated out – that is, if $a/z_h \gg 1$ – the corresponding extra-dimensional interval will be approximately flat, as shown in Fig. 4.1, and the integrated-out region will generate large kinetic terms on the UV brane.

These results lead us to believe that the $SO(4) \times U(1)$ model with a flat background, and large kinetic terms on the brane where the electroweak symmetry is unbroken, can potentially be realistic. Of course a model like this is only an effective field theory with a cutoff in the TeV range, and an unknown UV completion. However this does

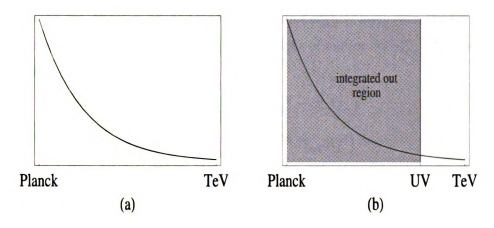


Figure 4.1: Background of a Randall-Sundrum model (a). The same model after integrating out a large slice of AdS₅ near the Planck brane (b). The new model has a smaller radius, an approximately flat background, and a large brane kinetic term on the UV brane.

not bother us. The corresponding action, for the gauge sector, is³

$$S_{\text{gauge}} = \int d^4x \int_0^{\pi R} dx^5 \left[-\frac{1}{4g_5^2} A_{LMN}^a A_L^{MN} - \frac{1}{4g_5^2} A_{RMN}^a A_R^{aMN} - \frac{1}{4g_5^2} B_{MN} B^{MN} - \frac{\delta(x^5)}{4g^2} A_{L\mu\nu}^a A_L^{a\mu\nu} - \frac{\delta(x^5)}{4g^2} B_{\mu\nu} B^{\mu\nu} \right],$$
 (4.14)

with the BCs

$$A^{\pm}_{R\mu}(0) = 0$$
, $A^3_{R\mu}(0) = B_{\mu}(0)$,
 $A^{\pm}_{-\mu}(\pi R) = 0$, $\partial_5 A^4_{+\mu}(\pi R) = 0$. (4.15)

From (4.15) we see that the last term could have been equally written as

$$-\frac{\delta(x^5)}{4q'^2}A_{R\mu\nu}^3A_R^{3\mu\nu}$$
.

This model was first introduced in Ref. [49]. Notice that the presence of δ -functions on the $x^5 = 0$ brane generates discontinuities in the ∂_5 -derivatives of the gauge fields.

³Here and in the following we omit the gauge-fixing terms. We always assume BCs which do not allow for a scalar zero mode, and work in unitary gauge, where all gauge-field fifth components are set to zero.

This can be seen by pushing the brane kinetic terms slightly away from the boundary, to make them part of the bulk. Then the equations of motion for $A^a_{L\mu}$, $A^3_{R\mu}$, and B_{μ} become

$$\frac{1}{g_{5}^{2}} \left(\partial^{\mu} A_{L\mu\nu}^{a} - \varepsilon^{abc} A_{L\mu\nu}^{b} A_{L}^{c\mu} - \partial_{5}^{2} A_{L\nu}^{a} \right)
+ \frac{1}{g^{2}} \delta(x^{5} - \epsilon) \left(\partial^{\mu} A_{L\mu\nu}^{a} - \varepsilon^{abc} A_{L\mu\nu}^{b} A_{L}^{c\mu} \right) = 0 ,
\frac{1}{g_{5}^{2}} \left(\partial^{\mu} A_{R\mu\nu}^{3} - \varepsilon^{3bc} A_{R\mu\nu}^{b} A_{R}^{c\mu} - \partial_{5}^{2} A_{R\nu}^{3} \right)
+ \frac{1}{g^{\prime 2}} \delta(x^{5} - \epsilon) \left(\partial^{\mu} A_{R\mu\nu}^{3} - \varepsilon^{3bc} A_{R\mu\nu}^{b} A_{R}^{c\mu} \right) = 0 ,
\frac{1}{g_{5}^{\prime 2}} \left(\partial^{\mu} B_{\mu\nu} - \partial_{5}^{2} B_{\nu} \right) + \frac{1}{g^{\prime 2}} \delta(x^{5} - \epsilon) \partial^{\mu} B_{\mu\nu} = 0 ,$$
(4.16)

where $0 < \epsilon \ll 1$, and ε^{abc} is the SU(2) antisymmetric tensor. An integration around the delta functions picks the discontinuity of $\partial_5 A_{L\mu}^a$, $\partial_5 A_{R\mu}^3$, and $\partial_5 B_{\mu}$:

$$-\frac{1}{g_{5}^{2}} [\partial_{5} A_{L\nu}^{a}]_{\epsilon_{-}}^{\epsilon^{+}} + \frac{1}{g^{2}} \left(\partial^{\mu} A_{L\mu\nu}^{a} - \varepsilon^{abc} A_{L\mu\nu}^{b} A_{L}^{c\mu} \right)_{\epsilon} = 0 ,$$

$$-\frac{1}{g_{5}^{2}} [\partial_{5} A_{R\nu}^{3}]_{\epsilon_{-}}^{\epsilon^{+}} + \frac{1}{g^{\prime 2}} \left(\partial^{\mu} A_{R\mu\nu}^{3} - \varepsilon^{3bc} A_{R\mu\nu}^{b} A_{R}^{c\mu} \right)_{\epsilon} = 0 ,$$

$$-\frac{1}{g_{5}^{\prime 2}} [\partial_{5} B_{\nu}]_{\epsilon_{-}}^{\epsilon^{+}} + \frac{1}{g^{\prime 2}} \left(\partial^{\mu} B_{\mu\nu} \right)_{\epsilon} = 0 .$$

$$(4.17)$$

With the brane terms as part of the bulk, the BCs $\partial_5 A_{L\mu}^a(0) = 0$ and $\partial_5 (g_5^{\prime 2} A_{R\mu}^3 + g_5^2 B_{\mu}(0)) = 0$ should be imposed, since these are the BCs which leave the electroweak symmetry unbroken on the $x^5 = 0$ boundary (see eq. (3.29)). Then, taking the limit $\epsilon \to 0$, and using the bulk equations of motion, (4.17) gives

$$\lim_{x^{5} \to 0^{+}} \left(\partial_{5}^{2} A_{L\mu}^{a} - \frac{g^{2}}{g_{5}^{2}} \partial_{5} A_{L\mu}^{a} \right) = 0 ,$$

$$\lim_{x^{5} \to 0^{+}} \left(\partial_{5}^{2} (A_{R\mu}^{3} + B_{\mu}) - \frac{g'^{2}}{g_{5}^{2} g_{5}'^{2}} \partial_{5} (g_{5}'^{2} A_{R\mu}^{3} + g_{5}^{2} B_{\mu}) \right) = 0 .$$
(4.18)

These equations, together with the BCs (4.15), give rise to non-trivial mass spectra, for both charged sector and neutral sector. We do not show here the solutions, since our focus will be on a simpler model, which will be introduced in the next section. However, it is clear that with a flat background the wavefunctions are superpositions of sines and cosines, rather than Bessel functions. This makes this class of models considerably simpler than the warped extra-dimension scenario.

4.3 A Minimal Higgsless Model

In section 4.2 we introduced an $SO(4)\times U(1)$ gauge theory on a flat extra-dimensional interval, with large localized kinetic terms on the brane where the electroweak symmetry is unbroken. The deconstructed model is represented by the moose diagram of Fig. 1.2 (a), where the couplings of the SU(2) and U(1) groups corresponding to $x^5 = 0$ are the gauge couplings of the brane fields. The same moose diagram can be unfolded to a single chain of SU(2) groups followed by a chain of U(1) groups, as shown in Fig. 1.2 (b).

A simpler model can be obtained by eliminating all U(1) sites, with the only exception of the first one, which corresponds to the U(1) gauge group on the $x^5=0$ brane. What is left is an $SU(2)^{N+2}$ NLSM whose $SU(2)\times SU(2)^N\times U(1)$ part is gauged, and the corresponding moose diagram is shown in Fig. 1.3. In this section we study the gauge sector of this model for N=1, arbitrary N, and $N\to\infty$, where the latter corresponds to the continuum limit [42]. We find the unitarity bounds of longitudinal gauge boson scattering amplitudes for each case, where our analysis is restricted to unitarity of the $W_L^+W_L^-\to W_L^+W_L^-$ scattering. We will work in tree-level approximation throughout the rest of this dissertation.

4.3.1 The $SU(2)_0 \times SU(2)_1 \times U(1)$ Model

We begin by studying the simplest Higgsless extension of the SM model, namely an $SU(2)_0 \times SU(2)_1 \times SU(2)_2$ NLSM whose $SU(2)_0 \times SU(2)_1 \times U(1)$ part is gauged. The corresponding moose diagram is shown in Fig. 4.2. The NLSM fields,

$$\Sigma_1(x) = e^{2i\pi_1^a(x)T^a/f_1}$$
 , $\Sigma_2(x) = e^{2i\pi_2^a(x)T^a/f_2}$ (4.19)

consist of two SU(2) triplets, which are coupled to the gauge fields by the covariant derivatives⁴

$$D_{\mu}\Sigma_{1} = \partial_{\mu}\Sigma_{1} - igT^{a}W^{a}_{0\mu}\Sigma_{1} + i\tilde{g}\Sigma_{1}T^{a}W^{a}_{1\mu} \ ,$$

⁴In this section and in the next one we will work in canonical normalization, where the coefficient of the gauge kinetic terms is -1/4.

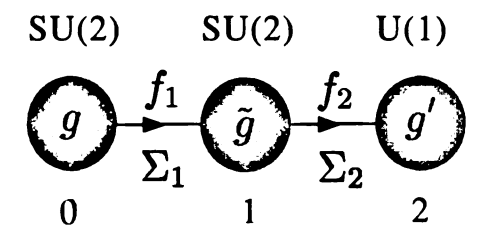


Figure 4.2: Moose diagram for a global $SU(2)_0 \times SU(2)_1 \times SU(2)_2$ NLSM whose $SU(2)_0 \times SU(2)_1 \times U(1)$ part is gauged. All parameters are taken to be independent quantities.

$$D_{\mu}\Sigma_{2} = \partial_{\mu}\Sigma_{2} - i\tilde{g}T^{a}W_{1\mu}^{a}\Sigma_{2} + ig'\Sigma_{2}T^{3}B_{\mu} . \tag{4.20}$$

Notice that, in order to maintain generality, we take the VEVs of the Σ fields to be independent parameters. The Lagrangian for this model is

$$\mathcal{L} = -\frac{1}{4} W_{0\mu\nu}^{a} W_{0}^{a\mu\nu} - \frac{1}{4} W_{1\mu\nu}^{a} W_{1}^{a\mu\nu} - \frac{1}{4} B_{\mu\nu} B^{\mu\nu}$$

$$+ \frac{f_{1}^{2}}{4} \text{Tr} \left((D_{\mu} \Sigma_{1})^{\dagger} D^{\mu} \Sigma_{1} \right) + \frac{f_{2}^{2}}{4} \text{Tr} \left((D_{\mu} \Sigma_{2})^{\dagger} D^{\mu} \Sigma_{2} \right) , \qquad (4.21)$$

where we only kept the lowest dimension opertors. After the Σ fields acquire the VEV, $<\Sigma_i>=1$, the $\mathrm{SU}(2)_0\times\mathrm{SU}(2)_1\times\mathrm{U}(1)$ gauge symmetry breaks down to U(1), and the last two terms in the Lagrangian become mass terms for the gauge fields. The mass spectrum consists of a neutral massless gauge boson, which will be identified with the photon, a tower of two charged gauge bosons, and a tower of two neutral gauge bosons. The light modes of these towers will be identified with the SM W and Z bosons. The heavy modes are two new particles, which will be denoted as W' and Z'.

There are overall five independent parameters: $g, \tilde{g}, g', f_1, f_2$. We can trade three of these for the electromagnetic coupling, e, and the W and Z boson masses, $m_{W'}$ and m_{Z} . The remaining two parameters can be expressed in terms of the W' and Z' masses, $m_{W'}$ and $m_{Z'}$. The gauge eigenstates, W_0^a , W_1^a , and B can be expanded in terms of the mass eigenstates. We have

$$W_0^{\pm} = a_{00}W^{\pm} + a_{01}W'^{\pm},$$

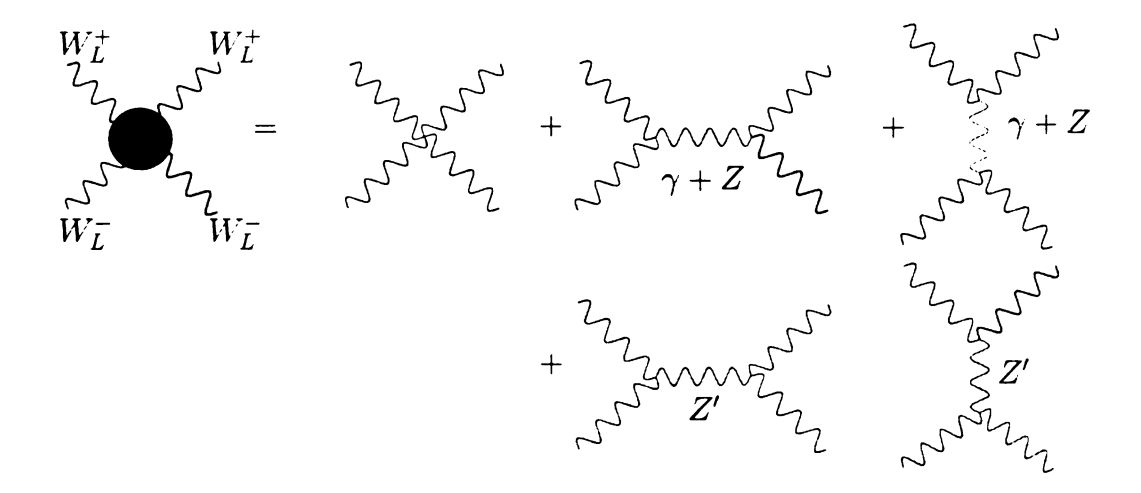


Figure 4.3: Tree-level diagrams for the $W_L^+W_L^- \to W_L^+W_L^-$ elastic scattering, in the $SU(2)_0 \times SU(2)_1 \times U(1)$ NLSM model.

$$W_1^{\pm} = a_{10}W^{\pm} + a_{11}W'^{\pm} , \qquad (4.22)$$

for the charged sector, and

$$W_0^3 = (e/g)A + b_{00}Z + b_{01}Z',$$

$$W_1^3 = (e/\tilde{g})A + b_{10}Z + b_{11}Z',$$

$$B = (e/g')A + b_{20}Z + b_{21}Z',$$
(4.23)

for the neutral sector. Formulas for the original parameters g, \tilde{g} , g', f_1 , f_2 , and the mixing matrices a_{jn} , b_{jn} , as functions of the physical parameters e, m_W , m_Z , $m_{W'}$, $m_{Z'}$, can be found in appendix A. Notice that the coefficients of the photon field are necessarily e/g, e/\tilde{g} , and e/g', because the photon is the gauge field of an unbroken symmetry, and must couple to the Σ fields (as well as to any other field) with its gauge coupling e. Inserting this result in the Lagrangian (4.21) gives

$$\frac{1}{e^2} = \frac{1}{g^2} + \frac{1}{\tilde{g}^2} + \frac{1}{g'^2} \ . \tag{4.24}$$

Having set up the model, we would like now to study the high energy behavior of longitudinal gauge boson scattering amplitudes, restricting our analysis to the

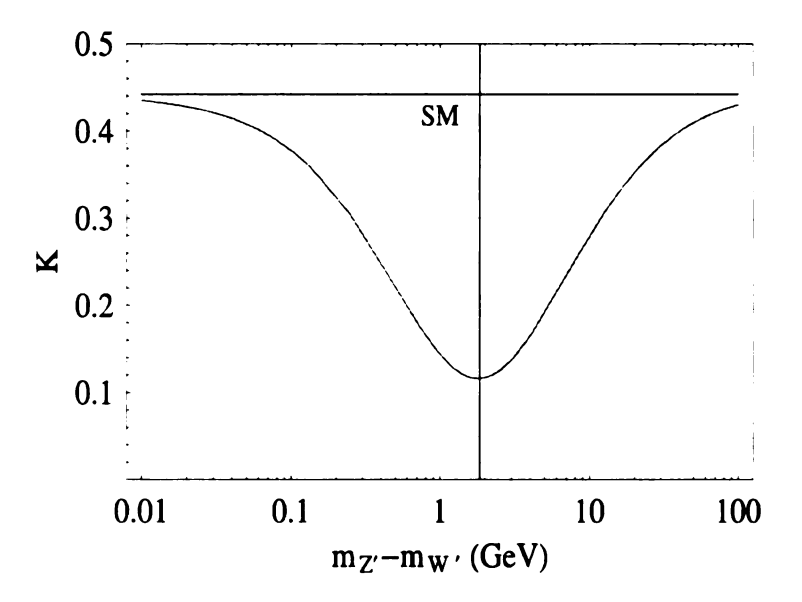


Figure 4.4: The coefficient of the $(E/m_W)^2$ term in the $W_L^+W_L^- \to W_L^+W_L^-$ scattering amplitude in the $\mathrm{SU}(2)_0\times\mathrm{SU}(2)_1\times\mathrm{U}(1)$ model (blue) as a function of the Z' and W' mass difference, with $m_{W'}=500$ GeV fixed. The same quantity in the SM without a Higgs boson (red) is also plotted. The vertical line indicates the position where $m_{Z'}^2 - m_{W'}^2 = m_Z^2 - m_{W'}^2$.

 $W_L^+W_L^- \to W_L^+W_L^-$ scattering. In addition to the SM exchanges of virtual photons and Z bosons, there are exchanges of virtual Z' bosons, in the s- and t-channel, as shown in Fig. 4.3. The amplitude is an easy generalization of (2.10):

$$M = \frac{g_{WWWW}^2}{m_W^4} \left[p^2 E^2 (-2 + 6\cos\theta) - E^4 \sin^2\theta \right]$$

$$+ \frac{1}{m_W^4} \left[\frac{e^2}{s} + \frac{g_{WWZ}^2}{s - m_Z^2} + \frac{g_{WWZ'}^2}{s - m_{Z'}^2} \right] \left(-4p^2 (p^2 - 3E^2)^2 \right) \cos\theta$$

$$+ \frac{1}{m_W^4} \left[\frac{e^2}{t} + \frac{g_{WWZ}^2}{t - m_Z^2} + \frac{g_{WWZ'}^2}{t - m_{Z'}^2} \right]$$

$$\times \left[-4E^2 \left(p^2 + (E^2 - 2p^2) \cos\theta \right)^2$$

$$-2p^2 (1 + \cos\theta) \left(2E^2 - p^2 - E^2 \cos\theta \right)^2 \right]. \tag{4.25}$$

The quartic and cubic couplings are obtained by inserting the expansions (4.22),

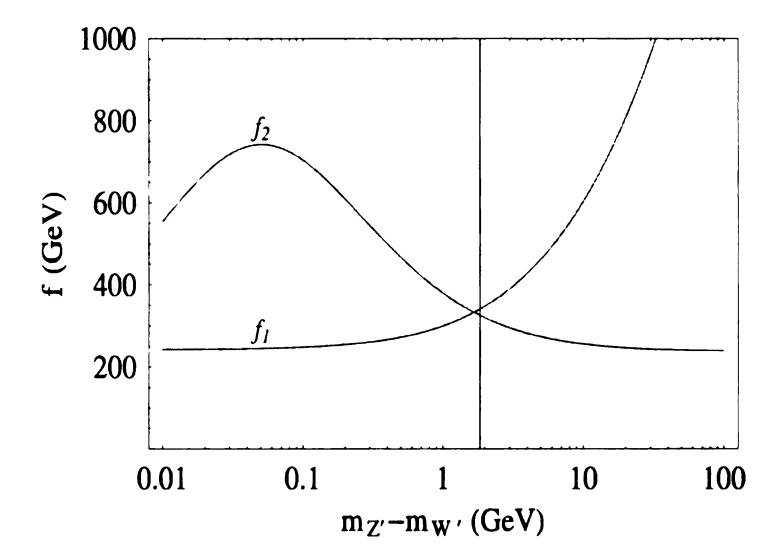


Figure 4.5: The quantities f_1 (blue) and f_2 (red) as a function of the Z' and W' mass difference, with $m_{W'} = 500$ GeV fixed. The vertical line indicates the position where $m_{Z'}^2 - m_{W'}^2 = m_Z^2 - m_{W'}^2$.

(4.23) into the gauge kinetic terms of the Lagrangian (4.21). This gives

$$\begin{array}{rcl} g_{WWZ} & = & g \; a_{00}^2 b_{00} + \tilde{g} \; a_{10}^2 b_{10} \; , \\ \\ g_{WWZ'} & = & g \; a_{00}^2 b_{01} + \tilde{g} \; a_{10}^2 b_{11} \; , \\ \\ g_{WWWW}^2 & = & g^2 \; a_{00}^4 + \tilde{g}^2 \; a_{10}^4 \; . \end{array} \tag{4.26}$$

At high energy the amplitude can be expanded in powers of E/m_W . The term proportional to $(E/m_W)^4$ exactly vanishes due to gauge invariance. The leading contribution is then proportional to $(E/m_W)^2$:

$$M = \left(\frac{E}{m_W}\right)^2 \frac{1 + \cos\theta}{2} K + \mathcal{O}\left((m_W/E)^0\right) , \qquad (4.27)$$

where

$$K = 4g_{WWWW}^2 - \frac{3}{m_W^2} \left(m_Z^2 g_{WWZ}^2 + m_{Z'}^2 g_{WWZ'}^2 \right) . \tag{4.28}$$

Using the formulae in appendix A, we can treat $K \equiv K(m_{W'}, m_{Z'})$ as a function of $m_{W'}$ and $m_{Z'}$.

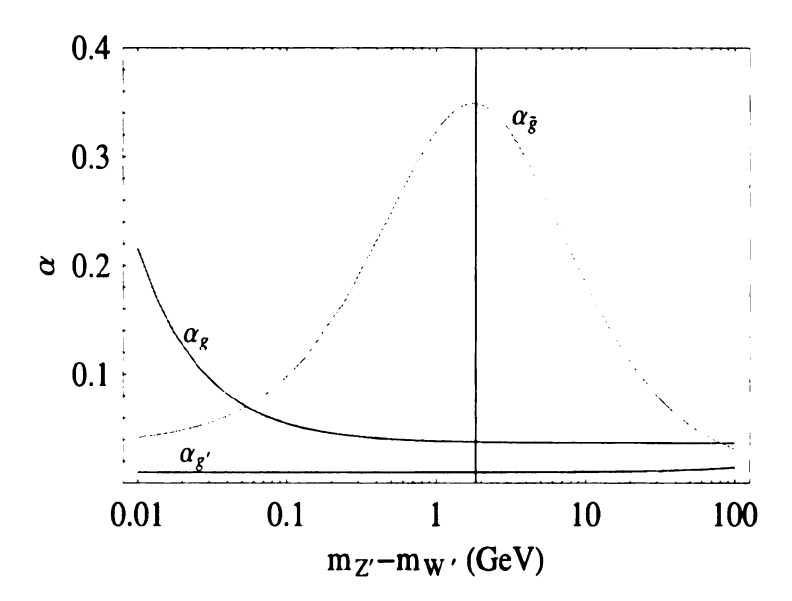


Figure 4.6: The coupling constants $\alpha_g = g^2/4\pi$ (blue), $\alpha_{g'} = g'^2/4\pi$ (red), and $\alpha_{\tilde{g}} = \tilde{g}^2/4\pi$ (green), as a function of the Z' and W' mass difference, with $m_{W'} = 500$ GeV fixed. The vertical line indicates the position where $m_{Z'}^2 - m_{W'}^2 = m_Z^2 - m_W^2$.

In Fig. 4.4 we plot K as a function of the mass difference, $m_{Z'} - m_{W'}$, for $m_{W'} = 500$ GeV fixed. As a comparison we also plot the same quantity in the SM without the Higgs boson. Notice that K is significantly suppressed for $m_{Z'}^2 - m_{W'}^2 \simeq m_Z^2 - m_W^2$. When this relation holds, the value of K is reduced by almost precisely a factor of 1/4, a result which does not depend on the particular value of $m_{W'}$. This indicates that the unitarity violation that occurs in the SM without the Higgs boson would be postponed to higher energy in this model.

We also plot in Fig. 4.5 the scales f_1 and f_2 , and in Fig. 4.6 the couplings constants $\alpha_g = g^2/4\pi$, $\alpha_{g'} = g'^2/4\pi$, and $\alpha_{\tilde{g}} = \tilde{g}^2/4\pi$, as a function of the Z' and W' mass difference, with $m_{W'} = 500$ GeV fixed. We notice that the relation $m_{Z'}^2 - m_{W'}^2 \simeq m_Z^2 - m_W^2$ also corresponds to $f_1 \simeq f_2$ and $\tilde{g} \gg g, g'$. In fact when this relation holds the couplings are given to a good approximation by $g = e/\sin\theta_W$, $g' = e/\cos\theta_W$, and $\tilde{g} = (m_{W'}/2m_W)g$, up to corrections of order $m_W^2/m_{W'}^2$. (We have used the tree level definition of $\cos\theta_W = m_W/m_Z$.) Thus, the SU(2)₀ and the U(1) act approximately

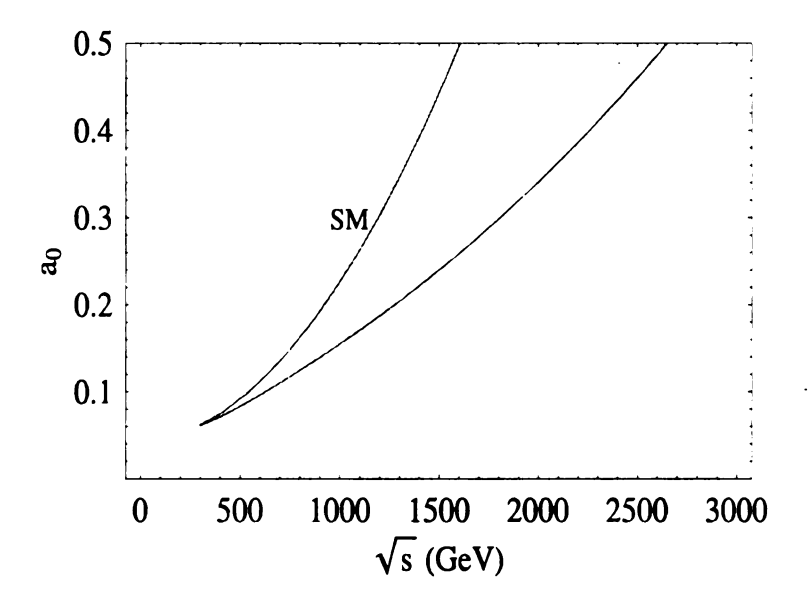


Figure 4.7: The J=0 partial wave amplitude as a function of \sqrt{s} for the SM without a Higgs boson (red) and the $SU(2)_0\times SU(2)_1\times U(1)$ model (blue) with $m_{W'}=500$ GeV and $m_{Z'}^2-m_{W'}^2=m_Z^2-m_W^2$.

like the $SU(2)_L$ and $U(1)_Y$ of the SM, while the intervening $SU(2)_1$ has the effect of softening the unitarity violation of the SM $W_L^+W_L^- \to W_L^+W_L^-$ scattering.

We can observe the effect of the delayed unitary violation by plotting the J=0 partial wave amplitude as a function of $\sqrt{s}=2E$. This is shown in Fig. 4.7 for both the SM without a Higgs boson and in the $SU(2)_0 \times SU(2)_1 \times U(1)$ model with $m_{W'}=500$ GeV and $m_{Z'}^2 - m_{W'}^2 = m_Z^2 - m_W^2$. Since unitarity requires $|\text{Re }a_0| < 1/2$, we can use this figure to infer that unitarity violation in this amplitude has been postponed from a scale of $\sqrt{s} \simeq 1.6$ TeV in the SM without a Higgs boson to $\sqrt{s} \simeq 2.65$ TeV in the $SU(2)_0 \times SU(2)_1 \times U(1)$ model with this choice of parameters.

We have found that the behavior of the $W_L^+W_L^- \to Z_LZ_L$ amplitude to be essentially identical to that for $W_L^+W_L^- \to W_L^+W_L^-$. In particular the corresponding value of K, the coefficient of the leading E^2/m_W^2 term in that amplitude, is reduced by the same factor of 1/4 when $m_{Z'}^2 - m_{W'}^2 \simeq m_Z^2 - m_W^2$.

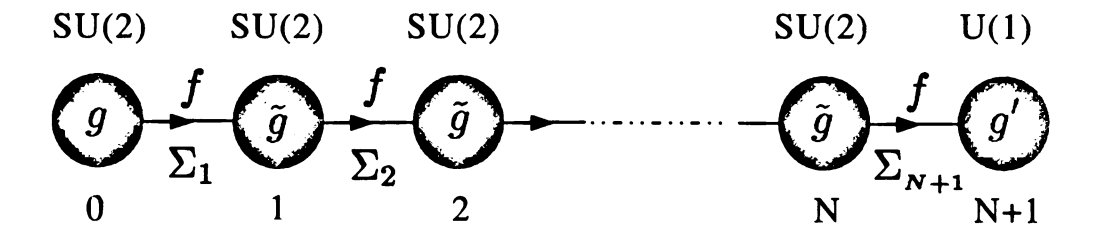


Figure 4.8: Moose diagram for the $SU(2) \times SU(2)^N \times U(1)$ Higgsless model.

4.3.2 The $SU(2)\times SU(2)^N\times U(1)$ Model

In section 4.3.1 we saw that the choice of parameters which produced the greatest postponement of unitarity led to a model where the SM $SU(2)_L$ and $U(1)_Y$ gauge groups were separated in TS by an extra intervening SU(2). Following the extra-dimensional analogue further, we now extend this to a series of intervening SU(2)'s, all with the same coupling and all VEVs chosen to be the same. The moose diagram for this theory is shown in Fig. 4.8.

The Lagrangian is

$$\mathcal{L} = -\frac{1}{4} W_{0\mu\nu}^{a} W_{0}^{\cdot a\mu\nu} - \frac{1}{4} \sum_{j=1}^{N} W_{j\mu\nu}^{a} W_{j}^{a\mu\nu} - \frac{1}{4} B_{\mu\nu} B^{\mu\nu} + \frac{f^{2}}{4} \sum_{j=1}^{N+1} \operatorname{tr} \left[(D_{\mu} \Sigma_{j})^{\dagger} D^{\mu} \Sigma_{j} \right], \qquad (4.29)$$

and the NLSM fields can be parameterized by

$$\Sigma_j = e^{2i\pi^a T^a/f} . (4.30)$$

The Σ_j 's are coupled to the gauge fields by the covariant derivatives

$$D_{\mu}\Sigma_{1} = \partial_{\mu}\Sigma_{1} - igT^{a}W_{0\mu}^{a}\Sigma_{1} + i\tilde{g}\Sigma_{1}T^{a}W_{1\mu}^{a} ,$$

$$D_{\mu}\Sigma_{j} = \partial_{\mu}\Sigma_{j} - i\tilde{g}T^{a}W_{j-1\mu}^{a}\Sigma_{j} + i\tilde{g}\Sigma_{j}T^{a}W_{j\mu}^{a} , \qquad (j = 2, ..., N) ,$$

$$D_{\mu}\Sigma_{N+1} = \partial_{\mu}\Sigma_{N+1} - i\tilde{g}T^{a}W_{N\mu}^{a}\Sigma_{N+1} + ig'\Sigma_{N+1}T^{3}B_{\mu} . \qquad (4.31)$$

As in the previous model, the Σ fields can be removed in unitary gauge, giving a mass to the gauge bosons. We can then expand the charged fields in terms of the

mass eigenstates

$$W_j^{\pm} = a_{j0}W^{\pm} + \sum_{n=1}^{N} a_{jn}W_n^{\prime \pm} , \qquad (4.32)$$

and similarly for the neutral fields

$$W_0^3 = (e/g)A + b_{00}Z + \sum_{n=1}^N b_{0n}Z_n',$$

$$W_j^3 = (e/\tilde{g})A + b_{j0}Z + \sum_{n=1}^N b_{jn}Z_n', \qquad (j = 2, ..., N),$$

$$B = (e/g')A + b_{(N+1)0}Z + \sum_{n=1}^N b_{(N+1)n}Z_n', \qquad (4.33)$$

where the photon A is exactly massless as required. Inserting these expansions in the kinetic terms we obtain, for the coupling of the unbroken U(1),

$$\frac{1}{e^2} = \frac{1}{g^2} + \frac{N}{\tilde{g}^2} + \frac{1}{g'^2} \ . \tag{4.34}$$

We give the general solution for the diagonalization of these mass matrices in Appendix B. For this model there are four independent parameters, g', \tilde{g} , g, f, which can be fixed by e, m_W , m_Z , and the mass of W_1' , $m_{W_1'}$. In accordance with the results of section 4.3.1, we assume $g, g' \ll \tilde{g}/\sqrt{N+1}$, and let $\lambda^2 \equiv g^2(N+1)/\tilde{g}^2$ and $\lambda'^2 \equiv g'^2(N+1)/\tilde{g}^2$. Then a perturbative expansion in λ^2 , and λ'^2 gives the masses

$$m_{W}^{2} = \frac{g^{2} f^{2}}{4(N+1)} \left(1 + \mathcal{O}(\lambda^{2}) \right) ,$$

$$m_{Z}^{2} = \frac{(g^{2} + g'^{2}) f^{2}}{4(N+1)} \left(1 + \mathcal{O}(\lambda^{2}) \right) ,$$

$$m_{W'_{n}}^{2} = \tilde{g}^{2} f^{2} \left(\sin \frac{n\pi}{2(N+1)} \right)^{2} + 2m_{W}^{2} \left(\cos \frac{n\pi}{2(N+1)} \right)^{2} \left(1 + \mathcal{O}(\lambda^{2}) \right) ,$$

$$m_{Z'_{n}}^{2} = \tilde{g}^{2} f^{2} \left(\sin \frac{n\pi}{2(N+1)} \right)^{2} + 2m_{Z}^{2} \left(\cos \frac{n\pi}{2(N+1)} \right)^{2} \left(1 + \mathcal{O}(\lambda^{2}) \right) .$$

$$(4.35)$$

It is easy to check that for N=1 this gives $m_{Z_1'}^2-m_{W_1'}^2\simeq m_Z^2-m_W^2$, and $\tilde{g}=(m_{W_1'}/2m_W)g$, up to corrections of order $m_W^2/m_{W_1'}^2$, as found in section 4.3.1.

The scattering of longitudinal W's is easily generalized from the N=1 case, since the exchanges of a single Z' in the s- and the t-channel are replaced by echanges of N

$$W_{L}^{+} \qquad W_{L}^{+} \qquad + \qquad \qquad \times \gamma + Z$$

$$W_{L}^{-} \qquad W_{L}^{-} \qquad + \qquad \qquad \qquad + \qquad \qquad + \qquad \qquad \times \sum_{n=1}^{N} Z_{n}' \qquad \qquad + \qquad \qquad \times \sum_{n=1}^{N} Z_{n}' \qquad \qquad \times \gamma + Z \qquad \qquad \times$$

Figure 4.9: Tree-level diagrams for the $W_L^+W_L^- \to W_L^+W_L^-$ elastic scattering, in the $SU(2)\times SU(2)^N\times U(1)$ model.

heavy neutral bosons, and shown in Fig. 4.9. The amplitude for $W_L^+W_L^- \to W_L^+W_L^-$ is

$$M = \frac{g_{WWWW}^{2}}{m_{W}^{4}} \left[p^{2}E^{2}(-2 + 6\cos\theta) - E^{4}\sin^{2}\theta \right]$$

$$+ \frac{1}{m_{W}^{4}} \left[\frac{e^{2}}{s} + \frac{g_{WWZ}^{2}}{s - m_{Z}^{2}} + \sum_{n=1}^{N} \frac{g_{WWZ'_{n}}^{2}}{s - m_{Z}^{2}} \right] \left(-4p^{2}(p^{2} - 3E^{2})^{2} \right) \cos\theta$$

$$+ \frac{1}{m_{W}^{4}} \left[\frac{e^{2}}{t} + \frac{g_{WWZ}^{2}}{t - m_{Z}^{2}} + \sum_{n=1}^{N} \frac{g_{WWZ'_{n}}^{2}}{t - m_{Z'_{n}}^{2}} \right] \left[-4E^{2} \left(p^{2} + (E^{2} - 2p^{2})\cos\theta \right)^{2} -2p^{2}(1 + \cos\theta) \left(2E^{2} - p^{2} - E^{2}\cos\theta \right)^{2} \right], \quad (4.36)$$

where the cubic and quartic couplings are

$$g_{WWZ} = g \ a_{00}^2 b_{00} + \tilde{g} \sum_{j=1}^N a_{j0}^2 b_{j0} ,$$

$$g_{WWZ'_n} = g \ a_{00}^2 b_{0n} + \tilde{g} \sum_{j=1}^N a_{j0}^2 b_{jn} ,$$

$$g_{WWWW}^2 = g^2 \ a_{00}^4 + \tilde{g}^2 \sum_{j=1}^N a_{j0}^4 .$$

$$(4.37)$$

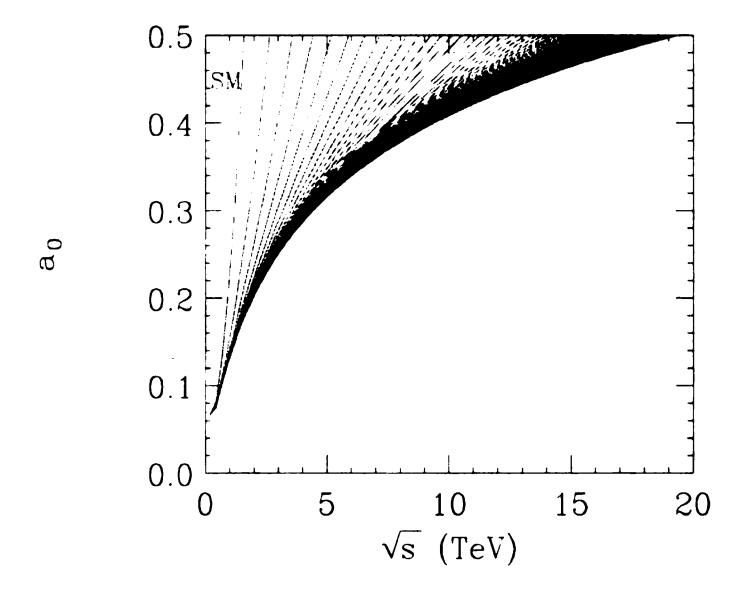


Figure 4.10: The J=0 partial wave amplitude as a function of \sqrt{s} for the SM without a Higgs boson (red) and the $\mathrm{SU}(2)\times\mathrm{SU}(2)^N\times\mathrm{U}(1)$ model (blue) for N=1 to 100 with $m_{W_1'}=500$ GeV.

Then the coefficient of the leading $(E/m_W)^2$ term, defined by (4.27), is

$$K = 4g_{WWWW}^2 - \frac{3}{m_W^2} \left(m_Z^2 g_{WWZ}^2 + \sum_{n=1}^N m_{Z_n'}^2 g_{WWZ_n'}^2 \right)$$
(4.38)

In Appendix B we obtain for this model

$$K = \frac{g^2}{(N+1)^2} + \mathcal{O}(\lambda^2)$$

$$= \frac{K(SM)}{(N+1)^2} + \mathcal{O}(\lambda^2) . \tag{4.39}$$

where the corrections also fall off as $(N+1)^{-2}$. As expected, this agrees with the results of the previous section for N=1.

In Fig. 4.10 we plot the J=0 partial wave amplitude as a function of \sqrt{s} for both the SM without a Higgs boson and in the $SU(2)\times SU(2)^N\times U(1)$ model with $m_{W_1'}=500$ GeV for N=1 to 100. For large N in this model the unitarity violation is delayed to an energy of about $\sqrt{s}=19$ TeV. Thus, we may expect that the effective

theory with a KK tower of vector bosons should be reliable up to about this scale.⁵ At high energies and large N, the partial wave amplitude asymptotes to

$$a_0 \approx \frac{1}{32\pi} \left[\frac{s}{4m_W^2} \frac{g^2}{(N+1)^2} + \frac{4\tilde{g}^2}{N+1} \left(\log \frac{s}{\Lambda^2} - \frac{1}{2} \right) \right]$$

$$\approx \frac{1}{32\pi} \left[\frac{s}{4m_W^2} \frac{g^2}{(N+1)^2} + \frac{4g^2}{\pi^2} \frac{m_{W_1'}^2}{m_W^2} \left(\log \frac{s}{\Lambda^2} - \frac{1}{2} \right) \right] , \qquad (4.40)$$

where Λ is a scale on the order of a few times $m_{W_1'}$.

4.3.3 The $N \to \infty$ Limit

From the analysis of section 3.5 we know that the limit $N \to \infty$ gives a gauge theory on an extra-dimensional interval, as long as \tilde{g} and f grow like N+1. The five-dimensional gauge coupling and the interval length are then given by

$$\pi R = \lim_{N \to \infty} \frac{2(N+1)}{\tilde{g}f} ,$$

$$g_5^2 = \lim_{N \to \infty} \frac{2\tilde{g}}{f} . \tag{4.41}$$

Since the gauge couplings of the edge sites are different, the five-dimensional action has localized kinetic terms on both branes,

$$S_{gauge} = \int d^4x \int_0^{\pi R} dy \left[-\frac{1}{4\hat{g}_5^2 \pi R} W_{MN}^a W^{a MN} - \delta(y) \frac{1}{4g^2} W_{\mu\nu}^a W^{a \mu\nu} - \delta(\pi R - y) \frac{1}{4g'^2} W_{\mu\nu}^3 W^{3 \mu\nu} \right] , \quad (4.42)$$

where the dimensionless five-dimensional coupling \hat{g}_5 is defined by $\hat{g}_5^2 \pi R = g_5^2$, and the five-dimensional coordinate x^5 has been renamed y.

As explained in section 4.2, the δ -functions should be intended as slightly pushed inside the bulk, with the BCs leaving SU(2) unbroken at y=0, and breaking SU(2) to U(1) at $y=\pi R$. These are the same BCs we met in the toy model (1) of section 3.2, which allow us to set $W_5^a\equiv 0$, in unitary gauge. Then, pushing the delta functions

⁵A coupled-channel analysis, as considered in Ref. [34], would give a lower energy scale for unitarity violation.

back to the branes, we obtain

$$\lim_{y \to 0^{+}} \left(\partial_{5}^{2} W_{\mu}^{a} - \frac{\lambda^{2}}{\pi R} \partial_{5} W_{\mu}^{a} \right) = 0 ,$$

$$\lim_{y \to \pi R^{-}} \left(\partial_{5}^{2} W_{\mu}^{3} + \frac{\lambda'^{2}}{\pi R} \partial_{5} W_{\mu}^{3} \right) = 0 ,$$

$$W_{\mu}^{\pm}(\pi R) = 0 , \qquad (4.43)$$

for the behavior of the gauge fields near the boundaries, where $\lambda^2 \equiv g^2/\hat{g}_5^2$, and $\lambda'^2 \equiv g'^2/\hat{g}_5^2$.

All of the results found in appendix B have a well-defined limit as $N \to \infty$, with the discrete label j becoming the continuous extra-dimensional variable y, and the vector expansions (4.32), (4.33) becoming KK expansions. An alternative method for deriving the solutions consists in working directly with the continuum model, as in section 3.1, and KK expanding the five-dimensional gauge fields,

$$W^{\pm\mu}(x,y) = \sum_{n=0}^{\infty} f_n(y) W_n^{\pm\mu}(x) ,$$

$$W^{3\mu}(x,y) = eA^{\mu}(x) + \sum_{n=0}^{\infty} g_n(y) Z_n^{\mu}(x) ,$$
(4.44)

where $W_0^{\pm}(x)$ and $Z_0(x)$ will be identified with the SM W and Z boson, respectively. The wavefunctions $f_n(y), g_n(y)$ are superpositions of the ∂_5^2 operator, namely sines and cosines. The photon wavefunction is trivially obtained to be constant and equal to e, where

$$\frac{1}{e^2} = \frac{1}{g^2} + \frac{1}{\hat{g}_5^2} + \frac{1}{g'^2} \ . \tag{4.45}$$

The $f_n(y)$ and $g_n(y)$ wavefunctions satisfying the BCs (4.43) are

$$f_n(y) = F_n \sin \left[m_{W_n} (\pi R - y) \right] ,$$

$$g_n(y) = G_n \left[\cos(m_{Z_n} y) - \frac{\hat{m}_{Z_n}}{\lambda^2} \sin(m_{Z_n} y) \right] ,$$

$$(4.46)$$

where the masses m_{W_n}, m_{Z_n} solve the transcendental equations

$$\hat{m}_{W_n} \tan \hat{m}_{W_n} = \lambda^2 ,$$

$$\left(\hat{m}_{Z_n} - \frac{\lambda^2 \lambda'^2}{\hat{m}_{Z_n}}\right) \tan \hat{m}_{Z_n} = \lambda^2 + \lambda'^2 ,$$
(4.47)

with $\hat{m} \equiv m\pi R$. The normalization constants F_n, G_n are determined by requiring a canonical orthonormalization of the mass eigenstates:

$$\int_{0}^{\pi R} dy \left[\frac{1}{\hat{g}_{5}^{2} \pi R} + \frac{1}{g^{2}} \delta(y) \right] f_{n}(y) f_{n'}(y) = \delta_{nn'},$$

$$\int_{0}^{\pi R} dy \left[\frac{1}{\hat{g}_{5}^{2} \pi R} + \frac{1}{g^{2}} \delta(y) + \frac{1}{g^{2}} \delta(\pi R - y) \right] g_{n}(y) g_{n'}(y) = \delta_{nn'}.$$
(4.48)

Notice that the integrands in (4.48), for equal values of n and n', should be interpreted as position probability densities in the extra-dimensional interval. The presence of δ -function terms tells us that the charged gauge bosons have non-zero probability of being exactly localized at y = 0, and the neutral gauge bosons have non-zero probability of being exactly localized at y = 0 and $y = \pi R$.

Using the mass equations, we obtain

$$F_{n} = \hat{g}_{5} \left[\frac{1}{2} \left(1 + \frac{\sin 2\hat{m}_{W_{n}}}{2\hat{m}_{W_{n}}} \right) \right]^{-1/2} ,$$

$$G_{n} = \hat{g}_{5} \left[\frac{1}{2} \left(1 - \frac{\sin 2\hat{m}_{Z_{n}}}{2\hat{m}_{Z_{n}}} \right) + \frac{1}{\lambda^{2}} \sin^{2} \hat{m}_{Z_{n}} + \frac{\hat{m}_{Z_{n}}^{2}}{2\lambda^{4}} \left(1 + \frac{\sin 2\hat{m}_{Z_{n}}}{2\hat{m}_{Z_{n}}} \right) \right]^{-1/2} ,$$

$$(4.49)$$

for the normalization constants.

Once the normalized wavefunctions are found, the cubic and quartic gauge coupings can be computed using the formulas

$$g_{W_{l}W_{m}Z_{n}} = \int_{0}^{\pi R} dy \left[\frac{1}{\hat{g}_{5}^{2}\pi R} + \frac{1}{g^{2}}\delta(y) \right] f_{l}(y) f_{m}(y) g_{n}(y) ,$$

$$g_{W_{k}W_{l}W_{m}W_{n}} = \int_{0}^{\pi R} dy \left[\frac{1}{\hat{g}_{5}^{2}\pi R} + \frac{1}{g^{2}}\delta(y) \right] f_{k}(y) f_{l}(y) f_{m}(y) f_{n}(y) ,$$

$$g_{W_{k}W_{l}Z_{m}Z_{n}} = \int_{0}^{\pi R} dy \left[\frac{1}{\hat{g}_{5}^{2}\pi R} + \frac{1}{g^{2}}\delta(y) \right] f_{k}(y) f_{l}(y) g_{m}(y) g_{n}(y) .$$

$$(4.50)$$

These formulas are also valid for couplings involving the photons, for it is sufficient to replace the $g_n(y)$'s with the photon wavefunction, $g_{\gamma}(y) = e$. Therefore, using also

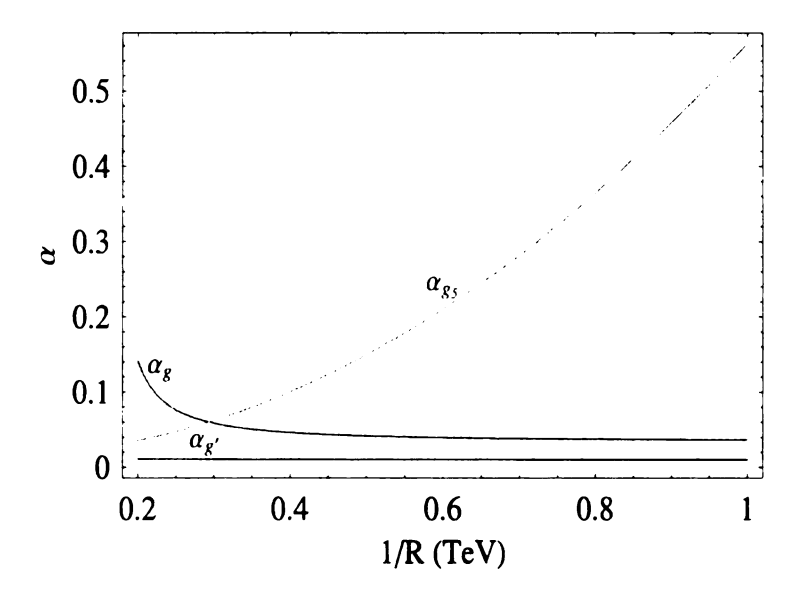


Figure 4.11: The coupling constants $\alpha_g=g^2/4\pi$ (blue), $\alpha_{g'}=g'^2/4\pi$ (red), and $\alpha_{\hat{g}_5}=\hat{g}_5^2/4\pi$ (green), as a function of 1/R.

the normalization conditions (4.48), we obtain

$$g_{W_m W_n \gamma} = e \delta_{mn} ,$$

$$g_{W_m W_n \gamma \gamma} = e^2 \delta_{mn} ,$$

$$g_{W_l W_m Z_n \gamma} = e g_{W_l W_m Z_n} .$$

$$(4.51)$$

In the examples with a finite number of sites we saw that the largest postponement of unitarity violation occurs for $g^2, g'^2 \ll \tilde{g}^2/(N+1)$, which in the continuum model corresponds to $g^2, g'^2 \ll \hat{g}_5^2$. Therefore, we can find the solutions perturbatively for $\lambda^2, \lambda'^2 \ll 1$. For the masses, we obtain

$$m_W^2 \equiv m_{W_0}^2 = \frac{\lambda^2}{(\pi R)^2} \left[1 - \frac{\lambda^2}{3} + \mathcal{O}(\lambda^4) \right] ,$$

$$m_Z^2 \equiv m_{Z_0}^2 = \frac{\lambda^2 + \lambda'^2}{(\pi R)^2} \left[1 - \frac{\lambda^2 + \lambda'^2}{3} + \frac{\lambda^2 \lambda'^2}{\lambda^2 + \lambda'^2} + \mathcal{O}(\lambda^4) \right] , \qquad (4.52)$$

for the SM gauge bosons, and

$$m_{W_n}^2 = \left(\frac{n}{R}\right)^2 \left[1 + 2\frac{\lambda^2}{(\pi n)^2} + \mathcal{O}(\lambda^4)\right] n = 1, 2, \dots,$$

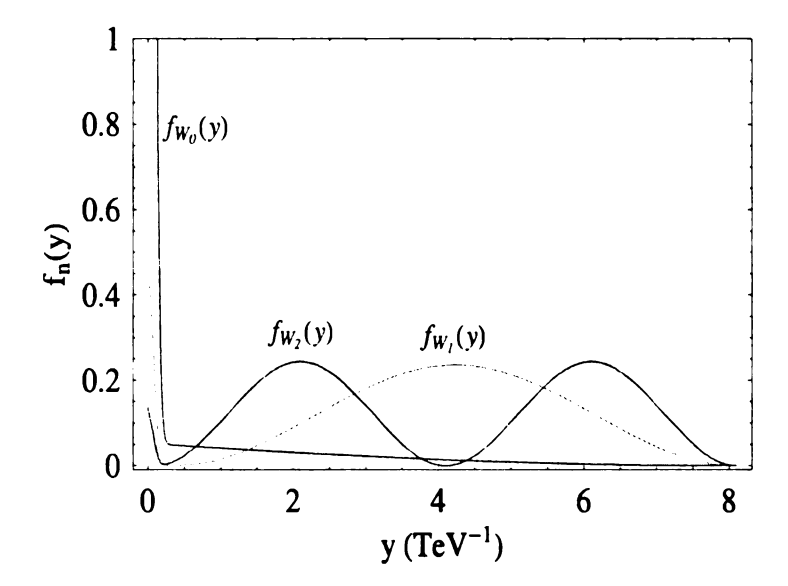


Figure 4.12: Probability density for the position of the W boson (red), W_1 (green), and W_2 (blue) in the extra-dimensional interval, for 1/R = 500 GeV, with $\delta(y)$ replaced by a narrow Gaussian.

$$m_{Z_n}^2 = \left(\frac{n}{R}\right)^2 \left[1 + 2\frac{\lambda^2 + {\lambda'}^2}{(\pi n)^2} + \mathcal{O}(\lambda^4)\right] \ n = 1, 2, \dots,$$
 (4.53)

for the heavy gauge bosons. Inserting these equations in (4.49) gives

$$F_{0} = \frac{g}{\lambda} \left[1 + \frac{\lambda^{2}}{6} + \mathcal{O}(\lambda^{4}) \right] ,$$

$$F_{n} = \frac{\sqrt{2}g}{\lambda} \left[1 - \frac{\lambda^{2}}{2(n\pi)^{2}} + \mathcal{O}(\lambda^{4}) \right] n = 1, 2, ...,$$

$$G_{0} = \frac{g\lambda}{\sqrt{\lambda^{2} + \lambda'^{2}}} \left[1 - \frac{\lambda^{4} + 2\lambda^{2}\lambda'^{2} - 2\lambda'^{4}}{6(\lambda^{2} + \lambda'^{2})} + \mathcal{O}(\lambda^{4}) \right] ,$$

$$G_{n} = \frac{\sqrt{2}g\lambda}{n\pi} \left[1 - \frac{3}{2} \frac{\lambda^{2} + \lambda'^{2}}{(n\pi)^{2}} + \mathcal{O}(\lambda^{4}) \right] n = 1, 2, ...,$$
(4.54)

for the normalization constants. Perturbative expansions for the couplings (4.50) are given in appendix C.

This model has four parameters: g, g', \hat{g}_5 , and the compactification scale R. We can trade g, g', \hat{g}_5 for e, m_W, m_Z , leaving R as the only parameter beyond the SM. In Fig. 4.11 we show the behavior of $\alpha_g = g^2/4\pi$, $\alpha_{g'} = g'^2/4\pi$, and $\alpha_{\hat{g}_5} = \hat{g}_5^2/4\pi$ as

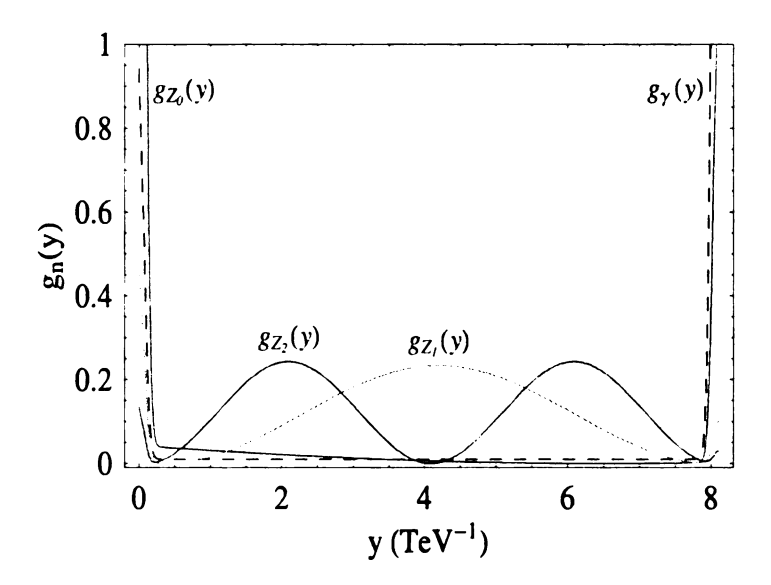


Figure 4.13: Probability density for the position of the photon (dashed), the Z boson (red), Z_1 (green), and Z_2 (blue) in the extra-dimensional interval, for 1/R = 500 GeV, with $\delta(y)$ and $\delta(\pi R - y)$ replaced by narrow Gaussians.

functions of 1/R, which, as shown by (4.53), is approximately equal to the mass of the W_1 and Z_1 bosons. We see that large values of 1/R correspond to small values of λ^2 and λ'^2 . This can be seen directly from the relations (4.52), which fix the W and Z mass, and is in agreement with the results we found for the deconstructed model.

Inserting the normalization factors (4.54) and the masses (4.52), (4.53) in (4.46), we obtain that near y=0 and $y=\pi R$ the wavefunctions of the SM gauge bosons are of order of the electroweak couplings, and are not suppressed by any power of λ . On the other hand, the wavefunctions of the heavy modes are suppressed by one power of λ . Since the position probability densities have δ -functions at y=0 and $y=\pi R$, with coefficients $1/\lambda^2$ and $1/\lambda'^2$, respectively (see eq. (4.48)), it follows that all gauge bosons have non-zero probability of being exactly localized on the two branes, but this probability is much larger for the SM gauge bosons than for the heavy KK modes. In Fig 4.12 we show the probability density for the position of the W boson, W_1 , and W_2 in the extra-dimensional interval, for 1/R = 500 GeV, where the δ -functions have

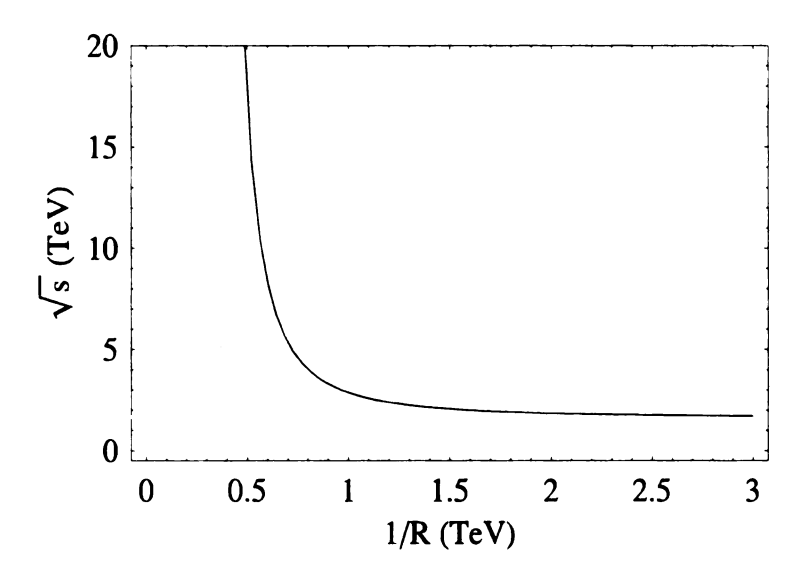


Figure 4.14: Unitarity violation curve for the $W_L^+W_L^- \to W_L^+W_L^-$ scattering, in the $(\sqrt{s}, 1/R)$ plane. For a given value of 1/R, unitarity is satisfied for values of \sqrt{s} below the curve.

been replaced with narrow Gaussians. In Fig. 4.13 we show the probability density for the photon, the Z boson, Z_1 , and Z_2 . We see that the SM gauge bosons spend indeed more time than the heavy modes near the branes. Therefore, in accordance to what we had found in the deconstructed models, the brane SU(2) and U(1) groups act approximately as the SM SU(2)_L and U(1)_Y. In the limit λ , $\lambda' \to 0$ we must also have $R \to 0$, and the heavy modes decouple. Therefore, the λ , $\lambda' \to 0$ limit corresponds to a four-dimensional theory, namely the SM without the Higgs boson.

With the model fully set up, we can calculate the unitarity bounds from longitudinal gauge boson scattering amplitudes. The $W_L^+W_L^- \to W_L^+W_L^-$ scattering is given by the diagrams of Fig. 4.9, and the amplitude by (4.36) (without the primes on the KK gauge bosons), with N replaced by ∞ , and the gauge couplings given by (4.50). The coefficient of the $(E/m_W)^2$ term, in the high energy expansion, is easily found to be zero by taking the $N \to \infty$ limit in (4.39). Alternatively we can prove this directly from the extra-dimensional model, as we did in section 3.3, with the difference that

the gauge couplings receive contributions from the δ -function terms.

Since R is the only free parameter, the amplitude M depends on E, θ , and R, $M = M(E, \theta, R)$. Therefore, the J = 0 partial wave amplitude depends on E and R, $a_0 = a_0(E, R)$. In Fig 4.14 we show the $a_0 = 1/2$ curve in the $(\sqrt{s}, 1/R)$ plane: unitarity is satisfied below the curve, where $a_0 < 1/2$. We observe that for a given energy, unitarity sets an upper bound on 1/R. This was expected, since the heavy neutral bosons must come into play early enough to unitarize the amplitude.

The asymptotic behavior of a_0 can be found by taking the limit $N \to \infty$ in (4.40), which gives

$$a_0 \approx \frac{1}{32\pi} \left[\frac{4g^2}{\pi^2} \frac{m_{W_1}^2}{m_W^2} \left(\log \frac{s}{\Lambda^2} - \frac{1}{2} \right) \right] ,$$
 (4.55)

where Λ is a scale of the order of a few times m_{W_1} . Using (4.52) and (4.53), we notice that, to leading order in λ^2 , the coefficient of the logarithmic term in (4.55) is \hat{g}_5^2 times a numerical factor. Therefore, the unitarity violation scale is approximately given by the reciprocal of the dimensionful coupling g_5^2 times a numerical factor, in agreement with the discussion at the end of section 3.3 [34] [37] [38].

Chapter 5

Coupling to Matter Fields and Experimental Constraints

In chapter 4 we have introduced the gauge sector of an $SU(2)\times SU(2)^N\times U(1)$ NLSM, where the $N\to\infty$ limit corresponds to an SU(2) gauge theory on an five-dimensional interval, with BCs breaking SU(2) to U(1) at one of the boundaries, and localized kinetic terms on the two branes. In this chapter we will add matter fields to this model.

Since the SU(2) and U(1) gauge groups localized at the endpoints of the interval act approximately as the SM $SU(2)_L$ and $U(1)_Y$, the simplest choice is to have the SM fermions charged under these groups only, with the usual quantum numbers. We will show that this manner of coupling fermions leads to tension between the constraints imposed by the EWP data and the unitarity constraints.

In order to release this tension, we let the fermion fields to have some leakage into the bulk – in a fashion similar to the gauge sector setup – with the left-handed fermions peaked at the boundary where SU(2) is unbroken, and the right-handed fermions peaked at the other boundary. We show that the correction to the SM electroweak observables can be tuned to zero by imposing a relation between the amount of leakage into the bulk of the gauge fields and the left-handed fermion fields. We also show that delocalized fermions in this model naturally allow for multiple generations and fermion mixings.

As the $N \to \infty$ model has been proved to be computationally easier than the finite-N NLSMs, we will only present our results in this limit. However we should not rely upon the extra-dimensional interpretation, because this would leave little freedom for model building: Gauge-fermion interactions would be forced to be local, in the five-dimensional interval, and "Yukawa" interactions between fermions and the gauge field fifth-component would be forced to have the same strength of the ordinary gauge interactions. We will then interpret the variable y of section 4.3.3 as a continuum index, and the interval from which y picks its values as a TS interval, rather than an extra-dimensional interval. We will take advantage of this interpretation in both this chapter and the next one.

5.1 Model I

In section 4.3.3 we considered an SU(2) gauge theory on a $[0, \pi R]$ extra-dimensional interval, with BCs breaking SU(2) at $y = \pi R$, and localized kinetic terms on both branes. The action, for the gauge sector, is given by (4.42). Fig. 4.11 shows that, as 1/R grows, the dimensionless bulk coupling \hat{g}_5^2 becomes larger than the brane couplings, g^2 and g'^2 . Fig. 4.12 and Fig. 4.13 show that, for small values of g^2/\hat{g}_5^2 and g'^2/\hat{g}_5^2 , the SM gauge bosons are much more peaked on the two branes than the heavy KK gauge bosons. (The W boson is only peaked on the y=0 brane, since SU(2) is broken to U(1) at $y=\pi R$.) Therefore, as previously stressed, the SU(2) and U(1) gauge groups on the two branes act approximately as the SM SU(2)_L and U(1)_Y.

It is therefore reasonable to try first coupling the SM fermions to the SU(2) and U(1) brane fields only, in exactly the same way they are coupled to the electroweak gauge bosons in the GWS theory. With this choice, the action for one generation of fermions is

$$S_{\text{fermion}}^{(I)} = \int d^4x \int_0^{\pi R} dy \left[\delta(y) \bar{\psi}_L i \gamma^\mu D_\mu \psi_L + \delta(\pi R - y) \left(\bar{u}_R i \gamma^\mu D_\mu u_R + \bar{d}_R i \gamma^\mu D_\mu d_R \right) \right]$$
(5.1)

where $\psi_L = (u_L, d_L)$ is an SU(2) doublet, and u_R , d_R are SU(2) singlets. The covariant derivatives are

$$D_{\mu}\psi_{L} = \left(\partial_{\mu} - iT^{a}W_{\mu}^{a}(y) - iY_{L}W_{\mu}^{3}(\pi R)\right)\psi_{L},$$

$$D_{\mu}u_{R} = \left(\partial_{\mu} - iY_{R}W_{\mu}^{3}(y)\right)u_{R},$$

$$D_{\mu}d_{R} = \left(\partial_{\mu} - iY_{R}W_{\mu}^{3}(y)\right)d_{R}.$$
(5.2)

Notice that the left-handed field ψ_L lives at y=0 but couples also to the gauge field W^3 at $y=\pi R$. This is not allowed in a five-dimensional Yang-Mills theory, but is perfectly reasonable in continuum TS. The fermion action could be made local by folding the SU(2) gauge group at $y=\pi R$, as in example (2) of section 3.2, and coupling all fermions at y=0. However, a mass term for the fermions can only arise in this model from a Wilson line connecting the two branes. This is again a non-local operator in 5D, but is fine from a four-dimensional standpoint. Therefore, as previously argued, we see that giving up on the five-dimensional interpretation opens new possibilities for model building, and our choice of labelling the x^5 coordinate as y is to emphasize this point.

The four-dimensional charged-current and neutral-current Lagrangians are

$$\mathcal{L}_{CC}^{(I)} = \sum_{n=0}^{\infty} \left[\frac{g_{Ln}^{CC(I)}}{\sqrt{2}} \bar{\psi} \gamma^{\mu} P_{L} T^{+} \psi W_{n\mu}^{+} + \text{h.c.} \right] ,$$

$$\mathcal{L}_{NC}^{(I)} = \sum_{n=0}^{\infty} \left[\bar{\psi} \gamma^{\mu} \left(g_{Ln}^{NC(I)} P_{L} T^{3} + g_{Qn}^{NC(I)} Q \right) \psi Z_{n\mu} \right] , \qquad (5.3)$$

where W_0 , and Z_0 are the SM W and Z boson, respectively, and $\psi = \psi_L + \psi_R$. The couplings are

$$g_{Ln}^{CC(I)} = f_n(0) ,$$

 $g_{Ln}^{NC(I)} = g_n(0) - g_n(\pi R) ,$
 $g_{Qn}^{NC(I)} = g_n(\pi R) ,$ (5.4)

where $f_n(y)$ and $g_n(y)$ are given by (4.46).

5.2 Experimental Constraints on Model I

In this section we study the most immediate phenomenological implications of model I. We will first briefly consider the direct constraints from producing the heavy gauge bosons at colliders, and then consider the indirect constraints from the EWP data.

5.2.1 Direct Constraints on Heavy Boson Production

The most significant bounds on the W_1 and Z_1 masses come from the Tevatron and LEP II, respectively. The Tevatron (CDF) limit on a W' that couples with SM strength is presented in Fig. 2 of Ref. [72]. In our case, the ratio $\sigma(q\bar{q} \to W_1 \to \ell\nu)/\sigma(q\bar{q} \to W \to \ell\nu)$ is suppressed by the small value of the W_1 wavefunction on the boundary where the fermions are localized. The coupling of SM fermions with W_1 is $g_{L0}^{CC(I)} = f_1(0)$, which gives the suppression factor $(f_1(0)/g)^2$. Using (4.46), together with (4.53) and (4.54), this gives

$$\left[\frac{\sigma(q\bar{q}\to W_1\to\ell\nu)}{\sigma(q\bar{q}\to W\to\ell\nu)}\right]^{(I)} = 2\frac{m_W^2}{m_{W_1}^2} \left[\frac{\sigma(q\bar{q}\to W_1\to\ell\nu)}{\sigma(q\bar{q}\to W\to\ell\nu)}\right]^{(SM)} .$$
(5.5)

By rescaling the cross sections shown in the figure, we estimate that the corresponding limits in our case would be about $m_{W_1} > 500$ GeV.

The LEP II bound on new four fermion contact interactions are presented (for the case of strong coupling) in Ref. [73] by making fits to $\sigma(e^+e^- \to f\bar{f})$. This can be translated to a bound on m_{Z_1} since a heavy Z' effectively induces a four fermion contact interaction. Extracting the relevant contact interactions induced in our model, and comparing to the results of the LEP II analysis, we estimate that the mass bound is about $m_{Z_1} > 480$ GeV.

5.2.2 Indirect Constraints on the Low Energy Fermion Lagrangians

The fermion couplings with the gauge boson are given by the values of the corresponding wavefunctions at the two interval ends, as shown by (5.4). In section 4.3.3 we have

argued that the wavefunctions of the heavy modes are suppressed by one power of λ at y=0 and $y=\pi R$: This is shown explicitly in Fig. 4.12 and Fig. 4.13. Therefore, four-fermion operators arising from exchanges of heavy gauge bosons are suppressed by λ^4 , with two powers of λ coming from the couplings, and two powers from the large mass in the gauge boson propagator $(1/R \sim m_W/\lambda, \text{ see } (4.52))$. The couplings of the SM gauge bosons with the heavy gauge bosons are also suppressed by one power of λ , due to the little overlap of the corresponding wavefunctions. This means that dimension five operators, with two SM fermions and two SM gauge bosons, only arise at λ^4 order.

As a consequence, at order λ^2 the new-physics corrections to the low-energy observables are purely oblique, and are therefore entirely parametrized by the Peskin-Takeuchi S, T, and U parameters, where S = T = U = 0 corresponds to the SM [43] [44] [59]. The way these quantities enter in the charged-current and neutral-current effective Lagrangians depends on the chosen set of input observables. It is customary to take the electromagnetic coupling strength at the Z-pole, the Z boson mass, and the Fermi constant, because these observables have been measured with a high level of precision. The current estimates are [53]

$$\alpha(m_Z)^{-1} = 128.80 \pm 0.12$$
,
 $m_Z = 91.1876 \pm 0.0021$,
 $G_F = (1.16637 \pm 0.00001) \times 10^{-5} \text{ GeV}^{-2}$. (5.6)

However here we take m_W instead of G_F , even though m_W is not known as precisely as m_Z :

$$m_W = 80.425 \pm 0.038 \ . \tag{5.7}$$

This choice is in fact useful, because it is independent of the fermion profiles, and will pay off in section 5.3, where we compare this model, in which fermions are localized, with a different model, in which fermions are delocalized.

Taking α, m_Z , and m_W as input observables, and defining s by,

$$s^2 \equiv 1 - \frac{m_W^2}{m_Z^2} \,, \tag{5.8}$$

with $c \equiv \sqrt{1-s^2}$, we find the following expressions for the low-energy charged-current and neutral-current Lagrangians:

$$\mathcal{L}_{CC} = \frac{g_L^{CC}}{\sqrt{2}} \bar{\psi} \gamma^{\mu} P_L T^+ \psi W_{\mu}^+ + \text{h.c.} ,$$

$$\mathcal{L}_{NC} = \bar{\psi} \gamma^{\mu} \left(g_L^{NC} P_L T^3 + g_Q^{NC} Q \right) \psi Z_{\mu} , \qquad (5.9)$$

where

$$g_L^{CC} = \frac{e}{s} \left[1 + \frac{\alpha S}{4s^2} - \frac{c^2 \alpha T}{2s^2} - \frac{(c^2 - s^2)\alpha U}{8s^4} \right] ,$$

$$g_L^{NC} = \frac{e}{sc} \left[1 + \frac{\alpha S}{4s^2} - \frac{(c^2 - s^2)\alpha T}{2s^2} - \frac{(c^2 - s^2)\alpha U}{8s^4} \right] ,$$

$$g_Q^{NC} = -\frac{es}{c} \left[1 + \frac{\alpha T}{2s^2} + \frac{\alpha U}{8s^4} \right] .$$
(5.10)

This equations show that T is related to the ρ parameter by

$$\alpha T = \rho - 1 \ . \tag{5.11}$$

This relation is however only valid as long as the new-physics contribution to the low-energy interactions is purely oblique.

Inserting (4.46) in (5.4), and using the perturbative expansions (4.52) and (4.54) for the masses and the normalization factors, respectively, leads to the following tree-level expressions for the couplings in model I:

$$\begin{split} g_L^{CC(I)} &= \frac{e}{s} \left[1 + \lambda^2 / 6 + \mathcal{O}(\lambda^4) \right] , \\ g_L^{NC(I)} &= \frac{e}{sc} \left[1 + \lambda^2 / 6 + \mathcal{O}(\lambda^4) \right] , \\ g_Q^{NC(I)} &= -\frac{es}{c} \left[1 + \mathcal{O}(\lambda^4) \right] . \end{split} \tag{5.12}$$

Comparing these equations with (5.10), we obtain for this theory

$$\alpha S = 2s^2 \lambda^2 / 3 ,$$

$$\alpha T = 0 ,$$

$$\alpha U = 0 .$$
(5.13)

The fact that T=0 at order $\mathcal{O}(\lambda^2)$ is an expected result, because this model has an approximate custodial symmetry: This is most easily seen in the deconstructed

version, from the choice of coupling B_{μ} as the T^3 component of a global SU(2). U is usually expected to differ from T by a percent, and is accordingly approximately zero in this model. However S is not zero at order $\mathcal{O}(\lambda^2)$. This is in agreement with a general result found in Ref. [55]: In an arbitrary $\mathrm{SU}(2)_0 \times \mathrm{SU}(2)^N \times \mathrm{U}(1)_{N+1} \times \mathrm{U}(1)^M$ NLSM, with matter fields charged under $\mathrm{SU}(2)_0$ and $\mathrm{U}(1)_{N+1}$ only, it is always true that $S-4\cos\theta_W T>\mathcal{O}(1)$. In our model T is naturally suppressed, thus the previous relation reads $S>\mathcal{O}(1)$, in agreement with (5.13), since $\alpha \sim \lambda^2$.

Recent experimental constraints on S and T can be found in Ref.[78], where the limits are given as a function of the Higgs boson mass. In principle, its contributions must be subtracted from the above S and T parameters, since there is no Higgs boson in our model. However, given that the dependence on m_H is not too large, we can still obtain an estimate of how these constraints impact our model. For $m_H = 600$ GeV with the constraint $S \geq 0$, and using Bayesian statistics, the limit on S is $S \leq 0.14$. This result corresponds to $m_{W_1} > 3$ TeV. Unfortunately, for models in which m_{W_1} is so large, unitarity will be violated even before the scale of m_{W_1} is reached, as shown by Fig. 4.14. Therefore, it appears that the method used in this section to incorporate matter fields into the model is not viable.

5.2.3 Indirect Constraints on the Low Energy Gauge Lagrangian

Although we have already proved that brane localized fermions violate the bounds imposed by unitarity and the EWP data, we press on and consider the indirect constraints of this model on the low-energy gauge interactions. The results we find here will be useful later in this chapter.

Additional constraints on the W_1 mass can be found from the analysis of anomalous couplings in the WWZ vertex. To leading order, in the absence of CP-violation, the triple gauge boson vertices may be written in the Hagiwara-Peccei-Zeppenfeld-Hikasa notation [74],

$$\mathcal{L}_{\text{gauge}}^{(3)} = -ie \frac{c_Z}{s_Z} (1 + \Delta \kappa_Z) W_{\mu}^+ W_{\nu}^- Z^{\mu\nu} - ie (1 + \Delta \kappa_{\gamma}) W_{\mu}^+ W_{\nu}^- A^{\mu\nu}$$

$$- ie \frac{c_Z}{s_Z} \left(1 + \Delta g_1^Z \right) (W^{+\mu\nu} W_{\mu}^- - W^{-\mu\nu} W_{\mu}^+) Z_{\nu}$$
$$- ie (W^{+\mu\nu} W_{\mu}^- - W^{-\mu\nu} W_{\mu}^+) A_{\nu} , \qquad (5.14)$$

where the two-index Lorentz tensors denote the $U(1)_Q$ -invariant field strength tensors of the corresponding field, and the "Z standard" weak mixing angle is defined in terms of e, m_Z , and G_F by

$$s_Z^2 c_Z^2 \equiv \frac{e^2}{4\sqrt{2}G_F m_Z^2} \,, \tag{5.15}$$

where, as usual $s_Z^2 + c_Z^2 = 1$.

In the SM, $\Delta \kappa_Z = \Delta \kappa_\gamma = \Delta g_1^Z = 0$. In our Higgsless model, like in any vector-resonance model, the interactions (5.14) come from re-expressing the nonabelian couplings of the original Lagrangian in terms of the mass eigenstates, in which case one obtains equal contributions to the deviation from the SM in the first and the third terms, and in the second and the fourth terms [75]. Moreover, the contribution to the fourth term is fixed by electromagnetic gauge invariance. Therefore, we obtain

$$\Delta \kappa_Z = \Delta g_1^Z \qquad \Delta \kappa_\gamma = 0 \ . \tag{5.16}$$

In order to express the WWZ vertex in terms of s_Z , rather than $s \equiv m_W/m_Z$, we must find an expression for G_F . To order λ^2 , we simply have

$$\sqrt{2}G_F = \frac{\left(g_L^{CC(I)}\right)^2}{4m_W^2} \,, \tag{5.17}$$

because, as previously noticed, the heavy KK exchanges only contribute at order λ^4 . Using (5.10) and (5.13), we find

$$G_{F} = \frac{1}{4\sqrt{2}m_{W}^{2}} \frac{e^{2}}{s^{2}} \left[1 + \frac{\alpha S}{2s^{2}} \right]$$

$$= \frac{1}{4\sqrt{2}m_{W}^{2}} \frac{e^{2}}{s^{2}} \left[1 + \frac{(m_{W}\pi R)^{2}}{3} + \mathcal{O}\left((m_{W}\pi R)^{4}\right) \right] , \qquad (5.18)$$

where we used (4.52) to express λ in terms of m_W and R. Inserting this equation in (5.15) gives

$$s = s_Z \left[1 + \frac{1}{1 - s_Z^2 / c_Z^2} \frac{\alpha S}{4s_Z^2} \right]$$

$$= s_Z \left[1 + \frac{1}{1 - s_Z^2 / c_Z^2} \frac{(m_W \pi R)^2}{6} + \mathcal{O}\left((m_W \pi R)^4 \right) \right]$$
 (5.19)

The WWZ vertex can be found in appendix C. Expressing it in terms of e, s_Z , and $(m_W \pi R)$ gives

$$g_{WWZ} = e^{\frac{c_Z}{s_Z}} \left[1 + \frac{(m_W \pi R)^2}{12c_Z^2} - \frac{1}{c_Z^2 - s_Z^2} \frac{\alpha S}{4s_Z^2} + \mathcal{O}\left((m_W \pi R)^4\right) \right]$$

$$= e^{\frac{c_Z}{s_Z}} \left[1 - \frac{(m_W \pi R)^2}{12} \left(\frac{2}{c_Z^2 - s_Z^2} - \frac{1}{c_Z^2} \right) + \mathcal{O}\left((m_W \pi R)^4\right) \right] , \qquad (5.20)$$

whence, comparing with (5.14),

$$\Delta g_1^Z = -\frac{(m_W \pi R)^2}{12} \left(\frac{2}{c_Z^2 - s_Z^2} - \frac{1}{c_Z^2} \right) < 0.$$
 (5.21)

The 95% C.L. upper limit from LEP-II is $|\Delta g_1^Z| < 0.028$ [76]. Using the experimental results (5.6), (5.7) and eq. (5.15), the upper bound on Δg_1^Z translates into the lower bound $1/R \simeq m_{W_1} > 682$ GeV, which is considerably stronger than the direct-search bound found in section 5.2.1.

5.3 Model II

Drawing on the analogy of the gauge action (4.42), which has SU(2) and U(1) kinetic terms peaked at the two ends of the interval and connected through the bulk kinetic term, we now consider a theory with left-handed and right-handed fermion kinetic terms peaked at the two ends of the interval and connected through a bulk fermion kinetic term [45],[50]. The fermion action is

$$S_{\text{fermion}}^{(II)} = \int d^4x \int_0^{\pi R} dy \left[\frac{1}{\pi R} \left(\frac{1}{2} \bar{\psi} i \Gamma^M D_M \psi + \text{ h.c.} - M \bar{\psi} \psi \right) + \delta(y) \frac{1}{t_L^2} \bar{\psi}_L i \gamma^\mu D_\mu \psi_L + \delta(\pi R - y) \left(\frac{1}{t_{u_R}^2} \bar{u}_R i \gamma^\mu D_\mu u_R + \frac{1}{t_{d_R}^2} \bar{d}_R i \gamma^\mu D_\mu d_R \right) \right].$$
(5.22)

The five-dimensional Dirac matrices were introduced in section 4.1, and are defined in terms of the four-dimensional ones by $\Gamma^M = (\gamma^{\mu}, -i\gamma^5)$. The five-dimensional

fermion is equivalent to a four-dimensional Dirac fermion, $\psi = \psi_L + \psi_R$, where ψ_L and ψ_R are SU(2) doublets,

$$\psi_L = \left(egin{array}{c} u_L \ d_L \end{array}
ight) \;\; , \; \psi_R = \left(egin{array}{c} u_R \ d_R \end{array}
ight).$$

We have written the action for one doublet, consisting of an up and a down quark. We will discuss the possibility of more generations and mixing in Section 5.3.2. We can assume the bulk mass M to be real in (5.22) without any loss of generality. In fact any imaginary part of M can be removed by the replacement $\psi \to e^{(i\operatorname{Im} My)}\psi$. The sign of M, however, is physical. In analogy with the gauge brane kinetic terms (see section 4.2), the fermion brane kinetic term at y=0 is defined by interpreting the δ -function as $\delta(y-\epsilon)$ for $\epsilon \to 0^+$ with the boundary condition $\psi_R=0$ at y=0. Similarly, the boundary term at $y=\pi R$ is defined by interpreting the δ -function as $\delta(\pi R - y + \epsilon)$ with the boundary condition $\psi_L=0$ at $y=\pi R$. The general treatment of possible fermion boundary conditions can be found in Ref. [71].

The covariant derivative in (5.22) is

$$D_M \psi = \left(\partial_M - i T^a W_M^a(y) - i Y_L W_M^3(\pi R)\right) \psi, \tag{5.23}$$

where Y_L is the ψ_L hypercharge. At the interval ends the four-dimensional part of the covariant derivative (5.23) becomes:

$$(D_{\mu}\psi_{L})_{y=0} = \left(\partial_{\mu} - iT^{a}W_{\mu}^{a}(0) - iY_{L}W_{\mu}^{3}(\pi R)\right)\psi_{L},$$

$$(D_{\mu}\psi_{R})_{y=\pi R} = \left(\partial_{\mu} - iT^{3}W_{\mu}^{3}(\pi R) - iY_{L}W_{\mu}^{3}(\pi R)\right)\psi_{R}$$

$$= \left(\partial_{\mu} - iY_{R}W_{\mu}^{3}(\pi R)\right)\psi_{R},$$
(5.24)

where the ψ_R hypercharge, Y_R , is related to Y_L by $Y_R = T^3 + Y_L$, as in the SM. Note that Y_R is a 2×2 diagonal matrix, with the u_R hypercharge on the upper left, and the d_R hypercharge on the lower right. Therefore, at $y = \pi R$ the covariant derivative term, $\bar{\psi}_R \gamma^\mu D_\mu \psi_R$, splits into two separately gauge invariant terms, $\bar{u}_R \gamma^\mu D_\mu u_R$ and $\bar{d}_R \gamma^\mu D_\mu d_R$, as in (5.22). Note also that in the limit of small t_L , t_{u_R} , and t_{d_R} the action $\mathcal{S}^{(II)}_{\text{fermion}}$ describes massless left-handed fermions gauged under an SU(2)×U(1)

group living on the left end of the fifth-dimensional interval, and massless right-handed fermions gauged under a U(1) living on the right end of the interval, exactly as in model I. It is the presence of the bulk fields which allow these light states to communicate with each other, supplying the analog of the Yukawa coupling of the SM, and giving mass to the fermions.

5.3.1 Fermion Masses and Wave Functions

In order to find the KK eigenstates for all fermion fields, we must diagonalize the free action. Let χ denote either u, the up-type fermions, or d, the down-type fermions. Turning off the gauge couplings, the action of (5.22) becomes $S_u^{(0)} + S_d^{(0)}$, where

$$S_{\lambda}^{(0)} = \int d^{4}x \int_{0}^{\pi R} dy \left[\frac{1}{\pi R} \left(\bar{\chi}_{L} i \gamma^{\mu} \partial_{\mu} \chi_{L} + \bar{\chi}_{R} i \gamma^{\mu} \partial_{\mu} \chi_{R} \right) \right]$$

$$- \frac{1}{2} \left(\bar{\chi}_{R} \partial_{5} \chi_{L} - \bar{\chi}_{L} \partial_{5} \chi_{R} + \text{ h.c.} \right) - M \left(\bar{\chi}_{R} \chi_{L} + \bar{\chi}_{L} \chi_{R} \right)$$

$$+ \delta(y - \epsilon) \frac{1}{t_{L}^{2}} \bar{\chi}_{L} i \gamma^{\mu} \partial_{\mu} \chi_{L} + \delta(\pi R - \epsilon - y) \frac{1}{t_{\chi_{R}}^{2}} \bar{\chi}_{R} i \gamma^{\mu} \partial_{\mu} \chi_{R} \right].$$
 (5.25)

In (5.25) we have explicitly included a finite ϵ to push the delta-function terms slightly away from the interval ends, allowing us to unambiguously impose the BCs

$$\chi_R(0) = 0 , \chi_L(\pi R) = 0.$$
(5.26)

The field equations in the bulk can be obtained by variation of $\mathcal{S}_{\chi}^{(0)}$. Integrating these equations around the δ -functions, taking the limit $\epsilon \to 0$, and using the boundary conditions (5.26), leads to alternative expressions for the boundary limits:

$$\lim_{y \to 0^{+}} \chi_{R} = -\frac{1}{t_{L}^{2}} i \gamma^{\mu} \partial_{\mu} \chi_{L}(0) ,$$

$$\lim_{y \to \pi R^{-}} \chi_{L} = -\frac{1}{t_{\lambda_{R}}^{2}} i \gamma^{\mu} \partial_{\mu} \chi_{R}(\pi R) . \qquad (5.27)$$

Comparing (5.26) with (5.27), we see that χ_R has a discontinuity at y = 0, but χ_L is continuous. Similarly, χ_L is discontinuous at $y = \pi R$, but χ_R is continuous.

The fermion fields can be expanded in a tower of four-dimensional KK states:

$$\chi_L(x,y) = \sum_{n=0}^{\infty} \alpha_{\chi_n}(y) \chi_{n_L}(x) ,$$

$$\chi_R(x,y) = \sum_{n=0}^{\infty} \beta_{\chi_n}(y) \chi_{n_R}(x) . \qquad (5.28)$$

The four dimensional fields χ_{n_L} and χ_{n_R} are the left-handed and right-handed projection, respectively, of a mass- m_n Dirac fermion, $\chi_n = \chi_{n_L} + \chi_{n_R}$. Wavefunctions and mass equations are obtained by diagonalizing (5.25). It is most convenient to treat the action as finite in the bulk (0 < y < πR) with (5.27) as BCs. In this case the bulk equations of motion become

$$\alpha_{\chi n}' + M\alpha_{\chi n} - m_n \beta_{\chi n} = 0 ,$$

$$\beta_{\chi n}' - M\beta_{\chi n} + m_n \alpha_{\chi n} = 0 ,$$
 (5.29)

with the BCs

$$\lim_{y \to 0^{+}} \beta_{\chi n}(0) = -\frac{\hat{m}_{n}}{t_{L}^{2}} \alpha_{\chi n}(0) ,$$

$$\lim_{y \to \pi R^{-}} \alpha_{\chi n}(\pi R) = -\frac{\hat{m}_{n}}{t_{\chi R}^{2}} \beta_{\chi n}(\pi R) .$$
(5.30)

(Recall that masses with a hat are expressed in units of $(\pi R)^{-1}$; i.e., $\hat{m} \equiv m\pi R$.) The wavefunctions must also satisfy the orthonormalization conditions

$$\int_{0}^{\pi R} dy \left[\frac{1}{\pi R} + \frac{1}{t_{L}^{2}} \delta(y) \right] \alpha_{\lambda n}(y) \alpha_{n'}(y) = \delta_{nn'} ,$$

$$\int_{0}^{\pi R} dy \left[\frac{1}{\pi R} + \frac{1}{t_{\chi R}^{2}} \delta(\pi R - y) \right] \beta_{\lambda n}(y) \beta_{n'}(y) = \delta_{nn'} , \qquad (5.31)$$

where the integrands, for equal n and n', should be interpreted as position probability densities for the left-handed and the right-handed fermions, respectively.

With the five-dimensional fermion fields propagating into the bulk, the four-dimensional charged-current and neutral-current Lagrangians involve not only KK gauge bosons, but also KK fermions. For one generation of quarks (or leptons), we have

$$\mathcal{L}_{CC}^{(II)} = \sum_{k,l,n} \frac{1}{\sqrt{2}} \, \bar{u}_k \gamma^{\mu} \left(g_{Ln,(u_k,d_l)}^{CC} P_L + g_{Rn,(u_k,d_l)}^{CC} P_R \right) d_l \, W_{n\mu}^{+} + \text{h.c.} ,$$

$$\mathcal{L}_{NC}^{(II)} = \sum_{k,l,n} \sum_{\chi=u,d} \bar{\chi}_k \gamma^{\mu} \left(g_{Ln,(\chi_k,\chi_l)}^{NC} P_L T^3 + g_{Rn,(\chi_k,\chi_l)}^{NC} P_R T^3 + g_{Qn}^{NC} Q \right) \chi_l \, Z_{n\mu}$$
(5.32)

where the coupling constants are given by

$$\begin{split} g^{CC}_{Ln,(u_k,d_l)} &= \int d^4x \int_0^{\pi R} dy \left[\frac{1}{\pi R} + \frac{\delta(y)}{t_L^2} \right] \alpha_{u_k}(y) \alpha_{d_l}(y) f_n(y) \;, \\ g^{CC}_{Rn,(u_k,d_l)} &= \int d^4x \int_0^{\pi R} \frac{dy}{\pi R} \beta_{u_k}(y) \beta_{d_l}(y) f_n(y) \;, \\ g^{NC}_{Ln,(\chi_k,\chi_l)} &= \int d^4x \int_0^{\pi R} dy \left[\frac{1}{\pi R} + \frac{\delta(y)}{t_L^2} \right] \alpha_{\chi_k}(y) \alpha_{\chi_l}(y) \left(g_n(y) - g_n(\pi R) \right) \;, \\ g^{NC}_{Rn,(\chi_k,\chi_l)} &= \int d^4x \int_0^{\pi R} \frac{dy}{\pi R} \beta_{\chi_k}(y) \beta_{\chi_l}(y) \left(g_n(y) - g_n(\pi R) \right) \;, \\ g^{NC}_{On} &= g_n(\pi R) \;. \end{split}$$
 (5.33)

Perturbative expressions for the fermion couplings can be found in appendix C for M=0.

The solutions to the mass equations are simplest in the case of zero bulk mass M. We study this case first and then look at the numerical solutions for nonzero M.

(i) M = 0. With no bulk mass, the solutions of (5.29) are

$$\alpha_{\lambda n} = A_n \left[\cos(m_n y) - \frac{\hat{m}_n}{t_L^2} \sin(m_n y) \right] ,$$

$$\beta_{\lambda n} = -A_n \left[\frac{\hat{m}_n}{t_L^2} \cos(m_n y) + \sin(m_n y) \right] . \tag{5.34}$$

Applying the boundary conditions given in (5.30) to these solutions leads to an equation for the fermion masses,

$$(t_L^2 + t_{\chi_R}^2)\hat{m}_n \tan \hat{m}_n + \hat{m}_n^2 = t_L^2 t_{\chi_R}^2 . {(5.35)}$$

The lowest mass state of the KK tower corresponds to a standard model fermion. This light mass can be easily obtained in a perturbation expansion if we assume t_L^2 to be small:

$$\hat{m}_0 = \frac{t_L t_{\chi_R}}{\sqrt{1 + t_{\chi_R}^2}} \left[1 - \frac{1 + t_{\chi_R}^2 + t_{\chi_R}^4/3}{2\left(1 + t_{\chi_R}^2\right)^2} t_L^2 + \mathcal{O}(t_L^4) \right] . \tag{5.36}$$

If we also assume $t_{\chi_R}^2$ to be small, the heavy state masses are

$$\hat{m}_n = \pi \left(n - \frac{1}{2} \right) \left[1 + \frac{t_L^2 + t_{\chi_R}^2}{\pi^2 \left(n - \frac{1}{2} \right)^2} + \mathcal{O}(t^4) \right] \quad n = 1, 2, \dots$$
 (5.37)

The normalization factor A_n can be fixed by requiring the KK states to be canonically normalized in the four-dimensional Lagrangian. We obtain

$$A_n = \left[\frac{1}{2} \left(1 + \frac{\sin 2\hat{m}_n}{2\hat{m}_n} \right) + \frac{1}{t_L^2} \cos^2 \hat{m}_n + \frac{\hat{m}_n^2}{2t_L^4} \left(1 - \frac{\sin 2\hat{m}_n}{2\hat{m}_n} \right) \right]^{-1/2} . \tag{5.38}$$

For t_L^2 small this gives

$$A_0 = t_L \left[1 - \frac{1 + t_{\chi_R}^2 + t_{\chi_R}^4 / 3}{2 \left(1 + t_{\chi_R}^2 \right)^2} t_L^2 + \mathcal{O}(t_L^4) \right] , \qquad (5.39)$$

for the lightest state, and for both t_L^2 and $t_{\chi_R}^2$ small this gives

$$A_n = \frac{\sqrt{2}t_L^2}{\pi \left(n - \frac{1}{2}\right)} \left[1 - \frac{3}{2} \frac{t_L^2 + t_{\chi R}^2}{\pi^2 \left(n - \frac{1}{2}\right)^2} + \mathcal{O}(t^4) \right] \quad n = 1, 2, ...,$$
 (5.40)

for the heavy states.

From (5.36) we see that the lightest fermion mass is suppressed by the factor $t_L t_{\chi_R}$. For small values of these parameters this lightest Dirac fermion lies mainly on the branes, with small contribution from the bulk. The left-handed bulk wave function $\alpha_0(y)$ goes to zero as $t_L \to 0$, and the right-handed bulk wave function $\beta_0(y)$ goes to zero as $t_R \to 0$. Since the fermion masses arise from the ∂_5 -terms, which mix left-handed and right-handed wave functions, it follows that m_0 goes to zero, as either $t_L \to 0$ or $t_R \to 0$.

Notice also that (5.36) and (5.37) are symmetric in t_L and t_{χ_R} . This was expected, since the mass equation is $t_L - t_{\chi_R}$ symmetric. However, we shall treat t_L and t_{χ_R} differently. For starters, t_L is an SU(2) invariant parameter, whereas t_{χ_R} can have different values for the up and down fermions. We shall take this distinction further by assuming that t_L is universal for all quarks and leptons, and that the different particle masses are determined by t_{χ_R} . We shall find in section 5.4 that if t_L is of order λ , it can be used to cancel the positive contribution to the S-parameter that comes from the gauge sector. To have an idea of the orders of magnitude involved, let us assume $R^{-1} \sim 1$ TeV and $t_L \sim \lambda \sim 10^{-1}$. Then t_{χ_R} ranges from $\sim 10^{-11}$ for the lightest neutrino, to $\sim 10^{-2}$ for the charm quark.

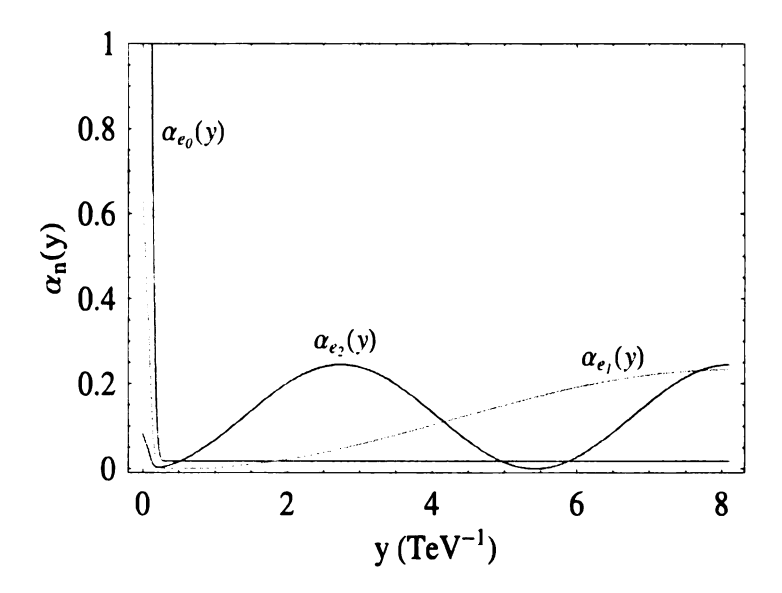


Figure 5.1: Probability density for the position of the left-handed electron (red), and its KK resonances, e_{L_1} (green), and e_{L_2} (blue) in the extra-dimensional (or TS) interval, for 1/R =500 GeV, and $t_L = \lambda/\sqrt{3}$, with $\delta(y)$ and $\delta(\pi R - y)$ replaced by narrow Gaussians.

All these features are made explicit in Fig. 5.1 and Fig. 5.2, where we show the position probability density in the $[0, \pi R]$ interval for the left-handed and the right-handed electron, respectively, together with the first two KK resonances, for 1/R = 500 GeV, and $t_L = \lambda/\sqrt{3}$. As we did previously for the gauge boson probability densities, we replaced $\delta(y)$ and $\delta(\pi R - y)$ with narrow Gaussians (with the same width, for a faithful comparison). We can directly observe the suppression in the bulk of $\alpha_e(y)$, and the very large suppression of $\beta_e(y)$. Correspondingly, the left-handed electron spends most of its time near the y=0 brane, while the right-handed electron spends virtually 100% of its time in proximity of the $y=\pi R$ brane. Notice that these considerations apply only to light fermions. We shall return to the issue of the third generation in chapter 6.

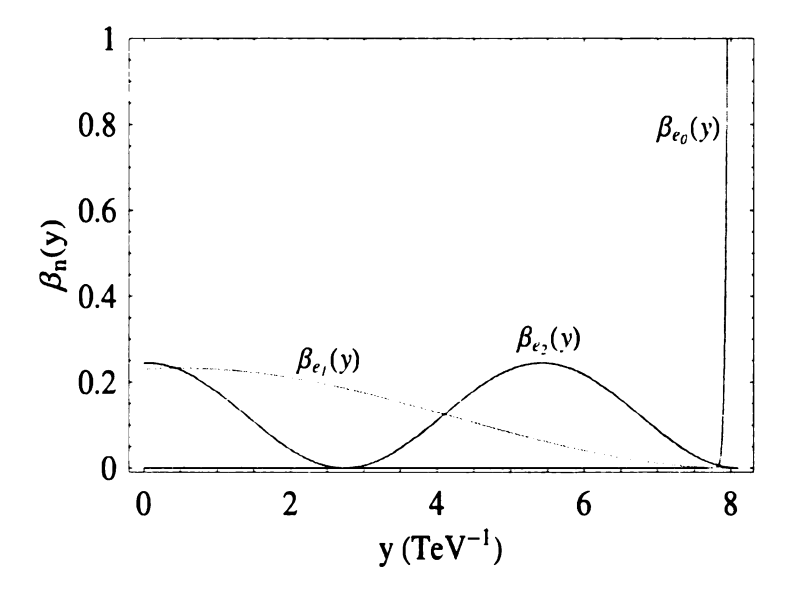


Figure 5.2: Probability density for the position of the right-handed electron (red), and its KK resonances, e_{R_1} (green), and e_{R_2} (blue) in the extra-dimensional (or TS) interval, for 1/R =500 GeV, and $t_L = \lambda/\sqrt{3}$, with $\delta(y)$ and $\delta(\pi R - y)$ replaced by narrow Gaussians.

(ii) $M \neq 0$. For nonzero bulk mass, the analysis is similar; the equations are just a bit longer. The equation for the fermion masses becomes

$$\left[\left(\hat{m}_n^2 + t_L^2 t_{\lambda R}^2 \right) \hat{M} + \left(t_L^2 + t_{\lambda R}^2 \right) \hat{m}_n^2 \right] T(m_n) = t_L^2 t_{\lambda R}^2 - \hat{m}_n^2 , \qquad (5.41)$$

where the function $T(m_n)$ depends on the relation between m_n and M:

$$T(m_n) = \begin{cases} \frac{1}{\sqrt{\hat{m}_n^2 - \hat{M}^2}} \tan \sqrt{\hat{m}_n^2 - \hat{M}^2} & \text{for } m_n > |M|, \\ \frac{1}{\sqrt{\hat{M}^2 - \hat{m}_n^2}} \tanh \sqrt{\hat{M}^2 - \hat{m}_n^2} & \text{for } |M| > m_n. \end{cases}$$
(5.42)

For a large and positive bulk mass $\hat{M} > 0$, $\hat{M} \gg 1$, there is one light solution to this mass equation, given approximately by

$$\hat{m}_0^2 \approx t_L^2 t_{\lambda R}^2 e^{-2\hat{M}} \ . \tag{5.43}$$

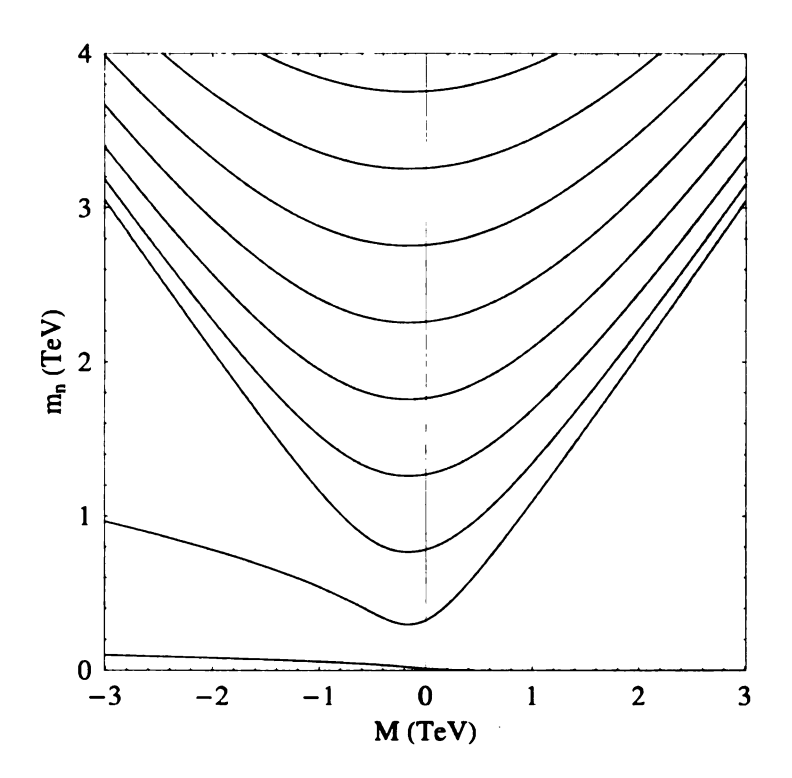


Figure 5.3: Masses of fermions, as a function of the bulk mass, for $t_L = 10^{-1}$, $t_R = 1$, and 1/R = 500 GeV.

For a large and negative bulk mass $\hat{M} < 0$, $|\hat{M}| \gg 1$, there are two light solutions, which are asymptotically given by (for $t_L < t_{\chi_R}$)

$$\hat{m}_{0}^{2} \approx 2|\hat{M}|t_{L}^{2}$$

 $\hat{m}_{1}^{2} \approx 2|\hat{M}|t_{\lambda R}^{2}$ (5.44)

This behavior is displayed in Fig. 5.3, where we plot the mass states as a function of the bulk mass M, with the other parameters fixed at $t_L = 10^{-1}$, $t_{\chi_R} = 1$, and 1/R = 500 GeV. The transformation $M \to -M$ can be shown to be equivalent to a reflection in the fifth dimension. Since the boundary conditions (5.26) that we have imposed are asymmetric in this reflection, we obtain the asymmetric behavior in $M \to -M$ of Fig. 5.3, even in the absence of the brane kinetic terms. The heavier modes are less asymmetric, because they are less affected by the boundaries.

5.3.2 Generation Mixings

It is not difficult to implement multiple generations in our fermion model II. In general the bulk mass, M, and the normalizations of the brane kinetic terms, t_L^{-2} , $t_{u_R}^{-2}$, and $t_{d_R}^{-2}$, would be independent 3×3 matrices for both the leptons and the quarks. However, this proliferation of mixing matrices would open the door to large flavor-changing neutral currents, which must somehow be avoided. The simplest way to achieve this is to restrict all of the flavor physics to the right brane, and impose a global $U(3)_{quark} \times U(3)_{lepton}$ symmetry on the quark and lepton doublets in the bulk and on the left brane. This flavor symmetry would only be broken by the kinetic terms on the right brane (which, incidentally, is also the only place where the SU(2) weak gauge symmetry is broken). The generalization of the fermion action in (5.22) is

$$S_{\text{fermion}}^{(II)} = \int d^4x \int_0^{\pi R} dy \left[\frac{1}{\pi R} \left(\frac{1}{2} \bar{\psi}^i i \Gamma^M D_M \psi^i + \text{ h.c.} - M \bar{\psi}^i \psi^i \right) \right] + \delta(y) \frac{1}{t_L^2} \bar{\psi}_L^i i \gamma^\mu D_\mu \psi_L^i + \delta(\pi R - y) \left(\bar{u}_R^i K_u^{ij} i \gamma^\mu D_\mu u_R^j + \bar{d}_R^i K_d^{ij} i \gamma^\mu D_\mu d_R^{j\prime} \right) \right],$$
(5.45)

where i and j are generation indices, and there is an equivalent contribution for leptons. In principle the t_L and M parameters, as well as the K matrices, can be different for the lepton and quark sectors. The five-dimensional fermion fields ψ^i 's can be considered four-dimensional Dirac fermions, which are also SU(2) doublets:

$$\psi^{i} = \psi_{L}^{i} + \psi_{R}^{i} = \begin{pmatrix} u_{L}^{i} \\ d_{L}^{i'} \end{pmatrix} + \begin{pmatrix} u_{R}^{i} \\ d_{R}^{i'} \end{pmatrix}$$
 (5.46)

The quark sector matrices K_u and K_d are arbitrary Hermitian matrices; however, we can exploit the U(3)_{quark} symmetry of the quark fields in the bulk and on the left brane to reduce the number of real physical parameters to 9 + 9 - (9 - 1) = 10, where we have taken into account the fact that the U(1) part of U(3) is just an overall phase symmetry. We can identify these 10 parameters as the six quark masses, and the four physical parameters of the CKM matrix. To see how this works, we first perform an SU(3) transformation on the ψ^i to diagonalize K_u . Thus, without loss of generality,

we can assume $K_u^{ij}=(t_{u_iR}^{-2})\delta^{ij}$. We can also assume that K_d^{ij} is diagonalized by a unitary matrix V, so that $K_d^{ij}=V^{ik}(t_{d_kR}^{-2})(V^\dagger)^{kj}$. We now relate the (primed) gauge eigenstates to the (unprimed) mass eigenstates by the redefinition $d_{L,R}^{ij}=V^{ij}d_{L,R}^{j}$. The action now becomes

$$S_{\text{fermion}}^{(II)} = \int_{0}^{\pi R} dy \int d^{4}x \left[\frac{1}{\pi R} \left(\frac{1}{2} \bar{\psi}^{i} i \Gamma^{M} D_{M} \psi^{i} + \text{h.c.} - M \bar{\psi}^{i} \psi^{i} \right) \right] + \delta(y) \frac{1}{t_{L}^{2}} \bar{\psi}_{L}^{i} i \gamma^{\mu} D_{\mu} \psi_{L}^{i} + \delta(\pi R - y) \left(\frac{1}{t_{u_{iR}}^{2}} \bar{u}_{R}^{i} i \gamma^{\mu} D_{\mu} u_{R}^{i} + \frac{1}{t_{d_{iR}}^{2}} \bar{d}_{R}^{i} i \gamma^{\mu} D_{\mu} d_{R}^{i} \right) \right],$$
(5.47)

where

$$\psi_L^i = \begin{pmatrix} u_L^i \\ V^{ij} d_L^j \end{pmatrix} , \quad \psi_R^i = \begin{pmatrix} u_R^i \\ V^{ij} d_R^j \end{pmatrix} . \tag{5.48}$$

The unitary matrix V corresponds precisely to the CKM matrix in the SM, only arising in terms that involve the exchange of charged SU(2) gauge bosons. Just as for the CKM matrix, it can be reduced to three real parameters and one phase, via five independent phase redefinitions of the $u_{L,R}$ and $d_{L,R}$ fields.

It is not difficult to see that any implementations of the SM can be mapped into this picture. In the lepton sector, for example, we could induce a see-saw mechanism by including a Majorana mass term for the neutrino, at $y = \pi R$. In that case the matrix V would contain two more physical parameters, corresponding to the Majorana phases of the MNS matrix. Alternatively, we could have a zero-mass neutrino, by imposing the boundary condition $\nu_R = 0$ at $y = \pi R$. In that case the number of physical parameters would be 9-(9-3)=3, corresponding to the three lepton masses.

5.4 Experimental Constraints on Model II

We would like now to study the experimental constraints on model II, starting from the four-dimensional Lagrangians (5.32), and the coupling strengths given in appendix C. We consider first the direct constraints on W_1 and Z_1 production, and then the indirect constraints of EWP data on the low energy effective Lagrangians.

5.4.1 Direct Constraints on Heavy Boson Production

With the fermions in the bulk, the overlap of the light fermion wavefunctions, with the heavy gauge boson wavefunctions is enhanced, relative to model I, by a factor of order $1/\lambda^2$. However the probability for the light fermions to be in the bulk is suppressed by a factor of order t_L^2 , and thus we expect the coupling of light fermions to heavy gauge bosons to be of the same size in model I and model II (for $t_L^2 \sim \lambda^2$).

However the cross sections for W_1 and Z_1 production change by numerical factors. The relation between the ratio $\sigma(q\bar{q}\to W_1\to\ell\nu)/\sigma(q\bar{q}\to W\to\ell\nu)$ in the SM and in model II is now

$$\label{eq:continuous} \left[\frac{\sigma(q\bar{q}\to W_1\to\ell\nu)}{\sigma(q\bar{q}\to W\to\ell\nu)}\right]^{(II)} = 2\frac{m_W^2}{m_{W_1}^2} \left(1-2\frac{t_L^2}{\lambda^2}\right)^2 \left[\frac{\sigma(q\bar{q}\to W_1\to\ell\nu)}{\sigma(q\bar{q}\to W\to\ell\nu)}\right]^{(\mathrm{SM})} \ , \ (5.49)$$

for M=0. In accordance with the results of the next section, we set $t_L=\lambda/\sqrt{3}$, so that last expression becomes

$$\left[\frac{\sigma(q\bar{q}\to W_1\to\ell\nu)}{\sigma(q\bar{q}\to W\to\ell\nu)}\right]^{(II)} = \frac{2}{9}\frac{m_W^2}{m_{W_1}^2} \left[\frac{\sigma(q\bar{q}\to W_1\to\ell\nu)}{\sigma(q\bar{q}\to W\to\ell\nu)}\right]^{(SM)} .$$
(5.50)

The suppression factor is nine times smaller than in model I (see eq. (5.5)). Rescaling the cross section shown in Fig. 2 of Ref. [72], we find $m_{W_1} > 350$ GeV, which is significantly weaker than the corresponding bound in model I. It can be shown that numerical factors also significantly weaken the bounds on m_{Z_1} , relative to the model with localized fermions.

5.4.2 Indirect Constraints on the Low Energy Fermion Lagrangians

In section 5.4.1 we argued that the couplings of light fermions (and SM gauge bosons) to heavy gauge bosons are also suppressed in model II as they were in model I. Therefore, dimension-five and dimension-six operators do not arise at λ^2 order, in the low-energy effective Lagrangian. Also, we observe that although the delocalization of fermion fields give rise to anomalous right-handed couplings, these must vanish as $t_{\lambda R} \to 0$, because in this limit the right-handed fields become exactly localized on the

 $y=\pi R$ boundary, where the five-dimensional $W^{\pm}(x,y)$ is zero, and $W^{3}(x,y)$ only couple with $Y_{R}\equiv Q_{R}$. Since $t_{\chi_{R}}$ is negligibly small for light fermions, no anomalous interactions are relevant at low energy.

Therefore, the new-physics constribution to the low-energy interactions is still oblique, with the charged-current and neutral-current Lagrangians given by (5.9). The couplings are now

$$g_L^{CC(II)} = g_L^{CC(I)} \int d^4x \int_0^{\pi R} dy \left[\frac{1}{\pi R} + \frac{\delta(y)}{t_L^2} \right] \alpha_u(y) \alpha_d(y) \frac{f_0(y)}{f_0(0)} ,$$

$$g_L^{NC(II)} = g_L^{NC(I)} \int d^4x \int_0^{\pi R} dy \left[\frac{1}{\pi R} + \frac{\delta(y)}{t_L^2} \right] \alpha_{u_k}(y) \alpha_{d_l}(y) \frac{g_0(y) - g_0(\pi R)}{g_0(0) - g_0(\pi R)} ,$$

$$g_Q^{NC(II)} = g_Q^{NC(I)} , \qquad (5.51)$$

where we used (5.4) and the normalization conditions (5.31). The ratios in (5.51) are positive and less than one,

$$0 \le \frac{f_0(y)}{f_0(0)} \approx \frac{g_0(y) - g_0(\pi R)}{g_0(0) - g_0(\pi R)} \approx 1 - \frac{y}{\pi R} \le 1 , \qquad (5.52)$$

and the suppression factors for g_L^{CC} and g_L^{NC} are identical to leading order in λ^2 .

Evaluating the integrals, we obtain

$$\begin{array}{lcl} g_L^{CC(II)} & = & g_L^{CC(I)}(1-At_L^2) \; , \\ g_L^{NC(II)} & = & g_L^{NC(I)}(1-At_L^2) \; , \\ g_Q^{NC(II)} & = & g_Q^{NC(I)} \; , \end{array} \tag{5.53}$$

where

$$A = e^{-\hat{M}} \frac{\sinh \hat{M}}{\hat{M}} - \frac{1}{2\hat{M}} \left(1 - e^{-\hat{M}} \frac{\sinh \hat{M}}{\hat{M}} \right) . \tag{5.54}$$

In the limit $\hat{M} \to 0$ we find $A \to 1/2$ [45]. By allowing the fermions to extend into the bulk, as in model II, one can cancel the effects of S in electroweak measurements. Comparing (5.53) with (5.12), we see that S can effectively be set to zero (while retaining T = U = 0) by the choice

$$t_L^2 = \frac{\lambda^2}{6A} \,. \tag{5.55}$$

5.4.3 Indirect Constraints on the Low Energy Gauge Lagrangian

In section 5.2.3 we analyzed in the constraints imposed by the EWP data on the WWZ vertex in model I. The results we found there can be easily adapted to model II. In fact, in equations (5.18), (5.19), and (5.20), the first line is also applicable to model II, because it is generically written in terms of the S parameter. We have just seen that the latter can be adjusted to zero in model II by setting $t_L = \lambda/\sqrt{3}$, for M = 0. Therefore, with this choice we obtain

$$G_F = \frac{1}{4\sqrt{2}m_W^2} \frac{e^2}{s^2} \left[1 + \mathcal{O}\left((m_W \pi R)^4 \right) \right] , \qquad (5.56)$$

for the Fermi constant,

$$s = s_Z \left[1 + \mathcal{O}\left((m_W \pi R)^4 \right) \right] , \qquad (5.57)$$

for the relation between the $\sin \theta_W$'s defined by (5.8) and (5.15), and

$$g_{WWZ} = e \frac{c_Z}{s_Z} \left[1 + \frac{(m_W \pi R)^2}{12c_Z^2} + \mathcal{O}\left((m_W \pi R)^4\right) \right]$$
 (5.58)

for the coupling in the WWZ vertex.

Comparing last equation with (5.14) gives

$$\Delta g_1^Z = \frac{(m_W \pi R)^2}{12c_Z^2} > 0 \ . \tag{5.59}$$

With this result, the 95% C.L. upper limit $|\Delta g_1^Z| < 0.028$ from LEP-II [76] translates into the lower bound $m_{W_1} > 498$ GeV for the W_1 mass. This is weaker than the corresponding bound with localized fermions, but stronger than the direct search bound we found in section 5.4.1.

The analyses of direct and indirect constraints in model II show that delocalizing fermions can always relieve the tension between unitarity and experimental data. However we have not yet considered the constraints imposed by the top quark phenomenology, which might be severe. In fact t_R may not be small enough to suppress anomalous right-handed couplings. Worse, there might not even be a t_R which gives a realistic top mass. We will see that this is indeed the case, and offer a solution to this problem in the next chapter.

Chapter 6

The Top Sector

In Section 5.3.1 it was shown that the fermion masses are suppressed by the factor $t_L t_{\chi_R}$. In Section 5.4.2, we saw that we could choose t_L to cancel gauge sector contributions to the S parameter, thereby relating t_L to λ by (5.55). Thus, we are left with t_{χ_R} as the final degree of freedom to fit the fermion masses. In this chapter we will see that this works well for all of the light fermions, except the top quark. In fact, accommodating a realistic top mass would require the increase of the value of 1/R beyond the bounds imposed by unitarity of the $W_L^+W_L^- \to W_L^+W_L^-$ scattering. We will then show that this problem can be solved by breaking the five-dimensional Lorentz symmetry, which leads to two independent compactification radii, or mass scales: One for the gauge sector, and one for the fermion sector. Upper bounds on the latter are then shown to arise from the $t\bar{t} \to W_L^+W_L^-$ scattering, and lower bounds from EWP data on the tbW vertex.

6.1 The Top Mass in Theory Space

In chapters 4 and 5 we have presented a Higgsless model of EWSB from continuum TS, whose full action is given by the sum of the gauge action (4.42), and the fermion action of model II, given by (5.22) (or (5.45), for multiple generations). In this model the overall mass scale is set by 1/R – which is required to be less than about a TeV in order to sufficiently delay unitarity in $W_L^+W_L^- \to W_L^+W_L^-$ scattering – and the other

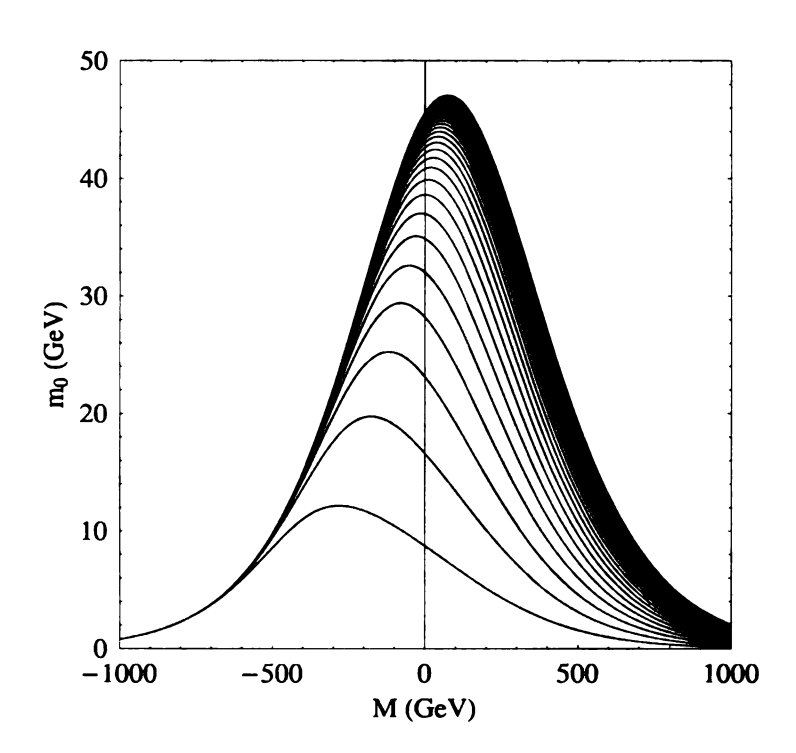


Figure 6.1: Mass of the lightest fermion, as a function of the bulk mass, for t_L chosen to adjust the S-parameter to zero, and 1/R = 500 GeV. The curves correspond to several values of t_{χ_R} , from 10^{-1} to infinity.

independent parameter is t_L (which measures the amount of leakage of left-handed fermions into the bulk) while the t_{χ_R} 's (which measure the amount of leakage of right-handed fermions into the bulk) are in a one-to-one correspondence with the SM fermion masses. In section 5.4.2 we saw that we could choose t_L to cancel gauge sector contributions to the S parameter, by relating t_L to λ by (5.55). Therefore, 1/R is left as the only free parameter beyond the SM.

With this setup, however, it is impossible to obtain a realistic top quark mass of 175 GeV. For example, for 1/R = 500 GeV, M = 0, and t_L fixed by (5.55), the lightest fermion mass solution to (5.41) has a maximum value of about 45 GeV. Even if we allow the bulk mass M to be nonzero, we cannot do much better, since (5.55) involves M in a dramatic way. In particular, when $M \to -\infty$, t_L tends exponentially

to zero, and so does m_0 . In the other limit of $M \to \infty$, the solution for m_0 itself is exponentially suppressed, as shown in (5.43). Thus we find a peak near M=0 in the curve for m_0 as a function of M (for fixed t_{χ_R}), as shown in Fig. 6.1. From this curve with 1/R=500 GeV, we find that the maximum possible quark mass for any value of M is about 47 GeV, which occurs for t_{χ_R} set to infinity.

One possible way to solve this problem is to allow a different t_L for the third generation of quarks. This approach might be viable, since the constraints on the S parameter do not directly involve the third generation fermions. However, we find it unattractive, since universality of t_L (and M) was the simplest way to avoid any dangerous flavor-changing neutral currents. Moreover, large values of t_L for the top-bottom doublet could lead to a violation of the experimental constraints on the $Zb\bar{b}$ vertex. An alternate solution that we prefer is to allow a different size of R for the gauge sector and the fermion sector. This possibility had been suggested in the context of the warped-space model in Ref. [46]. It is even more sensible in the context of a theory space, since there is no reason for the coefficients of $\bar{\psi}\Gamma^{\mu}D_{\mu}\psi$ and $\bar{\psi}\Gamma^{5}D_{5}\psi$ to be identical, in the bulk sector of (5.22). In terms of the deconstructed version of the theory, this just corresponds to allowing the gauge couplings and the Yukawa couplings to be independent of each other [20]. The most general extension of model II, with y-independent parameters, is described by the action $S_{\text{gauge}} + S_{\text{fermion}}^{(II)}$, where S_{gauge} is just the gauge sector action given in (4.42, and

$$S_{\text{fermion}}^{(II)\prime} = \int_{0}^{\pi R} dy \int d^{4}x \left[\frac{1}{\pi R} \left(\bar{\psi} i \Gamma^{\mu} D_{\mu} \psi + \kappa \left(\frac{1}{2} \bar{\psi} i \Gamma^{5} D_{5} \psi + \text{ h.c.} \right) - M \bar{\psi} \psi \right) \right.$$

$$+ \delta(y) \frac{1}{t_{L}^{2}} i \bar{\psi}_{L} \gamma^{\mu} D_{\mu} \psi_{L} + \delta(\pi R - y) \left(\frac{1}{t_{u_{R}}^{2}} i \bar{u}_{R} \gamma^{\mu} D_{\mu} u_{R} + \frac{1}{t_{d_{R}}^{2}} i \bar{d}_{R} \gamma^{\mu} D_{\mu} d_{R} \right) \right],$$

$$(6.1)$$

where κ is a new parameter. Notice that from an extra-dimensional point of view, this action corresponds to a theory with a microscopic breaking of the Lorentz invariance along the fifth dimension, in addition to the macroscopic breaking due to the compactification. Rescaling the parameter y by $y \to y' = y/\kappa$, the action $\mathcal{S}_{\text{fermion}}^{(II)\prime}$

becomes identical to $\mathcal{S}^{(II)}$, with R replaced by R/κ . Therefore, the gauge sector mass scale, $1/R_g \equiv 1/R$, and the fermion sector mass scale, $1/R_f \equiv \kappa/R$, are independent quantities in theory space: setting $R_f = R_g$ is an unnecessary and arbitrary choice.

With the action $S_{\text{fermion}}^{(II)\prime}$ replacing $S_{\text{fermion}}^{(II)}$, the fermion masses are (for M=0),

$$\hat{m}_0 = \kappa \frac{t_L t_{\chi_R}}{\sqrt{1 + t_{\chi_R}^2}} \left[1 - \frac{1 + t_{\chi_R}^2 + t_{\chi_R}^4/3}{2\left(1 + t_{\chi_R}^2\right)^2} t_L^2 + \mathcal{O}(t_L^4) \right] , \qquad (6.2)$$

$$\hat{m}_n = \kappa \pi \left(n - \frac{1}{2} \right) \left[1 + \frac{t_L^2 + t_{\chi_R}^2}{\pi^2 \left(n - \frac{1}{2} \right)^2} + \mathcal{O}(t^4) \right] \quad n = 1, 2, \dots$$
 (6.3)

Now we can account for m_t by simply increasing κ . Of course κ cannot be too large, due to unitarity constraints similar to those which give bounds on $1/R_g$. In the case of $1/R_f$ the limits come from scattering processes such as $t\bar{t} \to W_L^+ W_L^-$. We shall investigate these unitarity bounds in the next section.

6.2 Unitarity of Fermion Scattering Amplitudes

Here we shall restrict ourselves to considering the unitarity bounds coming from the $t\bar{t} \to W_L^+ W_L^-$ scattering process. General constraints on couplings in Higgsless models from this and related processes have been considered previously in Ref. [79]. In the SM, the tree-level $t\bar{t} \to W_L^+ W_L^-$ scattering amplitude is given by the four diagrams of Fig. 6.2(a). If t and \bar{t} have opposite helicities, the γ - and Z-exchange diagrams produce quadratically divergent terms, in the high-energy limit, which are cancelled by the b-exchange diagram [11]. The Higgs boson is not involved in this cancellation, which is confined to the J=1 partial wave, so there is no quadratic growth of the amplitude with energy, regardless of the Higgs boson mass. If t and \bar{t} have the same helicity, the b-exchange diagram produces a linearly divergent high-energy term in the J=0 channel, which is cancelled by the Higgs boson exchange diagram.

In our Higgsless model the Higgs boson exchange diagram, of course, does not occur. The γ -, Z-, and b-exchange diagrams are supplemented by corresponding dia-

¹The only difference is the interaction term with W_5^a , which is zero in unitary gauge anyway.

$$t = \sum_{\gamma+Z} \begin{pmatrix} W_L^+ \\ W_L^- \end{pmatrix} + \sum_{n=1}^{\infty} Z_n \begin{pmatrix} A_n \\ A_n \end{pmatrix} + \sum_{n=1}^{\infty} A_n \begin{pmatrix} A_n \\ A_n$$

Figure 6.2: (a) Diagrams contributing to the $t\bar{t} \to W_L^+ W_L^-$ tree-level scattering amplitude in the SM. (b) Same process, in our Higgsless model.

grams with exchange of heavy Z_n 's and b_n 's, as shown in Fig. 6.2(b). As $1/R_f \to \infty$, these heavy Z_n 's and b_n 's are removed from the theory, which becomes equivalent to the SM without the Higgs boson. Thus, it is reasonable to expect that the cancellation that occurs for opposite helicity t and \bar{t} in the SM also occurs in our Higgsless model, and that the amplitude does not display quadratic energy growth at any scale. We have directly verified this in our model. However, if the t and \bar{t} have the same helicity, the linear growth in energy, that was cancelled by Higgs boson exchange in the SM, now must be cancelled by some other sector of the theory. In our Higgsless model this cancellation occurs through the b_n -exchange diagrams. In this respect, the heavy b-quarks play the role of the SM Higgs boson for this scattering process.

In section 4.3.3 we used the quadratic growth in energy of the $W_L^+W_L^- \to W_L^+W_L^-$ scattering amplitude to place approximate bounds on the scale $1/R_g$, where the heavy vector states come in to restore unitarity. We can now do the same here, using the $t\bar{t} \to W_L^+W_L^-$ process to place approximate bounds on $1/R_f$. Note that, since the fermion amplitude only shows linear growth with energy in the high-energy limit, the

corresponding limits on the heavy fermion states will be significantly weaker.

For left-handed t and \bar{t} , the J=0 partial wave amplitude is given by

$$a_{0}(t_{L}\bar{t}_{L} \to W_{L}^{+}W_{L}^{-}) = \frac{1}{64\pi} \sum_{n=0}^{\infty} \frac{1}{p^{2} + k^{2} + m_{bn}^{2}} \left[\left((h_{Ln}^{CC})^{2} + (h_{Rn}^{CC})^{2} \right) \left(m_{t}kg(\xi_{n}) + 2\frac{m_{t}}{m_{W}^{2}} pE^{2}h(\xi_{n}) - m_{t}pf(\xi_{n}) \right) + \frac{m_{bn}}{m_{W}^{2}} h_{Ln}^{CC} h_{Rn}^{CC} \left(4kE^{2}g(\xi_{n}) - 2p(2E^{2} - m_{W}^{2})f(\xi_{n}) \right) \right],$$

$$(6.4)$$

where

$$\xi_n \equiv \frac{2pk}{p^2 + k^2 + m_{b_n}^2} \,, \tag{6.5}$$

E and p are the t (or \bar{t}) energy and momentum, respectively, k is the W_L^+ (or W_L^-) momentum, and m_{bn} is the b_n mass, with $m_{b0} \equiv m_b$. The functions f(x), g(x), and h(x) are

$$f(x) = \frac{1}{x} \ln \frac{1+x}{1-x} ,$$

$$g(x) = -\frac{2}{x} \left(1 - \frac{1}{2x} \ln \frac{1+x}{1-x} \right) ,$$

$$h(x) = \frac{2}{x^2} \left(1 - \frac{1-x^2}{2x} \ln \frac{1+x}{1-x} \right) .$$
(6.6)

Using the notation of eq. (5.33), the couplings are $h_{Ln}^{CC} \equiv g_{L0,(t_0,b_n)}^{CC}$ and $h_{Rn}^{CC} \equiv g_{R0,(t_0,b_n)}^{CC}$. For M=0, to leading order in t_L^2 , $t_{b_R}^2$, and λ^2 , the formulas of appendix C give

$$h_{L0}^{CC} = g \left[1 + \mathcal{O}(t^2) \right] ,$$

$$h_{Ln}^{CC} = g \frac{\sqrt{2}t_L}{1 + t_{t_R}^2} \left[\frac{(-1)^{n+1}}{\pi^2 \left(n - \frac{1}{2} \right)^2} + \frac{2t_{t_R}^2}{\pi^3 \left(n - \frac{1}{2} \right)^3} \right] \left[1 + \mathcal{O}(t^2) \right] \quad n = 1, 2, \dots ,$$

$$h_{R0}^{CC} = g \frac{t_{t_R} t_{b_R}}{2\sqrt{1 + t_{t_R}^2}} \left[1 + \mathcal{O}(t^2) \right] ,$$

$$h_{Rn}^{CC} = g \frac{\sqrt{2}}{\pi^2 \left(n - \frac{1}{2} \right)^2} \frac{t_{t_R}}{\sqrt{1 + t_{t_R}^2}} \left[1 + \mathcal{O}(t^2) \right] \quad n = 1, 2, \dots .$$

$$(6.7)$$

In the high energy limit, (6.4) becomes

$$a_0(t_L \bar{t}_L \to W_L^+ W_L^-) \simeq \frac{1}{32\pi} \frac{m_t E}{m_W^2} \sum_{n=0}^{\infty} \left((h_{Ln}^{CC})^2 + (h_{Rn}^{CC})^2 - 2 \frac{m_{b_n}}{m_t} h_{Ln}^{CC} h_{Rn}^{CC} \right). \tag{6.8}$$

It is straightforward to show that this vanishes, to leading order in t_L^2 , $t_{b_R}^2$, and λ^2 , using the couplings given in (6.7) and the masses given in (6.2) and (6.3), applied to m_t and m_{b_R} , respectively. In fact, using the completeness relations

$$\sum_{n=0}^{\infty} \left[\frac{1}{\pi R} + \frac{\delta(y)}{t_L^2} \right] \alpha_{bn}(y) \alpha_{bn}(y') = \delta(y - y') ,$$

$$\sum_{n=0}^{\infty} \left[\frac{1}{\pi R} + \frac{\delta(y)}{t_{bR}^2} \right] \beta_{bn}(y) \beta_{bn}(y') = \delta(y - y') ,$$
(6.9)

as well as the equations of motion, (5.29), and the boundary conditions, (5.30), for the t, and the b_n 's, it can be shown that

$$\sum_{n=0}^{\infty} \left[(h_{Ln}^{CC})^2 + (h_{Rn}^{CC})^2 - 2 \frac{m_{b_n}}{m_t} h_{Ln}^{CC} h_{Rn}^{CC} \right] \equiv 0 . \tag{6.10}$$

Therefore, this cancellation is exact in this model for any values of the couplings, and the linear growth in energy at high energies does not occur.

6.3 Bounds on the Model Parameters

Of course, the cancellation of the term that grows with energy is not a sufficient condition for the unitarization of the amplitude (6.4): The latter could stop growing after unitarity is already violated. The heavy b-quarks should come into play early enough to cancel the bad high-energy behavior, and this is only possible if $1/R_f$ is not too large. Enforcing (5.55), to keep S fixed at zero, and setting M=0, the only parameters that are not fixed by the light SM fermions and bosons are R_g and R_f , which set the scale for the heavy vector bosons and the heavy fermions, respectively. We can put some reasonable constraints on these two parameters by requiring that the $t_L \bar{t}_L \to W_L^+ W_L^-$ and the $W_L^+ W_L^- \to W_L^+ W_L^-$ scattering amplitudes remain unitary up to some value of the center-of-mass energy \sqrt{s} . As an example, in Fig. 6.3 we display the region in the $(1/R_g, 1/R_f)$ plane that is allowed by the requirement that $a_0 < 1/2$ up to $\sqrt{s} = 10$ TeV or $\sqrt{s} = 5$ TeV for both scattering amplitudes. As expected, we see that $1/R_f$ can indeed be much larger than $1/R_g$. If we require the theory to respect unitarity up to $\sqrt{s} = 10$ TeV in both amplitudes, we find $1/R_g < 10$

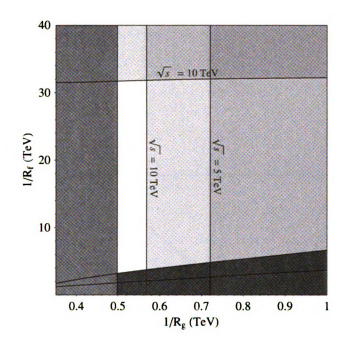


Figure 6.3: Bounds imposed by unitarity constraints on the $t\bar{t} \to W_L^+W_L^-$ scattering at $\sqrt{s}=10$ TeV (upper curve), and the $W_L^+W_L^- \to W_L^+W_L^-$ scattering at $\sqrt{s}=10$ TeV and $\sqrt{s}=5$ TeV (vertical lines), in the $(1/R_g,1/R_f)$ plane. Specifically, we have assumed the requirement of $a_0<1/2$ for both scattering processes. The $t\bar{t} \to W_L^+W_L^-$ scattering at $\sqrt{s}=5$ TeV imposes no bound, since at this energy the no Higgs boson is required to unitarize the amplitude. The two curves on the bottom correspond to the minimum value of $1/R_f$ which allows a top mass of 175 GeV to be a solution of the mass equation for M=0 (lower), and the minimum value of $1/R_f$ which gives a tbW right-handed coupling in agreement with the experimental constraint (upper). The vertical curve on the left corresponds to the experimental bound on m_{W_1} from analysis of the WWZ vertex.

570 GeV and $1/R_f < 32$ TeV. If we use the weaker requirement that the theory only respect unitarity up to $\sqrt{s} = 5$ TeV, then we find $1/R_g < 720$ GeV, while there is no constraint on $1/R_f$, since the $t_L \bar{t}_L \rightarrow W_L^+ W_L^-$ scattering amplitude does not violate unitarity at this energy even in the SM without a Higgs boson. Of course, any upper bounds on $1/R_g$ and $1/R_f$ depend on the somewhat arbitrary scale choice for \sqrt{s} ,

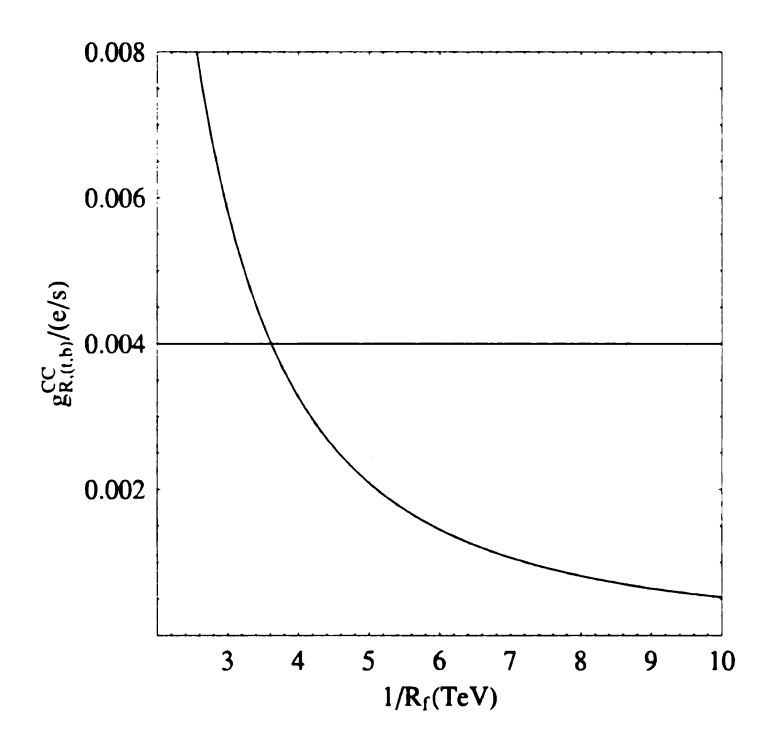


Figure 6.4: Right-handed tbW coupling, in units of e/s, for $1/R_g = 550$ GeV, as a function of $1/R_f$. The horizontal line corresponds to the experimental bound of Ref. [80].

where the low energy Higgsless theory has broken down.

Lower bounds on $1/R_g$ and $1/R_f$ can be obtained from experimental results. In section 5.4.3 we found the lower bound $1/R_g > 498$ GeV from indirect constraints on the WWZ vertex, while the corresponding direct search bounds were estimated in section 5.4.1 to be weaker. For the case of $1/R_f$, a minimal requirement is that it is large enough to accommodate a top quark mass of 175 GeV. This is displayed in the lower curve on the bottom of Fig. 6.3. It gives a lower bound of $1/R_f > 1-3$ TeV, with the dependence on $1/R_g$ entering through the condition imposed by (5.55). However, this curve corresponds to an infinite value of t_{t_R} , which is not viable. Tighter constraints can be obtained by limits on the right-handed tbW and

ttZ couplings, which in appendix C are evaluated to lowest order in t_{t_R} , t_{b_R} to be

$$g_{R,(t,b)}^{CC} = \frac{g}{2} t_{t_R} t_{b_R} \left[1 + \mathcal{O}(\lambda^2, t^2) \right] ,$$

$$g_{R,(t,t)}^{NC} = \frac{g}{2c} t_{R}^2 \left[1 + \mathcal{O}(\lambda^2, t^2) \right] .$$
(6.11)

For example, in Ref. [80] it is estimated, using experimental results on the $b\to s\gamma$ process, that $g_{R,(t,b)}^{NC}/g \leq 0.4\cdot 10^{-2}$, at the 2σ level. The corresponding bound on $1/R_f$ is displayed in the upper curve on the bottom of Fig. 6.3. For the particular value of $1/R_g = 550$ GeV, we can see how the coupling $g_R^{CC}(t,b,W^\pm)/g$ (where we have used $g \equiv e/s$) varies with $1/R_f$ in Fig. 6.4. The experimental bound is satisfied for this value of $1/R_g$ by $1/R_f$ 3.6 TeV, which corresponds to κ 6.5. An even stronger bound might be obtainable from limits on the right-handed neutral current coupling, since it is quadratic in the parameter t_R ; however, the extraction of this coupling requires more detailed analysis of higher order effects at the Z-pole in our model. Notice, however, that there is no tree-level constraint on $1/R_f$ coming from the right-handed $Zb\bar{b}$ coupling, because t_{bR} is a negligibly small quantity.

Chapter 7

Conclusions

In this dissertation we have built a phenomenologically viable Higgsless model from theory space, with inspiration from the physics of one compactified extra-dimension. It is a well known fact that a gauge theory on an extra-dimensional interval corresponds to a four-dimensional theory with an enhanced gauge symmetry. This large symmetry structure has the important property of unitarizing the longitudinal gauge boson scattering amplitudes. The unitarization occurs through exchanges of virtual Kaluza-Klein modes, which ensure the cancellation of the terms growing like E^4 and E^2 , playing in this way the role which is played by the Higgs boson in the Standard Model and its most common extensions. This is only true, however, for boundary conditions on the five-dimensional gauge fields which are consistent with the variational principle. Moreover, rather than restoring unitarity at (almost) all energies, as in the Standard Model, the Kaluza-Klein modes lead to a delay of unitarity violation to energy scales higher than the customary limits of Dicus-Mathur or Lee-Quigg-Thacker. Therefore, any Higgsless model should be regarded as an effective field theory, valid up to the energy scale of unitarity violation.

Our model contains three features, which are crucial to any viable Higgsless model of electroweak symmetry breaking. First, it contains a tower of vector bosons which delay the unitarity violation in the $W_LW_L \to W_LW_L$ and $W_LZ_L \to W_LZ_L$ scattering amplitudes, while giving the correct mass for the standard model W and Z (and photon) as the lightest states in the tower. Thus, it can extend the applicability

of the effective Higgsless theory up to a higher scale in the 5-10 TeV range. This is accomplished using an SU(2) gauge symmetry on a theory-space interval, broken down to U(1) at the right end of the interval, and with gauge kinetic terms on each end of the interval. The normalization (λ, λ') of the gauge kinetic terms on the boundaries are easily arranged to give the correct mass for the SM W and Z bosons.

Second, it incorporates a cancellation of the large vector boson contributions to the S parameter, which generically occur in Higgsless models. This cancellation is obtained by allowing the light fermion wave functions to leak away from the ends of the interval. In our model this leakage arises through boundary conditions and boundary kinetic terms for the fermions, where the light left-handed fields are predominantly located at the left end of the interval and the right-handed fields are predominantly located at the right end of the interval. The leakage of the left-handed fields into the bulk can be made to cancel the gauge boson contributions to S, while keeping the T and U parameters naturally suppressed, by tuning the normalization (t_L) of the universal left-handed fermion kinetic term on the left boundary. Meanwhile the normalization (t_{χ_R}) of the right-handed fermion kinetic terms on the right boundary can be used to give the correct mass for each of the light fermions. Furthermore, multiple generations and fermion mixings are implemented in the model, without introducing flavor-changing neutral currents, by confining all flavor physics to the right-handed fermion brane kinetic terms, and imposing a global $U(3)_{quark} \times U(3)_{lepton}$ symmetry on the bulk and left brane.

Third, it has a realistic top quark mass and small nonstandard right-handed top and bottom couplings. To obtain this goal, while maintaining the good unitarity properties of the W_LW_L scattering, it was necessary to separate the overall gauge sector scale $(1/R_g)$ from the overall fermion sector scale $(1/R_f)$. This requires an explicit breaking of the five-dimensional Lorentz symmetry, which is theoretically allowed, since such symmetry is already broken by compactification and brane kinetic terms. In fact, within a theory-space model it can be considered natural, since the difference in the size of the scales is analogous to having different sizes of gauge and Yukawa couplings. By making $1/R_f$ larger than $1/R_g$, it is possible to obtain the

top quark mass. It is also possible to suppress any nonstandard right-handed top and bottom couplings, since for a fixed fermion mass, an increase in $1/R_f$ requires a compensatory decrease in t_{χ_R} , leading to a decrease in right-handed couplings.

In this way, we have constructed a viable Higgsless model with only three undetermined parameters, $1/R_g$, $1/R_f$, and the bulk fermion mass M. Since the bulk fermion mass does not seem to add any qualitatively new features to the model, it is reasonable to set M=0, leaving us with a two-parameter model. The parameter $1/R_g$ sets the scale of the vector boson excitations, and the parameter $1/R_f$ sets the scale of the fermionic excitations. Just as the scale $1/R_g$ cannot be too large and still effectively delay unitarity violation in $W_L W_L \to W_L W_L$ scattering, the scale $1/R_f$ cannot be too large and still effectively delay unitarity violation in $t\bar{t} \to W_L W_L$ scattering. Thus, both of these scales are bounded from above, the exact bounds depending on the energy scale at which the effective Higgsless theory must be replaced by a more complete theory. A reasonable upper bound for $1/R_g$ is in the 570-720 GeV range, while the upper bound for $1/R_f$ is much weaker, of order 30 TeV or more. Experimental lower limits on $1/R_f$ from right-handed tbW couplings are in the range of 2-4 TeV. Precise experimental lower limits on $1/R_g$ require further investigation, although given the small couplings between the light fermions and the heavy W' and Z' states, there appears to be a reasonable range for this parameter that is still allowed.

In conclusion, we have presented an existence proof of a viable Higgsless model, that can satisfy all current experimental constraints, as far as we know. It is certainly not the only Higgsless model that may work, and it is probably too simplistic in many regards, but it has all of the features that any Higgsless model must have. Thus, it offers a concrete example for use to explore the phenomenology of Higgsless models at the Tevatron and the LHC. In particular, it is worthwhile to further investigate its most relevant phenomenological aspects, with careful attention to those features which are general, rather than characteristic of any particular model.

Appendix A

Solutions for the

$SU(2)_0 \times SU(2)_1 \times U(1)$ Model

In this model there are five independent parameters: $g, \tilde{g}, g', f_1, f_2$. We can express these in terms of the SM parameters e, m_W, m_Z , and the masses of the heavy vector bosons, $m_{W'}, m_{Z'}$:

$$g'^{2} = e^{2} \frac{m_{Z}^{2} m_{Z'}^{2}}{m_{W}^{2} m_{W'}^{2}},$$

$$\tilde{g}^{2} = g'^{2} \frac{(m_{W}^{2} + m_{W'}^{2})(m_{Z}^{2} + m_{Z'}^{2} - m_{W}^{2} - m_{W'}^{2}) + m_{W}^{2} m_{W'}^{2} - m_{Z}^{2} m_{Z'}^{2}}{(m_{Z}^{2} + m_{Z'}^{2} - m_{W}^{2} - m_{W'}^{2})},$$

$$g^{2} = g'^{2} \frac{m_{W'}^{2} m_{W'}^{2}((m_{W'}^{2} + m_{W'}^{2})(m_{Z}^{2} + m_{Z'}^{2} - m_{W}^{2} - m_{W'}^{2}) + m_{W}^{2} m_{W'}^{2} - m_{Z}^{2} m_{Z'}^{2})}{(m_{Z}^{2} - m_{Z'}^{2})(m_{Z'}^{2} - m_{W'}^{2})(m_{Z'}^{2} - m_{W}^{2})(m_{W'}^{2} - m_{Z}^{2})},$$

$$f_{1}^{2} = \frac{16}{g^{2} \tilde{g}^{2}} \frac{m_{W'}^{2} m_{W'}^{2}}{f_{2}^{2}},$$

$$f_{2}^{2} = \frac{4}{g'^{2}}(m_{Z}^{2} + m_{Z'}^{2} - m_{W'}^{2} - m_{W'}^{2}).$$
(A.1)

The charged boson mixing matrix, defined in (4.22) is given by $a_{00} = a_{11} = \cos \phi$ and $-a_{01} = a_{10} = \sin \phi$, where

$$\cos^2 \phi = \frac{m_{W'}^2 (m_{W'}^2 - m_Z^2) (m_{Z'}^2 - m_{W'}^2)}{m_{W'}^2 (m_{W'}^2 - m_Z^2) (m_{Z'}^2 - m_{W'}^2) + m_W^2 (m_{Z'}^2 - m_W^2) (m_Z^2 - m_W^2)},$$

$$\sin^2 \phi = \frac{m_W^2 (m_{Z'}^2 - m_W^2) (m_Z^2 - m_W^2)}{m_{W'}^2 (m_{W'}^2 - m_Z^2) (m_{Z'}^2 - m_{W'}^2) + m_W^2 (m_{Z'}^2 - m_W^2) (m_Z^2 - m_W^2)}.$$

(A.2)

The neutral boson mixing matrix, defined in (4.23), is given by

$$b_{00} = \left[\frac{m_{W'}^2 m_{W'}^2 (m_{Z'}^2 - m_{W}^2) (m_{Z'}^2 - m_{W'}^2)}{m_{Z}^2 (m_{Z'}^2 - m_{Z}^2) M^4} \right]^{1/2} ,$$

$$b_{10} = \left[\frac{(m_{Z}^2 - m_{W'}^2) (m_{W'}^2 - m_{Z}^2)}{m_{Z}^2 (m_{Z'}^2 - m_{Z}^2) M^4} \right]^{1/2} (m_{W'}^2 + m_{W}^2 - m_{Z'}^2) ,$$

$$b_{20} = -\left[\frac{(m_{Z}^2 - m_{W'}^2) (m_{W'}^2 - m_{Z}^2)}{m_{Z}^2 (m_{Z'}^2 - m_{Z}^2)} \right]^{1/2} ,$$

$$b_{01} = -\left[\frac{m_{W}^2 m_{W'}^2 (m_{Z}^2 - m_{W'}^2) (m_{W'}^2 - m_{Z}^2)}{m_{Z}^2 (m_{Z'}^2 - m_{Z}^2) M^4} \right]^{1/2} ,$$

$$b_{11} = \left[\frac{(m_{Z'}^2 - m_{W}^2) (m_{Z'}^2 - m_{W'}^2)}{m_{Z}^2 (m_{Z'}^2 - m_{Z}^2) M^4} \right]^{1/2} (m_{W'}^2 + m_{W}^2 - m_{Z}^2) ,$$

$$b_{21} = -\left[\frac{(m_{Z'}^2 - m_{W}^2) (m_{Z'}^2 - m_{W'}^2)}{m_{Z'}^2 (m_{Z'}^2 - m_{Z}^2)} \right]^{1/2} ,$$
(A.3)

where

$$M^{4} = (m_{W}^{2} + m_{W'}^{2})(m_{Z}^{2} + m_{Z'}^{2} - m_{W}^{2} - m_{W'}^{2}) + m_{W}^{2}m_{W'}^{2} - m_{Z}^{2}m_{Z'}^{2}.$$
 (A.4)

Appendix B

Solutions for the

$$SU(2)\times SU(2)^N\times U(1)$$
 Model

The mass matrix for the charged bosons is

$$M_W^2 = \frac{\tilde{g}^2 f^2}{4} \begin{bmatrix} \frac{\lambda^2}{N+1} & -\frac{\lambda}{\sqrt{N+1}} & 0 & \cdots \\ -\frac{\lambda}{\sqrt{N+1}} & 2 & -1 & \cdots \\ 0 & -1 & 2 & \cdots \\ \vdots & \vdots & \vdots & \ddots & \vdots & \vdots \\ & & \cdots & 2 & -1 & 0 \\ & & & \cdots & -1 & 2 & -1 \\ & & & \cdots & 0 & -1 & 2 \end{bmatrix}, \quad (B.1)$$

where $\lambda = g\sqrt{N+1}/\tilde{g}$. Note that the sequence of $(-1\ 2\ -1)$ in each row of this matrix (except the first and the last two) acts as a discrete second derivative, whose

eigenfunction is a sine function. Thus, we try a solution of the form

$$\psi_{(n)} = C_{(n)} \begin{bmatrix} \frac{\sqrt{N+1}}{\lambda} \sin(N+1)\omega_{(n)} \\ \sin N\omega_{(n)} \\ \sin(N-1)\omega_{(n)} \\ \vdots \\ \sin 3\omega_{(n)} \\ \sin 2\omega_{(n)} \\ \sin \omega_{(n)} \end{bmatrix}, \quad (B.2)$$

where $C_{(n)}$ is a normalization constant and the eigenvalues are

$$m_{W_n'}^2 = \tilde{g}^2 f^2 \sin^2 \frac{\omega_{(n)}}{2}$$
 (B.3)

The coefficients of $\omega_{(n)}$, in (B.2), have been chosen to run downward from N+1 to 1, because in the underlying extra-dimensional model $W^{\pm}=0$ at $x^5=\pi R$. This corresponds to the (N+2)-th component to be $\sin(0\cdot\omega_{(n)})\equiv 0$. The first row of the eigenvector equation $M_{W'}^2\psi_{(n)}=m_{W_n}^2\psi_{(n)}$ gives the characteristic equation for this system

$$\sin^2 \frac{\omega}{2} \sin (N+1)\omega = \frac{\lambda^2}{4(N+1)} \left[\sin (N+1)\omega - \sin N\omega \right], \qquad (B.4)$$

which has N+1 solutions, $\omega_{(n)}$. Using this equation and trigonometric identities [77], we obtain a simple formula for the normalization constant

$$C_{(n)} = \left[\frac{N+1}{2} + \frac{\sin\left[2(N+1)\omega_{(n)}\right]}{4\sin\omega_{(n)}} \right]^{-1/2}$$
 (B.5)

Solving (B.4) perturbatively, and identifying the SM $W \equiv W_0'$, we obtain for the charged boson masses

$$m_{W'}^{2} = \frac{g^{2}f^{2}}{4(N+1)} \left[1 - \lambda^{2} \frac{N(2N+1)}{6(N+1)^{2}} + \mathcal{O}(\lambda^{4}) \right]$$

$$m_{W'_{n}}^{2} = \tilde{g}^{2}f^{2} \left(\sin \frac{n\pi}{2(N+1)} \right)^{2} + 2m_{W}^{2} \left(\cos \frac{n\pi}{2(N+1)} \right)^{2} \left(1 + \mathcal{O}(\lambda^{2}) \right) . \tag{B.6}$$

The elements of the charged boson mixing matrix are

$$a_{00} = 1 - \lambda^{2} \frac{N(2N+1)}{12(N+1)^{2}} + \mathcal{O}(\lambda^{4}) ,$$

$$a_{j0} = \lambda \frac{N+1-j}{(N+1)^{3/2}} + \mathcal{O}(\lambda^{3}) ,$$

$$a_{0n} = -\lambda \frac{\sqrt{2}}{N+1} \frac{\sin(\pi n N/(N+1))}{4\sin^{2}(\pi n/2(N+1))} + \mathcal{O}(\lambda^{3}) ,$$

$$a_{jn} = \sqrt{\frac{2}{N+1}} \sin \frac{\pi (N+1-j)n}{N+1} + \mathcal{O}(\lambda^{2}) ,$$
(B.7)

where j and n run from 1 to N.

The mass matrix for the neutral bosons is

$$M_Z^2 = \frac{\tilde{g}^2 f^2}{4} \begin{bmatrix} \frac{\lambda^2}{N+1} & -\frac{\lambda}{\sqrt{N+1}} & 0 & \cdots \\ -\frac{\lambda}{\sqrt{N+1}} & 2 & -1 & \cdots \\ 0 & -1 & 2 & \cdots \\ \vdots & \vdots & \vdots & \ddots & \vdots & \vdots \\ & & \cdots & 2 & -1 & 0 \\ & & \cdots & -1 & 2 & -\frac{\lambda'}{\sqrt{N+1}} \\ & & \cdots & 0 & -\frac{\lambda'}{\sqrt{N+1}} & \frac{\lambda'^2}{N+1} \end{bmatrix}, \quad (B.8)$$

where $\lambda' = g'\sqrt{N+1}/\tilde{g}$. The eigenvector equation $M_Z^2\chi_{(n)} = m_{Z_n}^2\chi_{(n)}$ can be solved in a similar manner to the charged mass matrix. The eigenvectors are

$$\chi_{(n)} = D_{(n)} \begin{bmatrix} \frac{\sqrt{N+1}}{\lambda} \sin \left[(N+1)\rho_{(n)} + \phi_{(n)} \right] \\ \sin \left[N\rho_{(n)} + \phi_{(n)} \right] \\ \sin \left[(N-1)\rho_{(n)} + \phi_{(n)} \right] \\ \vdots \\ \sin \left[2\rho_{(n)} + \phi_{(n)} \right] \\ \sin \left[\rho_{(n)} + \phi_{(n)} \right] \\ \frac{\sqrt{N+1}}{\lambda'} \sin \phi_{(n)} \end{bmatrix}, \quad (B.9)$$

where $D_{(n)}$ is a normalization constant and the eigenvalues are

$$m_{Z_n'}^2 = \tilde{g}^2 f^2 \sin^2 \frac{\rho_{(n)}}{2} .$$
 (B.10)

The characteristic equation for this system is

$$\sin^2 \frac{\rho}{2} \sin (N+1)\rho = \frac{\lambda^2 + \lambda'^2}{4(N+1)} \left[\sin (N+1)\rho - \sin N\rho \right] + \frac{\lambda^2 \lambda'^2}{4(N+1)^2} \sin N\rho , \quad (B.11)$$

which has N+2 solutions, $\rho_{(n)}$. The phase constant $\phi_{(n)}$ satisfies

$$\tan \phi_{(n)} \tan \frac{\rho_{(n)}}{2} = \frac{\lambda'^2}{\lambda'^2 - 2(N+1)}.$$
 (B.12)

Using (B.11) and (B.12), we obtain for the normalization constant

$$D_{(n)} = \left[\frac{N+1}{2} + \frac{\sin\left[(N+1)\rho_{(n)} \right] \cos\left[(N+1)\rho_{(n)} + 2\phi_{(n)} \right]}{2\sin\rho_{(n)}} \right]^{-1/2}$$
(B.13)

There is one trivial solution to (B.11) and (B.12), which corresponds to the photon solution: $\rho_{(\gamma)} = 0$, $\phi_{(\gamma)} = \pi/2$. In section 4.3.2, the mixing matrix elements for the photons were shown to be constant, and equal to the U(1)_Q coupling e. Identifying the standard model $Z \equiv Z'_0$, we obtain for the tremaining neutral boson masses

$$m_Z^2 = \frac{(g^2 + g'^2)f^2}{4(N+1)} \left[1 - (\lambda^2 + \lambda'^2) \frac{N(2N+1)}{6(N+1)^2} + \frac{\lambda^2 \lambda'^2}{\lambda^2 + \lambda'^2} \frac{N}{N+1} + \mathcal{O}(\lambda^4) \right].$$

$$m_{Z'_n}^2 = \tilde{g}^2 f^2 \left(\sin \frac{n\pi}{2(N+1)} \right)^2 + 2m_Z^2 \left(\cos \frac{n\pi}{2(N+1)} \right)^2 \left(1 + \mathcal{O}(\lambda^2) \right).$$
(B.14)

The elements of the charged boson mixing matrix are

$$b_{00} = \frac{g}{\sqrt{g^2 + g'^2}} \left[1 - (\lambda^2 + \lambda'^2) \frac{N(2N+1)}{12(N+1)^2} + \frac{\lambda'^4}{2(\lambda^2 + \lambda'^2)} \frac{N}{N+1} + \mathcal{O}(\lambda^4) \right],$$

$$b_{j0} = \frac{\lambda^2}{\sqrt{\lambda^2 + \lambda'^2}} \frac{N+1-j}{(N+1)^{3/2}} - \frac{\lambda'^2}{\sqrt{\lambda^2 + \lambda'^2}} \frac{j}{(N+1)^{3/2}} + \mathcal{O}(\lambda^3),$$

$$b_{(N+1)0} = -\frac{g'}{\sqrt{g^2 + g'^2}} \left[1 - (\lambda^2 + \lambda'^2) \frac{N(2N+1)}{12(N+1)^2} + \frac{\lambda^4}{2(\lambda^2 + \lambda'^2)} \frac{N}{N+1} + \mathcal{O}(\lambda^4) \right],$$

$$b_{0n} = -\lambda \sqrt{\frac{2}{N+1}} \frac{\sin \pi n N/(N+1)}{4 \sin^2 \pi n/2(N+1)} + \mathcal{O}(\lambda^3),$$

$$b_{jn} = \sqrt{\frac{2}{N+1}} \sin \frac{\pi (N+1-j)n}{N+1} + \mathcal{O}(\lambda^2) ,$$

$$b_{(N+1)n} = -\lambda' \sqrt{\frac{2}{N+1}} \frac{\sin \pi n/(N+1)}{4 \sin^2 \pi n/2(N+1)} + \mathcal{O}(\lambda^3) , \qquad (B.15)$$

where j and n run from 1 to N.

Finally, we can use the characteristic equations, (B.4), (B.11), and (B.12), along with the orthonormality of the rows of the Z' mixing matrix, to obtain a simple expression for the leading $E^2/m_{W'_n}^2$ term in the $W'_n^+W'_n^- \to W'_n^+W'_n^-$ scattering amplitude, which is the generalization of K in (4.38). We find

$$K_{(n)} = C_{(n)}^{4} \left(\frac{m_{W_{n}'}^{2}}{f^{2}}\right) \left[\frac{3}{2}(N+1) + \frac{\sin\left[2(N+1)\omega_{(n)}\right]}{\sin\omega_{(n)}} + \frac{\sin\left[4(N+1)\omega_{(n)}\right]}{4\sin2\omega_{(n)}}\right].$$
(B.16)

It is interesting to note that this quantity is exactly independent of g', and it falls off as $(N+1)^{-2}$ for large N. Setting n=0, we obtain the result for W^+W^- scattering in this model which, to first non-zero order in λ^2 , is

$$K = \frac{g^2}{(N+1)^2} \,. \tag{B.17}$$

Appendix C

Coupling Constants in Model II

C.1 Gauge Boson Couplings

The Feynman rules for the cubic and quartic vertices, in the continuum TS gauge model of section 4.3.3, are shown in Fig. C.1, where W_0 and Z_0 correspond to the W and Z boson, respectively. The coupling constants are

$$\begin{split} g_{W_0,W_0,W_0,W_0}^2 &= g^2 \left[1 - \frac{7}{15} \lambda^2 + \mathcal{O}(\lambda^4) \right] \;, \\ g_{W_k,W_0,W_0,W_0}^2 &= g^2 \; \lambda \frac{6\sqrt{2}(-1)^k}{k^3\pi^3} \left[1 + \mathcal{O}(\lambda^2) \right] \;, \\ g_{W_k,W_l,W_0,W_0}^2 &= g^2 \left[\left(\frac{1}{3} - \frac{1}{2k^2\pi^2} \right) \delta_{k,l} \right. \\ &\quad \left. + \frac{8(-1)^{k+l} \; k \; l}{(k^2 - l^2)^2\pi^2} \left(1 - \frac{\sin[(k-l)\pi]}{(k-l)\pi} \right)^2 \right] \left[1 + \mathcal{O}(\lambda^2) \right] \;, \\ g_{W_k,W_l,W_m,W_0}^2 &= g \; \hat{g}_5 \frac{(-1)^{k+l+m}}{2\sqrt{2}\pi} \left[\left(\frac{1}{l+m} - \frac{1}{l} - \frac{1}{m} \right) \delta_{k,l+m} \right. \\ &\quad \left. + \left(\frac{1}{m+k} - \frac{1}{m} - \frac{1}{k} \right) \delta_{l,m+k} + \left(\frac{1}{k+l} - \frac{1}{k} - \frac{1}{l} \right) \delta_{m,k+l} \right. \\ &\quad \left. + \frac{16 \; k \; l \; m}{k+l+m} \frac{1 - \sin[(k-l-m)\pi]/(k-l-m)\pi}{k-l-m} \right. \\ &\quad \times \frac{1 - \sin[(k+l-m)\pi]/(k+l-m)\pi}{k+l-m} \frac{1 - \sin[(k-l+m)\pi]/(k-l+m)\pi}{k-l+m} \right] \\ &\quad \left. \times \left[1 + \mathcal{O}(\lambda^2) \right] \;, \\ g_{W_k,W_l,W_m,W_n}^2 &= \hat{g}_5^2 \frac{(-1)^{k+l+m+n}}{2} \left[\delta_{k+l,m+n} + \delta_{k+m,l+n} + \delta_{k+n,l+m} \right. \end{split}$$

$$\begin{split} -\delta_{k,l+m+n} - \delta_{l,m+n+k} - \delta_{m,n+k+l} - \delta_{n,k+l+m} \bigg] \Big[1 + \mathcal{O}(\lambda^2) \Big] \;, \\ g_{W_0,W_0,Z_0,Z_0}^2 &= \frac{g^4}{g^2 + g'^2} \bigg[1 - \frac{14g^2 + 27g'^2 - 18g'^4/g^2 - g'^6/g^4}{30(g^2 + g'^2)} \lambda^2 + \mathcal{O}(\lambda^4) \bigg] \;, \\ g_{W_k,W_0,Z_0,Z_0}^2 &= \left(3g^2 + (1 + 2(-1)^k)g'^2 \right) \lambda^2 \frac{2\sqrt{2}(-1)^k}{k^3\pi^3} \bigg[1 + \mathcal{O}(\lambda^2) \bigg] \;, \\ g_{W_0,W_0,Z_m,Z_0}^2 &= \frac{(3g^2 + (2 + (-1)^m)g'^2)g}{\sqrt{g^2 + g'^2}} \lambda^2 \frac{2\sqrt{2}(-1)^k}{k^3\pi^3} \bigg[1 + \mathcal{O}(\lambda^2) \bigg] \;, \\ g_{W_k,W_l,Z_0,Z_0}^2 &= \bigg[\left(\frac{1}{3} \frac{g^4 - g^2g'^2 + g'^4}{g^2 + g'^2} - \frac{g^2 + g'^2}{2^k 2\pi^2} \right) \delta_{k,l} \\ &+ \frac{8 \left((-1)^{k+l}g^2 + g'^2 \right) k l}{(k^2 - l^2)^2\pi^2} \left(1 - \frac{\sin[(k - l)\pi]}{(k - l)\pi} \right)^2 \bigg] \left[1 + \mathcal{O}(\lambda^2) \right] \;, \\ g_{W_k,W_0,Z_m,Z_0}^2 &= \frac{g}{\sqrt{g^2 + g'^2}} \bigg[\left(\frac{g^2}{3} - \frac{g'^2}{6} - \frac{g^2 + g'^2}{2^k 2\pi^2} \right) \delta_{k,m} \\ &+ \frac{4(-1)^{k+m} \left(2g^2 + (1 + (-1)^{k+m})g'^2 \right) k m}{(k^2 - m^2)^2\pi^2} \left(1 - \frac{\sin[(k - m)\pi]}{(m - n)\pi} \right)^2 \bigg] \times \bigg[1 + \mathcal{O}(\lambda^2) \bigg] \;, \\ g_{W_0,W_0,Z_m,Z_0}^2 &= g^2 \bigg[\left(\frac{1}{3} - \frac{1}{2m^2\pi^2} \right) \delta_{m,n} \\ &+ \frac{8(-1)^{m+n} m n}{(m^2 - n^2)^2\pi^2} \left(1 - \frac{\sin[(m - n)\pi]}{(m - n)\pi} \right)^2 \bigg] \times \bigg[1 + \mathcal{O}(\lambda^2) \bigg] \;, \\ g_{W_k,W_l,Z_m,Z_0}^2 &= \sqrt{g^2 + g'^2} \, \hat{g}_5 \frac{(-1)^{k+l+m}}{2\sqrt{2\pi}} \bigg[\left(\frac{1}{l+m} - \frac{1}{l} - \frac{1}{l} \right) \delta_{k,l+m} \\ &+ \frac{g^2 + (-1)^{k+l+m}g'^2}{2^2 + g'^2} \frac{16 k l m}{k + l + m} \frac{1 - \sin[(k - l - m)\pi]/(k - l - m)\pi}{k - l - m} \\ \times \frac{1 - \sin[(k + l - m)\pi]/(k + l - m)\pi}{k + l - m} \frac{1 - \sin[(k - l - m)\pi]/(k - l + m)\pi}{k - l + m} \bigg] \\ \times \frac{1 - \sin[(k + l - m)\pi]/(k - l - m)\pi}{k + l - m} \frac{1 - \sin[(k - l + m)\pi]/(k - l + m)\pi}{k - l - m} \\ \times \frac{1 - (1 + k)^{k+m}}{k + l - m} \frac{1 - \sin[(k - l - m)\pi]/(k - l - m)\pi}{k - l - m} \\ \times \frac{1 - (1 + k)^{k+m}}{k + l - m} \frac{1 - \sin[(k - l - m)\pi]/(k - l - m)\pi}{k - l - m} \\ \times \frac{1 - (1 + k)^{k+m}}{k + l - m} \frac{1 - \sin[(k - l - m)\pi]/(k - l - m)\pi}{k - l - m} \\ \times \frac{1 - (1 + k)^{k+m}}{k + l - m} \frac{1 - \sin[(k - l - m)\pi]/(k - l - m)\pi}{k - l - m} \\ \times \frac{1 - (1 + k)^{k+m}}{k + l - m} \frac{1 - \sin[(k - l - m)\pi]/(k - l - m)\pi}{k - l - m} \\ \times \frac{1 - (1 + k)^{k+m}}{k + l - l - l - l} \frac{1}{k l m} \delta_{k,m+n} \\ \times \frac{1 - (1$$

$$W_{m}^{+} W_{n}^{+} W_{n}^{+} Z_{m} Z_{n}$$

$$= ig_{W_{k},W_{l},W_{m},W_{n}}^{2} S_{\mu\nu,\kappa\lambda} \qquad \qquad = ig_{W_{k},W_{l},Z_{m},Z_{n}}^{2} S_{\mu\nu,\kappa\lambda}$$

$$W_{k}^{-} W_{l}^{-} \qquad \qquad W_{k}^{-} W_{l}^{-}$$

$$S_{\mu\nu,\kappa\lambda} = 2g_{\mu\nu}g_{\kappa\lambda} - g_{\mu\kappa}g_{\nu\lambda} - g_{\mu\lambda}g_{\nu\kappa} \qquad (a)$$

$$k^{N_{k,\mu}^{+}} \underbrace{Z_{n,\sigma}^{q}}_{V_{l,\nu}^{-}} = ig_{W_{k}.W_{l}.Z_{n}} \left[g_{\mu\sigma}(k-q)_{\nu} + g_{\sigma\nu}(q-p)_{\mu} + g_{\nu\mu}(p-k)_{\sigma} \right]$$
(b)

Figure C.1: Feynman rules for gauge interactions.

$$\times \frac{1 - \sin[(k+m-n)\pi]/(k+m-n)\pi}{k+m-n} \frac{1 - \sin[(k-m+n)\pi]/(k-m+n)\pi}{k-m+n} \\ \times \left[1 + \mathcal{O}(\lambda^{2})\right] ,$$

$$g_{W_{k}.W_{l}.Z_{m},Z_{n}}^{2} = \hat{g}_{5}^{2} \frac{(-1)^{k+l+m+n}}{2} \left[\delta_{k+l,m+n} + \delta_{k+m,l+n} + \delta_{k+n,l+m} - \delta_{k,l+m+n} - \delta_{l,m+n+k} - \delta_{m,n+k+l} - \delta_{n,k+l+m}\right] \left[1 + \mathcal{O}(\lambda^{2})\right] , \quad (C.1)$$

for the quartic vertices, and

$$\begin{split} g_{W_0,W_0,Z_0} &= \frac{g^2}{\sqrt{g^2 + g'^2}} \left[1 - \frac{g^4 + 2g^2g'^2 - g'^4}{g^2(g^2 + g'^2)} \frac{\lambda^2}{4} + \mathcal{O}(\lambda^4) \right] \;, \\ g_{W_k,W_0,Z_0} &= -\frac{2\sqrt{2}\sqrt{g^2 + g'^2}\lambda}{n^3\pi^3} \left[(1 - (-1)^n) + \mathcal{O}(\lambda^4) \right] \;, \\ g_{W_0,W_0,Z_0} &= -\frac{2\sqrt{2}g\lambda}{n^3\pi^3} \left[(1 - (-1)^n) + \mathcal{O}(\lambda^4) \right] \;, \\ g_{W_k,W_l,Z_0} &= \frac{\sqrt{g^2 + g'^2}}{2} \left[kl(-1)^{k+l}\pi^2 \left(\frac{\sin\left((k+l)\pi/2\right)}{(k+l)\pi/2} \right)^2 \left(\frac{\sin\left((k-l)\pi/2\right)}{(k-l)\pi/2} \right)^2 + \delta_{kl} \frac{g^2 - g'^2}{g^2 + g'^2} \right] \left[1 + \mathcal{O}(\lambda^2) \right] \;, \end{split}$$

$$g_{W_k,W_0,Z_n} = \frac{g}{2} \left[kn(-1)^{k+n} \pi^2 \left(\frac{\sin((k+n)\pi/2)}{(k+n)\pi/2} \right)^2 \left(\frac{\sin((k-n)\pi/2)}{(k-n)\pi/2} \right)^2 + \delta_{kn} \right] \left[1 + \mathcal{O}(\lambda^2) \right] ,$$

$$g_{W_k,W_l,Z_n} = \frac{(-1)^n n \hat{g}_5}{\sqrt{2}\pi} \left[\frac{\sin((k+l+n)\pi/2)}{(k+l+n)/2} \frac{\sin((k+l-n)\pi/2)}{(k+l-n)/2} - \frac{\sin((k-l+n)\pi/2)}{(k-l+n)/2} \frac{\sin((k-l-n)\pi/2)}{(k-l-n)/2} \right] \left[1 + \mathcal{O}(\lambda^2) \right] , \quad (C.2)$$

for the cubic vertices. (In these expressions, and in the expressions below, whenever numerator and denominator vanish, the right formula can be obtained by taking the limit.) Notice that the vertices involving one or two photon lines can be obtained from (C.1), (C.2) by using the relations (4.51).

C.2 Fermion Couplings

The Feynman rules for the charged-current and neutral-current vertices in model II are shown in Fig. C.2. The corresponding coupling constants, for M=0, are

$$\begin{split} g^{CC}_{L0,(u_0.d_0)} &= g \left[1 - \frac{\lambda^2}{6} - \frac{t_L^2}{2} + \mathcal{O}(t^4) \right] \;, \\ g^{CC}_{L0,(u_k.d_0)} &= \frac{\sqrt{2} \; (-1)^{k+l} \; g \; t_L}{\left(k - \frac{1}{2} \right)^2 \pi^2} \left[1 + \mathcal{O}(t^2) \right] \;, \\ g^{CC}_{L0,(u_0.d_k)} &= \frac{\sqrt{2} \; (-1)^{k+l} \; g \; t_L}{\left(k - \frac{1}{2} \right)^2 \pi^2} \left[1 + \mathcal{O}(t^2) \right] \;, \\ g^{CC}_{L0,(u_k.d_l)} &= \frac{g}{2} \left[\left(\frac{\sin \left((k - l)\pi/2 \right)}{(k - l)\pi/2} \right)^2 - \left(\frac{\sin \left((k + l - 1)\pi/2 \right)}{(k + l - 1)\pi/2} \right)^2 \right] \left[1 + \mathcal{O}(t^2) \right] \;, \\ g^{CC}_{Ln,(u_0.d_0)} &= \frac{\sqrt{2} \; \hat{g}_5}{n\pi} \left[(1 - (-1)^n) t_L^2 + (-1)^n \lambda^2 + \mathcal{O}(t^4) \right] \;, \\ g^{CC}_{Ln,(u_0.d_0)} &= \frac{8}{\pi} \frac{n \; (-1)^{k+1} \; \hat{g}_5 \; t_L}{1 + 4k(k - 1) - 4n^2} \left[1 + \mathcal{O}(t^2) \right] \;, \\ g^{CC}_{Ln,(u_0.d_k)} &= \frac{8}{\pi} \frac{n \; (-1)^{k+1} \; \hat{g}_5 \; t_L}{1 + 4k(k - 1) - 4n^2} \left[1 + \mathcal{O}(t^2) \right] \;, \\ g^{CC}_{Ln,(u_k.d_l)} &= \frac{n \; \hat{g}_5}{\sqrt{2}\pi} \left[\frac{\sin \left((k - l + n)\pi/2 \right) \sin \left((k - l - n)\pi/2 \right)}{(k - l - n)/2} - \frac{\sin \left((k + l + n - 1)\pi/2 \right)}{(k + l + n - 1)/2} \frac{\sin \left((k + l - n - 1)\pi/2 \right)}{(k + l - n - 1)/2} \left[1 + \mathcal{O}(t^2) \right] \;, \end{split}$$

$$W_{n}^{+} = \frac{i}{\sqrt{2}} \left[g_{Ln,(u_{k},d_{l})}^{CC} P_{L} + g_{Rn,(u_{k},d_{l})}^{CC} P_{R} \right]$$
 (a)

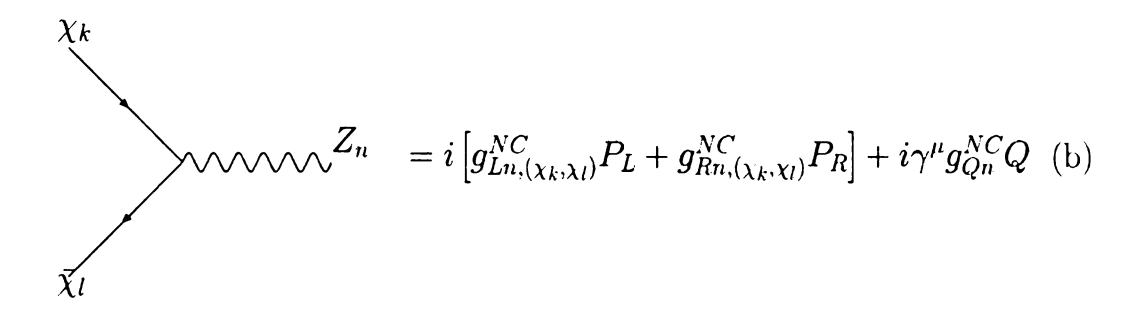


Figure C.2: Feynman rules for charge-current and neutral-current interactions.

$$\begin{split} g^{CC}_{R0,(u_0.d_0)} &= \frac{g \ tu_R \ td_R}{2} \left[1 + \mathcal{O}(t^2) \right] \ , \\ g^{CC}_{R0,(u_k.d_0)} &= \frac{\sqrt{2} \ g \ tu_R}{\left(k - \frac{1}{2} \right)^2 \pi^2} \left[1 + \mathcal{O}(t^2) \right] \ , \\ g^{CC}_{R0,(u_0.d_k)} &= \frac{\sqrt{2} \ g \ td_R}{\left(k - \frac{1}{2} \right)^2 \pi^2} \left[1 + \mathcal{O}(t^2) \right] \ , \\ g^{CC}_{R0,(u_k.d_l)} &= \frac{\left(-1 \right)^{k+l-1} g}{2} \left[\left(\frac{\sin \left((k-l)\pi/2 \right)}{(k-l)\pi/2} \right)^2 - \left(\frac{\sin \left((k+l-1)\pi/2 \right)}{(k+l-1)\pi/2} \right)^2 \right] \\ &\qquad \qquad \times \left[1 + \mathcal{O}(t^2) \right] \ , \\ g^{CC}_{Rn,(u_k.d_0)} &= \frac{8}{\pi} \frac{n \ (-1)^k \ \hat{g}_5 \ td_R}{1 + 4k(k-1) - 4n^2} \left[1 + \mathcal{O}(t^2) \right] \ , \\ g^{CC}_{Rn,(u_0.d_k)} &= \frac{8}{\pi} \frac{n \ (-1)^k \ \hat{g}_5 \ tu_R}{1 + 4k(k-1) - 4n^2} \left[1 + \mathcal{O}(t^2) \right] \ , \\ g^{CC}_{Rn,(u_k.d_l)} &= \frac{n \ (-1)^{k+l-n-1} \ \hat{g}_5}{\sqrt{2}\pi} \left[\frac{\sin \left((k-l+n)\pi/2 \right) \sin \left((k-l-n)\pi/2 \right)}{(k-l+n)/2} \frac{\sin \left((k-l-n)\pi/2 \right)}{(k-l-n)/2} \right. \\ &\qquad \qquad - \frac{\sin \left((k+l+n-1)\pi/2 \right) \sin \left((k+l-n-1)\pi/2 \right)}{(k+l+n-1)/2} \left[1 + \mathcal{O}(t^2) \right] \ . \end{split}$$

for the charged-current interactions, and

$$\begin{array}{ll} g^{NC}_{L0,(\chi_0,\chi_0)} &=& \sqrt{g^2+g'^2} \left[1 - \frac{g^4-g^2g'^2+g'^4}{g^2(g^2+g'^2)} \frac{\lambda^2}{6} - \frac{t_L^2}{2} + \mathcal{O}(l^4) \right] \;, \\ g^{NC}_{L0,(\chi_k,\chi_0)} &=& -\frac{\sqrt{2} \; (-1)^k \, \sqrt{g^2+g'^2} \; t_L}{\left(k-\frac{1}{2}\right)^2 \, \pi^2} \left[1 + \mathcal{O}(t^2) \right] \;, \\ g^{NC}_{L0,(\chi_k,\chi_0)} &=& \frac{\sqrt{g^2+g'^2}}{2} \left[\left(\frac{\sin\left((k-l)\pi/2\right)}{(k-l)\pi/2}\right)^2 - \left(\frac{\sin\left((k+l-1)\pi/2\right)}{(k+l-1)\pi/2}\right)^2 \right] \\ &\qquad \qquad \times \left[1 + \mathcal{O}(t^2) \right] \;, \\ g^{NC}_{Ln,(\chi_0,\chi_0)} &=& \frac{\sqrt{2} \; \hat{g}_5}{n\pi} \left[(1 - (-1)^n) t_L^2 + (-1)^n \frac{g^2 + (-1)^n g'^2}{g^2} \lambda^2 + \mathcal{O}(l^4) \right] \;, \\ g^{NC}_{Ln,(\chi_k,\chi_0)} &=& \frac{8}{\pi} \, \frac{n \; (-1)^{k+1} \; \hat{g}_5 \; t_L}{1 + 4k(k-1) - 4n^2} \left[1 + \mathcal{O}(t^2) \right] \;, \\ g^{NC}_{Ln,(\chi_k,\chi_0)} &=& \frac{n \; \hat{g}_5}{\sqrt{2}\pi} \left[\frac{\sin\left((k-l+n)\pi/2\right)}{(k-l+n)/2} \frac{\sin\left((k-l-n)\pi/2\right)}{(k-l-n)/2} \right] - \frac{\sin\left((k+l+n-1)\pi/2\right)}{(k+l+n-1)/2} \frac{\sin\left((k+l-n-1)\pi/2\right)}{(k+l-n-1)/2} \left[1 + \mathcal{O}(t^2) \right] \;, \\ g^{NC}_{R0,(\chi_0,\chi_0)} &=& \frac{\sqrt{2} \; g^2 + g'^2 \; t_R^2}{2} \left[1 + \mathcal{O}(t^2) \right] \;, \\ g^{NC}_{R0,(\chi_k,\chi_0)} &=& \frac{\sqrt{2} \; \hat{g}_5 \; t_R^2}{2} \left[1 + \mathcal{O}(t^2) \right] \;, \\ g^{NC}_{Rn,(\chi_0,\chi_0)} &=& \frac{\sqrt{2} \; \hat{g}_5 \; t_R^2}{n\pi} \left[1 - (-1)^n + \mathcal{O}(t^2) \right] \;. \\ g^{NC}_{Rn,(\chi_k,\chi_0)} &=& \frac{8}{\pi} \, \frac{n \; (-1)^k \, \hat{g}_5 \; t_{d_R}}{1 + 4k(k-1) - 4n^2} \left[1 + \mathcal{O}(t^2) \right] \;, \\ g^{NC}_{Rn,(\chi_k,\chi_0)} &=& \frac{n \; (-1)^{k+l-1} \; g}{n\pi} \left[\frac{\sin\left((k-l+n)\pi/2\right)}{(k-l+n)/2} \frac{\sin\left((k-l-n)\pi/2\right)}{(k-l-n)/2} - \frac{\sin\left((k-l-n)\pi/2\right)}{(k-l+n)/2} \frac{\sin\left((k-l-n)\pi/2\right)}{(k-l-n)/2} - \frac{\sin\left((k+l-n-1)\pi/2\right)}{(k+l-n-1)/2} \left[1 + \mathcal{O}(t^2) \right] \;, \\ g^{NC}_{Rn,(\chi_k,\chi_0)} &=& \frac{n \; (-1)^{k+l-n-1} \; \hat{g}_5}{\sqrt{2}\pi} \left[\frac{\sin\left((k-l+n)\pi/2\right)}{(k-l+n)/2} \frac{\sin\left((k-l-n)\pi/2\right)}{(k-l-n)/2} - \frac{\sin\left((k+l-n-1)\pi/2\right)}{(k+l-n-1)/2} \left[1 + \mathcal{O}(t^2) \right] \;, \\ g^{NC}_{Q0} &=& -\frac{g'^2}{\sqrt{a^2+g'^2}} \left[1 + \frac{2g^4 - 2g^2g'^2 - g'^4}{g^2(g^2+g'^2)} \frac{\delta}{6} + \mathcal{O}(\lambda^4) \right] \;, \end{array}$$

$$g_{Qn}^{NC} = -\frac{g'^2}{g} \frac{\sqrt{2} \lambda}{n\pi} \left[1 + \mathcal{O}(\lambda^2) \right] , \qquad (C.4)$$

for the neutral-current interactions.

Bibliography

- [1] P. W. Higgs, "Broken Symmetries And The Masses Of Gauge Bosons," Phys. Rev. Lett. 13, 508 (1964).
- [2] G. S. Guralnik, C. R. Hagen and T. W. B. Kibble, "Global Conservation Laws And Massless Particles," Phys. Rev. Lett. 13, 585 (1964).
- [3] F. Englert and R. Brout, "Broken Symmetry And The Mass Of Gauge Vector Mesons," Phys. Rev. Lett. 13, 321 (1964).
- [4] S. L. Glashow, "Partial Symmetries Of Weak Interactions," Nucl. Phys. 22, 579 (1961).
- [5] S. Weinberg, "A Model Of Leptons," Phys. Rev. Lett. 19, 1264 (1967).
- [6] C. H. Llewellyn Smith, "High-Energy Behavior And Gauge Symmetry," Phys. Lett. B 46, 233 (1973).
- [7] D. A. Dicus and V. S. Mathur, "Mass Differences In A Unified Theory Of Weak And Electromagnetic Interactions," Phys. Rev. D 7, 525 (1973).
- [8] J. M. Cornwall, D. N. Levin and G. Tiktopoulos, "Uniqueness Of Spontaneously Broken Gauge Theories," Phys. Rev. Lett. 30, 1268 (1973) [Erratum-ibid. 31, 572 (1973)].
- [9] J. M. Cornwall, D. N. Levin and G. Tiktopoulos, "Derivation Of Gauge Invariance From High-Energy Unitarity Bounds On The S Matrix," Phys. Rev. D 10, 1145 (1974) [Erratum-ibid. D 11, 972 (1975)].
- [10] B. W. Lee, C. Quigg and H. B. Thacker, "The Strength Of Weak Interactions At Very High-Energies And The Higgs Boson Mass," Phys. Rev. Lett. 38, 883 (1977).
- [11] B. W. Lee. C. Quigg and H. B. Thacker, "Weak Interactions At Very High-Energies: The Role Of The Higgs Boson Mass," Phys. Rev. D 16, 1519 (1977).
- [12] M. J. G. Veltman, "Second Threshold In Weak Interactions," Acta Phys. Polon. B 8, 475 (1977).
- [13] C. E. Vayonakis, "Born Helicity Amplitudes And Cross-Sections In Nonabelian Gauge Theories," Lett. Nuovo Cim. 17, 383 (1976).

- [14] M. S. Chanowitz and M. K. Gaillard, "The Tev Physics Of Strongly Interacting W's And Z's," Nucl. Phys. B **261**, 379 (1985).
- [15] Y. P. Yao and C. P. Yuan, "Modification Of The Equivalence Theorem Due To Loop Corrections," Phys. Rev. D 38, 2237 (1988).
- [16] J. Bagger and C. Schmidt, "Equivalence Theorem Redux," Phys. Rev. D 41, 264 (1990).
- [17] H. J. He, Y. P. Kuang and X. y. Li, "On the precise formulation of equivalence theorem," Phys. Rev. Lett. 69, 2619 (1992).
- [18] H. J. He, Y. P. Kuang and X. y. Li, "Further investigation on the precise formulation of the equivalence theorem," Phys. Rev. D 49, 4842 (1994).
- [19] H. J. He and W. B. Kilgore, "The equivalence theorem and its radiative correction-free formulation for all R(xi) gauges," Phys. Rev. D 55, 1515 (1997) [arXiv:hep-ph/9609326].
- [20] H. Georgi, "Chiral fermion delocalization in deconstructed Higgsless theories," arXiv:hep-ph/0508014.
- [21] I. Antoniadis, "A Possible New Dimension At A Few Tev," Phys. Lett. B 246, 377 (1990).
- [22] I. Antoniadis, C. Munoz and M. Quiros, "Dynamical supersymmetry breaking with a large internal dimension," Nucl. Phys. B 397, 515 (1993) [arXiv:hepph/9211309].
- [23] J. D. Lykken, "Weak Scale Superstrings," Phys. Rev. D 54, 3693 (1996) [arXiv:hep-th/9603133].
- [24] I. Antoniadis and M. Quiros, "Large radii and string unification," Phys. Lett. B 392, 61 (1997) [arXiv:hep-th/9609209].
- [25] N. Arkani-Hamed, S. Dimopoulos and G. R. Dvali, "The hierarchy problem and new dimensions at a millimeter," Phys. Lett. B 429, 263 (1998) [arXiv:hep-ph/9803315].
- [26] I. Antoniadis, N. Arkani-Hamed, S. Dimopoulos and G. R. Dvali, "New dimensions at a millimeter to a Fermi and superstrings at a TeV," Phys. Lett. B 436, 257 (1998) [arXiv:hep-ph/9804398].
- [27] G. Shiu and S. H. H. Tye, "TeV scale superstring and extra dimensions," Phys. Rev. D 58, 106007 (1998) [arXiv:hep-th/9805157].
- [28] K. R. Dienes, E. Dudas and T. Gherghetta, "Extra spacetime dimensions and unification," Phys. Lett. B 436, 55 (1998) [arXiv:hep-ph/9803466].
- [29] K. R. Dienes, E. Dudas and T. Gherghetta, "Grand unification at intermediate mass scales through extra dimensions," Nucl. Phys. B 537, 47 (1999) [arXiv:hep-ph/9806292].

- [30] A. Pomarol and M. Quiros, "The standard model from extra dimensions," Phys. Lett. B 438, 255 (1998) [arXiv:hep-ph/9806263].
- [31] H. C. Cheng, B. A. Dobrescu and C. T. Hill, "Gauge coupling unification with extra dimensions and gravitational scale effects," Nucl. Phys. B **573**, 597 (2000) [arXiv:hep-ph/9906327].
- [32] J. D. Lykken and S. Nandi, "Asymmetrical large extra dimensions," Phys. Lett. B 485, 224 (2000) [arXiv:hep-ph/9908505].
- [33] R. Sundrum, "To the fifth dimension and back. (TASI 2004)," arXiv:hep-th/0508134.
- [34] R. Sekhar Chivukula, D. A. Dicus and H. J. He, "Unitarity of compactified five dimensional Yang-Mills theory," Phys. Lett. B 525, 175 (2002) [arXiv:hep-ph/0111016].
- [35] R. S. Chivukula, D. A. Dicus, H. J. He and S. Nandi, "Unitarity of the higher dimensional standard model," Phys. Lett. B 562, 109 (2003) [arXiv:hepph/0302263].
- [36] C. Csaki, C. Grojean, H. Murayama, L. Pilo and J. Terning, "Gauge theories on an interval: Unitarity without a Higgs," Phys. Rev. D 69, 055006 (2004) [arXiv:hep-ph/0305237].
- [37] M. Soldate, "Partial Wave Unitarity And Closed String Amplitudes," Phys. Lett. B 186, 321 (1987).
- [38] M. Chaichian and J. Fischer, "Higher Dimensional Space-Time And Unitarity Bound On The Scattering Amplitude," Nucl. Phys. B **303**, 557 (1988).
- [39] H. C. Cheng, C. T. Hill, S. Pokorski and J. Wang, "The standard model in the latticized bulk," Phys. Rev. D 64, 065007 (2001) [arXiv:hep-th/0104179].
- [40] N. Arkani-Hamed, A. G. Cohen and H. Georgi, "(De)constructing dimensions," Phys. Rev. Lett. 86, 4757 (2001) [arXiv:hep-th/0104005].
- [41] R. S. Chivukula and H. J. He, "Unitarity of deconstructed five-dimensional Yang-Mills theory," Phys. Lett. B **532**, 121 (2002) [arXiv:hep-ph/0201164].
- [42] R. Foadi, S. Gopalakrishna and C. Schmidt, "Higgsless electroweak symmetry breaking from theory space," JHEP **0403**, 042 (2004) [arXiv:hep-ph/0312324].
- [43] M. E. Peskin and T. Takeuchi, "A New Constraint On A Strongly Interacting Higgs Sector," Phys. Rev. Lett. 65, 964 (1990).
- [44] M. E. Peskin and T. Takeuchi, "Estimation of oblique electroweak corrections," Phys. Rev. D 46, 381 (1992).
- [45] R. Foadi, S. Gopalakrishna and C. Schmidt, "Effects of fermion localization in Higgsless theories and electroweak constraints," Phys. Lett. B 606, 157 (2005) [arXiv:hep-ph/0409266].

- [46] G. Cacciapaglia, C. Csaki, C. Grojean and J. Terning, "Curing the ills of Higgsless models: The S parameter and unitarity," Phys. Rev. D 71, 035015 (2005) [arXiv:hep-ph/0409126].
- [47] C. Csaki, C. Grojean, L. Pilo and J. Terning, "Towards a realistic model of Higgsless electroweak symmetry breaking," Phys. Rev. Lett. **92**, 101802 (2004) [arXiv:hep-ph/0308038].
- [48] Y. Nomura, "Higgsless theory of electroweak symmetry breaking from warped space," JHEP **0311**, 050 (2003) [arXiv:hep-ph/0309189].
- [49] R. Barbieri, A. Pomarol and R. Rattazzi, "Weakly coupled Higgsless theories and precision electroweak tests," Phys. Lett. B 591, 141 (2004) [arXiv:hep-ph/0310285].
- [50] R. Foadi and C. Schmidt, "An effective Higgsless theory: Satisfying electroweak constraints and a heavy top quark," Phys. Rev. D 73, 075011 (2006) [arXiv:hepph/0509071].
- [51] L. Randall and R. Sundrum, "A large mass hierarchy from a small extra dimension," Phys. Rev. Lett. 83, 3370 (1999) [arXiv:hep-ph/9905221].
- [52] G. Cacciapaglia, C. Csaki, C. Grojean and J. Terning, "Oblique corrections from Higgsless models in warped space," Phys. Rev. D 70, 075014 (2004) [arXiv:hep-ph/0401160].
- [53] S. Eidelman et al. [Particle Data Group], "Review of particle physics," Phys. Lett. B 592, 1 (2004).
- [54] P. Sikivie, L. Susskind, M. B. Voloshin and V. I. Zakharov, "Isospin Breaking In Technicolor Models," Nucl. Phys. B 173, 189 (1980).
- [55] R. S. Chivukula, E. H. Simmons, H. J. He, M. Kurachi and M. Tanabashi. "The structure of corrections to electroweak interactions in Higgsless models," Phys. Rev. D 70, 075008 (2004) [arXiv:hep-ph/0406077].
- [56] A. Lewandowski, M. J. May and R. Sundrum, "Running with the radius in RS1," Phys. Rev. D 67, 024036 (2003) [arXiv:hep-th/0209050].
- [57] A. Lewandowski and M. Redi, "Spin and a running radius in RS1," Phys. Rev. D 68, 044012 (2003) [arXiv:hep-th/0305013].
- [58] A. Lewandowski, "The Wilsonian renormalization group in Randall-Sundrum. I," Phys. Rev. D 71, 024006 (2005) [arXiv:hep-th/0409192].
- [59] C. P. Burgess, S. Godfrey, H. Konig, D. London and I. Maksymyk, "Model independent global constraints on new physics," Phys. Rev. D 49, 6115 (1994) [arXiv:hep-ph/9312291].
- [60] C. Csaki, J. Erlich and J. Terning, "The effective Lagrangian in the Randall-Sundrum model and electroweak physics," Phys. Rev. D 66, 064021 (2002) [arXiv:hep-ph/0203034].

- [61] R. S. Chivukula, E. H. Simmons, H. J. He, M. Kurachi and M. Tanabashi, "Universal non-oblique corrections in Higgsless models and beyond," Phys. Lett. B 603, 210 (2004) [arXiv:hep-ph/0408262].
- [62] R. Sekhar Chivukula, E. H. Simmons, H. J. He, M. Kurachi and M. Tanabashi, "Electroweak corrections and unitarity in linear moose models," Phys. Rev. D 71, 035007 (2005) [arXiv:hep-ph/0410154].
- [63] R. Sekhar Chivukula, E. H. Simmons, H. J. He, M. Kurachi and M. Tanabashi, "Ideal fermion delocalization in Higgsless models," Phys. Rev. D 72, 015008 (2005) [arXiv:hep-ph/0504114].
- [64] R. Sekhar Chivukula, E. H. Simmons, H. J. He, M. Kurachi and M. Tanabashi, "Ideal fermion delocalization in five dimensional gauge theories," Phys. Rev. D 72, 095013 (2005) [arXiv:hep-ph/0509110].
- [65] M. E. Peskin and D. V. Schroeder, "An Introduction To Quantum Field Theory,"
- [66] Y. Kawamura, "Gauge symmetry reduction from the extra space S(1)/Z(2)," Prog. Theor. Phys. 103, 613 (2000) [arXiv:hep-ph/9902423].
- [67] A. Hebecker and J. March-Russell, "A minimal S(1)/(Z(2) x Z'(2)) orbifold GUT," Nucl. Phys. B **613**, 3 (2001) [arXiv:hep-ph/0106166].
- [68] Z. Chacko, M. A. Luty, A. E. Nelson and E. Ponton, "Gaugino mediated supersymmetry breaking," JHEP **0001**, 003 (2000) [arXiv:hep-ph/9911323].
- [69] M. Carena, T. M. P. Tait and C. E. M. Wagner, "Branes and orbifolds are opaque," Acta Phys. Polon. B 33, 2355 (2002) [arXiv:hep-ph/0207056].
- [70] M. Carena, E. Ponton, T. M. P. Tait and C. E. M. Wagner, "Opaque branes in warped backgrounds," Phys. Rev. D 67, 096006 (2003) [arXiv:hep-ph/0212307].
- [71] C. Csaki, C. Grojean, J. Hubisz, Y. Shirman and J. Terning, "Fermions on an interval: Quark and lepton masses without a Higgs," Phys. Rev. D 70, 015012 (2004) [arXiv:hep-ph/0310355].
- [72] A. A. Affolder *et al.* [CDF Collaboration], "Search for quark lepton compositeness and a heavy W' boson using the e nu channel in p anti-p collisions at s**(1/2) = 1.8-TeV," Phys. Rev. Lett. **87**, 231803 (2001) [arXiv:hep-ex/0107008].
- [73] [ALEPH Collaboration], "A combination of preliminary electroweak measurements and constraints on the standard model. ((B))," arXiv:hep-ex/0212036.
- [74] K. Hagiwara, R. D. Peccei, D. Zeppenfeld and K. Hikasa, "Probing The Weak Boson Sector In E+ E- → W+ W-," Nucl. Phys. B 282, 253 (1987).
- [75] R. S. Chivukula, E. H. Simmons, H. J. He, M. Kurachi and M. Tanabashi, "Multi-gauge-boson vertices and chiral Lagrangian parameters in higgsless models with ideal fermion delocalization," Phys. Rev. D 72, 075012 (2005) [arXiv:hep-ph/0508147].
- [76] The LEP Collaborations ALEPH, DELPHI, L3, OPAL and the LEP TGC Working Group. LEPEWWG/TC/2005-01; June 8, 2005.

- [77] I. S. Gradshteyn and I. M. Ryzhik, "Table of Integrals, Series, and Products," 5th edition, Academic Press (1994).
- [78] K. Hagiwara *et al.* [Particle Data Group Collaboration], "Review Of Particle Physics," Phys. Rev. D **66**, 010001 (2002).
- [79] C. Schwinn, "Unitarity constraints on top quark signatures of Higgsless models," Phys. Rev. D **71**, 113005 (2005) [arXiv:hep-ph/0504240].
- [80] F. Larios, M. A. Perez and C. P. Yuan, "Analysis of t b W and t t Z couplings from CLEO and LEP/SLC data," Phys. Lett. B 457, 334 (1999) [arXiv:hep-ph/9903394].



